

**The integration of freely available medium resolution optical sensors with Synthetic Aperture Radar (SAR) imagery capabilities for American bramble (*Rubus cuneifolius*) invasion detection and mapping**

by

**Perushan Rajah**

**December 2018**



Submitted in fulfilment of the academic requirements for the degree of Doctor of Philosophy in the School of Agriculture, Earth and Environmental Sciences,

Geography, University of KwaZulu-Natal,

Pietermaritzburg

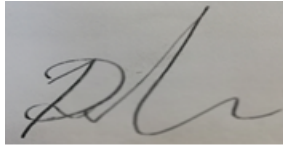
December 2018

## Preface

The work described in this thesis was carried out in the School of Agricultural, Earth and Environmental Sciences, University of KwaZulu-Natal, Pietermaritzburg. The research was undertaken from January 2015 to December 2018, under the supervision of Doctor John Odindi and Professor Onesimo Mutanga.

The work in this thesis represents the original work of the author and has never been submitted in any form to any other tertiary institution. Where use has been made of the work of others, it is duly acknowledged in both the text and reference sections of this thesis.

**Perushan Rajah:**



**December 2018**

As the candidate's supervisors, we certify the above statement and have approved this thesis for submission.

**1. Doctor John Odindi**

**Signed:**

**Date: 07/12/18**

**2. Prof. Onesimo Mutanga**

**Signed:**

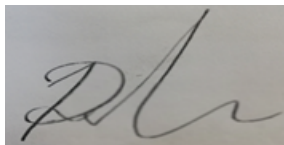
**Date: 07/12/18**

## Declaration 1: Plagiarism

I, Perushan Rajah, declare that:

1. The research reported in this thesis, except where otherwise indicated, is my original work.
2. This thesis has not been submitted for any degree or examination at any other university.
3. This thesis does not contain other persons' data, pictures, graphs, or other information, unless specifically acknowledged as being sourced from other persons.
4. This thesis does not contain other persons' writing, unless specifically acknowledged as being sourced from other researchers. Where other written sources have been quoted, then:
  - a. Their words have been re-written, but the general information attributed to them has been referenced.
  - b. Where their exact words have been used, their writing has been placed in italics and inside quotation marks, and referenced.
5. This thesis does not contain text, graphics, or tables copied and pasted from the internet, unless specifically acknowledged, and the source being detailed in the thesis and in the References sections.

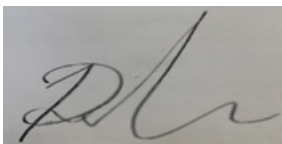
**Signed:**

A rectangular box containing a handwritten signature in black ink. The signature is cursive and appears to be 'Perushan Rajah'.

## Declaration 2: Publications

1. Rajah, P., Odindi, J., and Mutanga, O., 2018: Evaluating the potential of freely available multispectral remotely sensed imagery in mapping American bramble (*Rubus cuneifolius*). *South African Geographical Journal*, 100 (3), 291–307
2. Rajah, P., Odindi, J. and Mutanga, O., 2018. Feature level image fusion of optical imagery and Synthetic Aperture Radar (SAR) for invasive alien plant species detection and mapping. *Remote Sensing Applications: Society and Environment*, 10, 198-208.
3. Rajah, P., Odindi, J., Mutanga, O and Kiala, S., (*Under review: Resubmission - Journal of Applied Remote Sensing*): The fusion of optical imagery with SAR polarization combinations and ratios for invasive alien plant detection and mapping
4. Rajah, P., Odindi, J., Mutanga, O and Kiala, S., (*Under review - International Journal of Remote Sensing*): Assessing the synergistic potential of Sentinel-2 optical bands and derived vegetation indices for detecting and mapping invasive alien plant species
5. Rajah, P., Odindi, J., and Mutanga, O., (*Under review: Awaiting Subject editor's decision – Nature Conservation*): The utility of Sentinel-2 Vegetation Indices (VIs) and Sentinel-1 Synthetic Aperture Radar (SAR) for invasive alien species detection and mapping
6. Rajah, P., Odindi, J., and Mutanga, O., (*In preparation*): The synergistic potential of dual-polarized Synthetic Aperture Radar (SAR) fused with multispectral optical imagery for invasive alien species detection and mapping

Signed:

A rectangular box containing a handwritten signature in black ink. The signature is stylized and appears to be the initials 'PR' followed by a flourish.

# Contents

<b>Preface</b> .....	<b>2</b>
<b>Declaration 1: Plagiarism</b> .....	<b>3</b>
<b>Declaration 2: Publications</b> .....	<b>4</b>
Abstract .....	14
<b>Chapter One</b> .....	<b>17</b>
<b>General Introduction</b> .....	<b>17</b>
1. Introduction.....	17
1.2 Aim and objectives .....	20
1.3 Study area description .....	21
1.4 Outline of the thesis .....	22
<b>Chapter Two</b> .....	<b>24</b>
Abstract .....	24
2.1 Introduction.....	25
2.2 Methodology .....	27
2.2.1 Study area.....	27
2.2 Field data collection .....	29
2.2.2 SVM classification .....	30
2.2.3 Mapping and map validation .....	31
2.3 Results .....	32
2.3.1 Optimum band selection and band identification .....	32
2.3.2 Multi-seasonal discrimination .....	32
2.4. Discussion .....	37
2.5. Conclusion.....	39
<b>Chapter Three</b> .....	<b>40</b>
Abstract .....	40
3.1 Introduction.....	41
3.2 Methodology .....	43
3.2.1 Study area.....	43
3.2.2 Target species .....	44
3.2.4.1 Optical imagery .....	45
3.2.4.2 SAR imagery .....	46
3.2.5 Data fusion.....	47

3.2.6 Image classification .....	48
3.2.7 Spatial distribution maps and validation .....	48
3.3 Results .....	48
3.3.1 Seasonal comparisons of Bramble infestations in relation to other landcovers .....	48
3.3.1.1 Summer .....	48
3.3.1.2 Autumn .....	50
3.3.1.3 Winter .....	52
3.3.1.4 Spring .....	54
3.4 Discussion .....	56
3.5 Conclusion.....	58
<b>Chapter Four .....</b>	<b>60</b>
Abstract .....	60
4.1 Introduction.....	61
4.2 Methodology .....	63
4.2.1 Study area.....	63
4.2.1.1 Field data collection .....	64
4.2.2 Image acquisition .....	65
4.2.2.1 Optical imagery .....	65
4.2.2.2 SAR imagery .....	65
4.2.2.3 S1 SAR dual polarized indices .....	65
4.2.3 Data Fusion.....	66
4.2.4 Image classification.....	67
4.2.5 Map production and accuracy assessment.....	67
4.3 Results .....	67
4.4 Discussion .....	74
4.5 Conclusions.....	76
<b>Chapter Five .....</b>	<b>78</b>
Abstract .....	78
5.1 Introduction.....	79
5.2 Methodology .....	81
5.2.1 Study area.....	81
5.2.1.1 Target species.....	81
5.2.1.2 Field data collection .....	82
5.2.2 Image acquisition .....	83

5.2.2.1 Optical imagery .....	83
5.2.2.2 Vegetation indices .....	83
5.2.3 Variable selection .....	83
5.2.4 Image fusion: Optical bands and Vegetation Indices .....	84
5.2.5 Image classification .....	84
5.2.6 Spatial distribution map and accuracy assessment .....	85
5.3 Results .....	85
5.3.1 Optical and Vegetation Indices VIP band selection .....	85
5.3.2 Seasonal classification .....	87
5.3.2.1 S2 reflectance bands .....	87
5.3.2.2 Fused VIP S2 reflectance bands and Vegetation Indices .....	87
5.4 Discussion .....	90
5.5 Conclusion .....	92
<b>Chapter Six .....</b>	<b>93</b>
Abstract .....	93
6.1 Introduction .....	94
6.2 Methodology .....	96
6.2.1 Study site .....	96
6.2.1.1 Field data collection .....	97
6.2.2 Image acquisition .....	97
6.2.2.1 Optical Imagery .....	97
6.2.2.2 Sentinel-1 Synthetic Aperture Radar (SAR) Imagery .....	97
6.2.2.3 Sentinel-2 derived Vegetation Indices (VIs) .....	98
6.2.3 Image fusion .....	98
6.2.4 Image classification .....	99
6.2.5 Determination of spatial distribution and validation .....	99
6.3 Results .....	99
6.3.1 Vegetation Indices (VIs) .....	99
6.3.2 Sentinel-2 optical bands .....	100
6.3.3 Vegetation Indices (VIs) and S1 SAR imagery .....	102
6.4 Discussion .....	105
6.5 Conclusion .....	108
<b>Chapter Seven .....</b>	<b>109</b>

Abstract .....	109
7.1 Introduction.....	110
7.2 Methodology .....	112
7.2.1 Study area.....	112
7.2.2 Target species .....	112
7.2.3 Field data collection .....	113
7.2.5 Sentinel-2 optical imagery .....	115
7.2.6 Feature level image fusion .....	115
7.2.7 Image classification.....	116
7.2.8 Spatial distribution maps and validation .....	116
7.3 Results .....	116
7.4. Discussion .....	119
7.5. Conclusion.....	121
<b>Chapter Eight .....</b>	<b>123</b>
8.1 Introduction.....	124
8.2 Evaluating the potential of freely available multispectral remotely sensed imagery for mapping invasive alien plant species .....	125
8.3 Feature level image fusion of optical imagery and Synthetic Aperture Radar (SAR) for invasive alien plant species detection and mapping .....	127
8.4 The fusion of multispectral optical imagery and SAR polarization combinations/ratios for invasive alien plant detection and mapping .....	128
8.5 Assessing the combined potential of Sentinel-2 spectral reflectance bands, derived Vegetation Indices (VIs) and Synthetic Aperture Radar (SAR) for detecting and mapping invasive alien species .....	129
8.6 The synergistic potential of dual-polarized Synthetic Aperture Radar (SAR) fused with multispectral optical imagery for invasive alien species detection and mapping .....	131
<b>References .....</b>	<b>136</b>



## List of Figures

Figure 1.1: The invasive alien plant American bramble ( <i>Rubus cuneifolius</i> ) (a); its inflorescence (b-c) and bramble patches within the grassland landscape of the DP (d) and (e). .....	18
Figure 2.1: The study area (a and b) and the uKhahlamba Drakensberg Park (UDP) boundary (c). .....	28
Figure 2.3: Summer and spring classification maps from Landsat 8 and Sentinel-2 imagery. Where (a) = Landsat 8 summer; (b) = Sentinel-2 summer; (c) = Landsat 8 spring and (d) = Sentinel-2 Spring. ....	35
Figure 2.4: Summer and spring classification maps from Landsat 8 and Sentinel-2 imagery. Where (a) = Landsat 8 summer; (b) = Sentinel-2 summer; (c) = Landsat 8 spring and (d) = Sentinel-2 Spring. ....	36
Figure 3.1: The location of the Kwazulu-Natal (KZN) province within South Africa (a). Extent of the uKhahlamba Drakensberg Park (UDP), illustrating altitude as meters above sea level (b). .....	44
Figure 3.2: Feature level fusion processing chain. ....	47
Figure 3.3: Summer spatial distribution maps for fused Landsat 8 and Sentinel-2 VH and VV polarisations. Where (a) = Landsat 8 (VH); (b) = Landsat 8 (VV); (c) = Sentinel-2 (VH) and (d) = Sentinel-2 (VV) .....	50
Figure 3.4: Autumn spatial distribution maps for fused Landsat 8 and Sentinel-2 VH and VV polarisations. Where (a) = Landsat 8 (VH); (b) = Landsat 8 (VV); (c) = Sentinel-2 (VH) and (d) = Sentinel-2 (VV). ....	52
Figure 3.5: Winter spatial distribution maps for fused Landsat 8 and Sentinel-2 VH and VV polarisations. Where (a) = Landsat 8 (VH); (b) = Landsat 8 (VV); (c) = Sentinel-2 (VH) and (d) = Sentinel-2 (VV). ....	54
Figure 3.6: Spring spatial distribution maps for fused Landsat 8 and Sentinel-2 VH and VV polarisations. Where (a) = Landsat 8 (VH); (b) = Landsat 8 (VV); (c) = Sentinel-2 (VH) and (d) = Sentinel-2 (VV). ....	56
Figure 4.1: Ukhahlamba Drakensberg Park (UDP) boundary (c), within the KZN province (b) of South Africa (a). ....	64
Figure 4.2: Feature level fusion processing chain .....	66
Figure 4.3: Land cover maps produced using VV – VH and VH - VV S1 SAR dual polarized indices fused with S2 optical imagery and SVM classifier. ....	69

Figure 4.4: Land cover maps produced using VH/VV and VV/VH S1 SAR dual polarized indices fused with S2 optical imagery and SVM classifier. ....	71
Figure 4.5: Land cover maps produced using VH x VV and VH + VV S1 SAR dual polarized indices fused with S2 optical imagery.....	73
Figure 4.6: Overestimation and underestimation of Bramble classes across VH-VV; VV - VH; VH/VV; VV/VH; VH x VV and VV+VH band combinations and ratios .....	74
Figure 5.1: The Ukhahlamba Drakensberg Park (UDP) (c), located within the KwaZulu-Natal Province (b) of South Africa (a). ....	82
Figure 5.2: Multi-season classification maps produced using VIP selected optical bands and vegetation indices. Where (a) = Spring; (b) = Summer; (c) = Autumn and (d) = Winter. ....	90
Figure 6.1: The uKhahlamba Drakensberg Park (UDP) (C) located within the KwaZulu-Natal Province (B) of South Africa (A). ....	96
Figure 6.2: Support Vector Machine (SVM) classification maps produced utilizing (a) Vegetation Indices; (b) S2 optical bands and (c) Fused VIs and SAR. ....	102
Figure 6.3: Over-estimation and under-estimation of land-cover classes within an area of interest where (a) = S2 optical bands; (b) = Vegetation indices (VIs) and (c) = VIs and SAR imagery. ....	105
Figure 7.1: The uKhahlamba Drakensberg Park boundary (C), located within the KwaZulu-Natal province (B) of South Africa (A).....	113
Figure 7.2: Spatial distribution maps of fused S2 optical bands and (a) S1vv-vh; (b) S1vv-vv dual-polarized SAR imagery compared to (c) S2 optical band spatial distribution map.....	118
Figure 7.3: An example of mapped classification accuracies across S2+S1vv-vh ; S2+S1vv-vv and S2 optical bands .....	119
Figure 8.1: Comparison of Landsat 8 and Sentinel-2 spatial distribution of all landcover classes considered in this study.....	126
Figure 8.2: Overestimation and underestimation of Bramble classes across VH-VV; VV - VH; VH/VV; VV/VH; VH x VV and VV+VH band combinations and ratios .....	129
Figure 8.3: Support Vector Machine (SVM) classification maps produced utilizing (a) Vegetation Indices; (b) S2 optical bands and (c) Fused VIs and SAR. ....	131
Figure 8.4: Spatial distribution maps of fused S2 optical bands and (a) S1vv-vh; (b) S1vv-vv dual-polarized SAR imagery compared to (c) S2 optical band spatial distribution map.....	133

## List of tables

Table 2.1: Life-cycle phenology of American bramble ( <i>Rubus cuneifolius</i> ). .....	30
Table 2.2: Bands identified for discrimination analysis (NIR = Near infrared; SWIR1= Shortwave infrared1, SWIR2= Shortwave infrared 2, RE1= Red edge 1, RE2= Red edge 2 and RE3= Red edge 3. ....	32
Table 2.3: Support vector machine confusion matrices showing users, producers and overall accuracy for all four seasons using Landsat 8 imagery. Where BR = Bare rock; BBL = Bramble; FR = Forest; GR = grassland; PA= Producers accuracy; OA= Overall accuracy and UA.....	33
Table 2.4: Support vector machine confusion matrices showing users, producers and overall accuracy for all four seasons using Landsat 8 imagery. Where BR = Bare rock; BBL = Bramble; FR = Forest; GR = grassland; PA= Producers accuracy; OA= Overall accuracy and UA.....	34
Table 3.1: Image acquisition dates for individual optical and SAR imagery.....	46
Table 3.2: Summer confusion matrices of VH and VV fused polarisation for Landsat 8 and Sentinel-2. Where BR = Bare rock; BBL = Bramble; FR = Forest; GR = grassland; PA= Producers accuracy; OA= Overall accuracy and UA = Users accuracy.....	49
Table 3.3: Autumn confusion matrices for VH and VV fused polarisation for Landsat 8 and Sentinel-2. Where BR = Bare rock; BBL = Bramble; FR = Forest; GR = grassland; PA= Producers accuracy; OA= Overall accuracy and UA = Users accuracy.....	51
Table 3.4: Winter confusion matrices for VH and VV fused polarisation for Landsat 8 and Sentinel-2. Where BR = Bare rock; BBL = Bramble; FR = Forest; GR = grassland; PA= Producers accuracy; OA= Overall accuracy and UA = Users accuracy.....	53
Table 3.5: Spring confusion matrices of VH and VV fused polarisation for Landsat 8 and Sentinel-2. Where BR = Bare rock; BBL = Bramble; FR = Forest; GR = grassland; PA= Producers accuracy; OA= Overall accuracy and UA = Users accuracy.....	55
Table 4.1: Confusion matrices of VV - VH and VH - VV S1 SAR dual polarized indices fused with S2 optical imagery. Where BR = Bare rock; BBL = Bramble; FR = Forest; GR = grassland; PA= Producer's accuracy; OA= Overall accuracy and UA = User's accuracy. ..	68
Table 4.2: Confusion matrices of VH/VV and VV/VH SAR ratios fused with Sentinel-2 optical imagery. Where BR = Bare rock; BBL = Bramble; FR = Forest; GR = grassland; PA= Producers accuracy; OA= Overall accuracy and UA = Users accuracy.....	70

Table 4.3: Confusion matrices of VH x VV and VH + VV SAR combinations fused with Sentinel-2 optical imagery. Where BR = Bare rock; BBL = Bramble; FR = Forest; GR = grassland; PA= Producers accuracy; OA= Overall accuracy and UA = Users accuracy. ....	72
Table 5.1: Selected VIP optical bands and Vegetation Indices (VIs) across all seasonal imagery (Indices derived from the Index Database - <a href="http://www.indexdatabase.de">www.indexdatabase.de</a> ). ....	85
Table 5.2: S2 reflectance band Support Vector Machine (SVM) seasonal confusion matrices. Where BR = Bare rock; BBL = Bramble; FR = Forest; GR = grassland; PA= Producers accuracy; OA= Overall accuracy and UA = Users accuracy. ....	88
Table 5.3: Fused VIP S2 optical bands and Vegetation Indices Support Vector Machine (SVM) seasonal confusion matrices. Where BR = Bare rock; BBL = Bramble; FR = Forest; GR = grassland; PA= Producers accuracy; OA= Overall accuracy and UA = Users accuracy. ....	89
Table 6.1: Support Vector Machine (SVM) confusion matrix using Vegetation Indices for Bramble mapping and discrimination. Where BR = Bare rock; BBL = Bramble; FR = Forest; and GR = Grassland, UA = Users accuracy; PA = Producers accuracy and OA = Overall accuracy. ....	100
Table 6.2: Support Vector Machine (SVM) confusion matrix using Sentinel-2 optical bands for Bramble mapping and discrimination. Where BR = Bae rock; BBL = Bramble; FR = Forest; and GR = Grassland, UA = Users accuracy; PA = Producers accuracy and OA = Overall accuracy. ....	101
Table 6.3: Selected S2 derived VIP vegetation indices subsequently utilized for SAR fusion. .	103
Table 6.4: Support Vector Machine (SVM) confusion matrix using fused Vegetation Indices and SAR imagery for Bramble mapping and discrimination. Where BR = Bae rock; BBL = Bramble; FR = Forest; and GR = Grassland, UA = Users accuracy; PA = Producers accuracy and OA = Overall accuracy. ....	104
Table 7.1: Confusion matrices of fused S2 optical bands and (a) S1vv-vh ; (b) S1vv-vv SAR imagery compared to S2 optical band Confusion matrix. Where BR = Bare rock; BBL = Bramble; FR = Forest; GR = grassland; PA= Producers accuracy; OA= Overall accuracy and UA = Users accuracy. ....	117
Table 8.1: Seasonal overall classification accuracies resulting from Landsat 8 and Sentinel-2 imagery.....	126
Table 8.2: Seasonal overall accuracies of fused Landsat 8 and Sentinel-1 SAR and Sentinel-2 and Sentinel-1 SAR .....	127
Table 8.3: Overall accuracies of fused Sentinel-2 imagery and Sentinel-1 SAR polarization combinations and ratios .....	128

Table 8.4: Seasonal overall accuracies of stand alone Sentinel-2 imagery compared to fused Sentinel-2 and Vegetation Indices (VIs) .....	130
Table 8.5: Overall accuracies produced using stand-alone Sentinel-2 optical bands, VIP Vegetation Indices (Vis) and fused Sentinel-2 and Vegetation Indices .....	130
Table 8.6: Overall accuracies produced using Sentinel-2 optical imagery fused with dual-polarized Sentinel-1 SAR imagery .....	132

## **Abstract**

The emergence of American bramble (*Rubus cuneifolius*) across South Africa has caused severe ecological and economic damage. To date, most of the efforts to mitigate its effects have been largely unsuccessful due to its prolific growth and widespread distribution. Accurate and timeous detection and mapping of Bramble is therefore critical to the development of effective eradication management plans. Hence, this study sought to determine the potential of freely available, new generation medium spatial resolution satellite imagery for the detection and mapping of American Bramble infestations within the UNESCO world heritage site of the uKhahlamba Drakensberg Park (UDP).

The first part of the thesis determined the potential of conventional freely available remote sensing imagery for the detection and mapping of Bramble. Utilizing the Support Vector Machine (SVM) learning algorithm, it was established that Bramble could be detected with limited users (45%) and reasonable producers (80%) accuracies. Much of the confusion occurred between the grassland land cover class and Bramble.

The second part of the study focused on fusing the new age optical imagery and Synthetic Aperture Radar (SAR) imagery for Bramble detection and mapping. The synergistic potential of fused imagery was evaluated using multiclass SVM classification algorithm. Feature level image fusion of optical imagery and SAR resulted in an overall classification accuracy of 76%, with increased users and producers' accuracies for Bramble. These positive results offered an opportunity to explore the polarization variables associated with SAR imagery for improved classification accuracies.

The final section of the study dwelt on the use of Vegetation Indices (VIs) derived from new age satellite imagery, in concert with SAR to improve Bramble classification accuracies. Whereas improvement in classification accuracies were minimal, the potential of stand-alone VIs to detect and map Bramble (80%) was noteworthy. Lastly, dual-polarized SAR was fused with new age optical imagery to determine the synergistic potential of dual-polarized SAR to increase Bramble mapping accuracies. Results indicated a marked increase in overall Bramble classification accuracy (85%), suggesting improved potential of dual-polarized SAR and optical imagery in invasive species detection and mapping.

Overall, this study provides sufficient evidence of the complimentary and synergistic potential of active and passive remote sensing imagery for invasive alien species detection and mapping. Results of this study are important for supporting contemporary decision making relating to invasive species management and eradication in order to safeguard ecological biodiversity and pristine status of nationally protected areas.

## **Acknowledgements**

First and foremost, I would like to thank my parents for their constant support throughout my academic journey. Without your love, guidance and belief, my academic journey would have not been possible. I am eternally grateful.

To my principal supervisor and the person who always encouraged me to continue pressing forward even in the face of adversity, Dr. John, I will forever be thankful and indebted to you. Your patience and steadfast academic work ethic allowed me the opportunity to develop my passion for applied remote sensing. To my co-supervisor, Prof. Onesimo Mutanga, thank you for the constant encouragement and creating an atmosphere conducive to applied research.

I would also like to thank my dear friends who have shown patience and love during my research. Your understanding and belief in me and my will to achieve my goals allowed me to persevere through the toughest of times.

Finally, I would like to thank the Council for Scientific and Industrial Research (CSIR) and the UKZN School of Agricultural, Earth and Environmental Sciences for making it financially possible to read for my PhD through their joint bursary scheme.



# Chapter One

## General Introduction

### 1. Introduction

Global biodiversity has rapidly decreased in recent decades, with the estimated loss of terrestrial biodiversity costing the global economy approximately \$500 billion per annum (The Economics of Ecosystems and Biodiversity, 2009). Consequently, the United Nations Convention on Biological Diversity (CBD) has emphasized the Aichi 2020 targets, which aim to reduce pressure on biodiversity and improve biodiversity status by conserving ecosystems, species and genetic diversity (Proença *et al.*, 2017). An assessment of the targets found that while steps to offset the deterioration of biodiversity have increased, so have been the associated pressures (Tittensor *et al.*, 2014).

Global grassland ecosystems have particularly experienced an extreme decline in biodiversity in recent decades. With grassland ecosystems covering approximately 40% of the earth's surface (White *et al.*, 2000), significant efforts are necessary to ensure conservation of such a valuable ecosystem. Grasslands serve to sequester atmospheric carbon, reduce surface water runoff and erosion, store runoff as groundwater and provide grazing for livestock and wild animals. Globally, grasslands accommodate several important species and include 15% of the world's centres of plant endemism, 11% of endemic bird areas and 29% of ecoregions with outstanding biological distinctiveness (White *et al.*, 2000). In South Africa, the grassland biome is one of the most threatened of the seven biomes, with roughly 60% of natural grassland environments considered permanently transformed (Reyers and Tosh 2003; Fairbanks *et al.*, 2000). In addition, of the 339 237 km<sup>2</sup> (29% of South Africa's land surface area), only 2.8% is formally conserved (Reyers and Tosh, 2003). The decline in grassland ecosystems along with their associated biodiversity and ecosystem services demand urgent strategies to improve their condition (World Resource Institute, 2001).

Biological invasions are a major driver of grassland ecosystem and biodiversity degradation, hence understanding their spatial distribution patterns and processes is becoming increasingly important (McLean *et al.*, 2017). Considering that invasive plant species costs the South African economy an estimated R6.5 billion a year (De Lange and Van Wilgen, 2012), timely, accurate and cost-effective detection and mapping of specific invasive species is critical. In the KwaZulu-

Natal Province of South Africa, the increasing proliferation of the American bramble (*Rubus cuneifolius*) has particularly become a concern. Bramble is an alien deciduous shrub of the *Rosaceae* family originally imported into South Africa from northern America during the late 1800s and early 1900s, for commercial cultivation and production of jam from its berries (Erasmus, 1984). Subsequent to its introduction, Bramble has successfully escaped cultivated ranges and spread throughout KwaZulu-Natal, with disastrous effects (Figure 1.1).

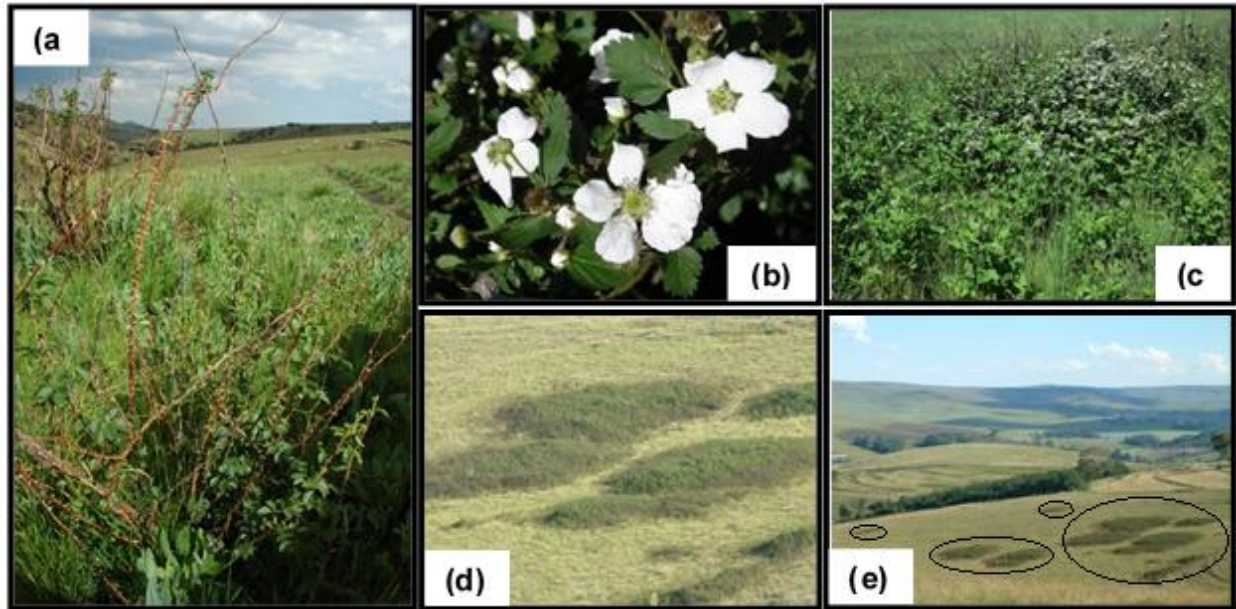


Figure 1.1: The American bramble (*Rubus cuneifolius*) (a); its inflorescence (b-c) and bramble patches within the grassland landscape of the UDP (d) and (e).

The thorny, thickety nature of Bramble has adverse impacts on natural grazing lands, along roadsides and in riparian zones (Shezi and Poona, 2010). Generally, Bramble is known to adversely affect nutrient cycling, increase soil erosion, reduce animal carrying capacity and population viability, hinder natural plant succession, reduce quality and quantity of water production and promote changes in fire patterns and behaviour. Furthermore, the establishment of Bramble patches is known to have negative effects on specialist grassland species. In order to reduce these harmful impacts, the development of efficient and cost-effective Bramble management strategies is required.

According to He *et al* (2011), repeated monitoring, detection and collation of spatial distributions of invasive alien plant species by conventional field-based survey is time consuming and expensive. The use of remotely sensed imagery in invasive alien species detection and mapping has attracted significant attention over recent decades and could significantly

contribute to reliable and accurate information relating to Bramble spatial distributions. While there have been numerous studies conducted on detection and mapping of invasive alien species using a range of satellite imagery, with reasonable accuracy (Van den Berg *et al.*, 2013; Masocha and Skidmore, 2011; Kimothi and Dasari, 2010; Rocchini *et al.*, 2015), satellite specifications have always been the limiting factor in generating reliable and accurate spatial distribution maps. Bradley *et al* (2014), for instance notes that when using remotely sensed data, researchers are faced with the dilemma of trade-offs between spatial extent (swath width), spectral resolution (number of bands), spatial resolution (pixel size) and temporal resolution (revisit time).

Currently, Earth Observation (EO) technology is characterized by an abundance of airborne and spaceborne sensors, providing a large variety of remotely sensed data (Schmitt *et al.*, 2017). The abundance and improvements in remote sensing satellite technology have the potential to allow for improved accuracy in detecting and mapping of invasive alien species. For instance, the European Union, through its first Earth Observation (EO) programme Copernicus, launched the Sentinel-1 (S1) and Sentinel-2 (S2) satellites. Sentinel-1 (S1) is a Synthetic Aperture Radar (SAR) sensor providing unprecedented 250 km<sup>2</sup> SAR imagery in single and dual polarization, while Sentinel-2 (S2) is a multispectral optical sensor, providing 290 km<sup>2</sup> optical imagery in 13 optical bands (Ramoelo *et al.*, 2015). Gao *et al* (2017) notes that the tandem operation and the respective unique characteristics of these two satellites have established a new paradigm for remote sensing applications. In addition, Schmidt *et al* (2017) suggests that the timeous launch of S1 and S2 could serve to increase the applicability of remote sensing-based approaches for practical environmental monitoring and mapping tasks.

The synergistic potential of multi-source remotely sensed imagery (eg. S1 SAR and S2 optical imagery) could potentially improve the analysis of Bramble's functional and structural properties, and consequently increase accuracies associated with mapping their spatial distributions (Peerbhay *et al.*, 2016 and Fard *et al.*, 2014). SAR sensors operate at longer wavelengths and provide complimentary information relating to shape, moisture and roughness, information not provided by optical imagery (Chen *et al.*, 2010). Since multispectral optical imagery record surface information regarding reflectance and emissivity characteristics, while SAR imagery capture the structure and dielectric properties of earth surface materials (Zhu *et al.*, 2012), studies have suggested that the synergistic potential and complementarity of optical and SAR imagery has potential to cost-effectively improve vegetation classification accuracies (Talab-Ou-Ali *et al.*, 2017). Whereas the technique has been successfully applied in the computer vision,

medical imaging and defence security realms (Zhang, 2010), studies on fusion of optical and SAR imagery for the detection and mapping of invasive alien species spatial distribution are limited.

Remote sensing image fusion seeks to combine information from multiple sources to achieve inferences that are not feasible from a single sensor or source. The approach seeks to integrate different data in order to obtain more information that can be derived from each of the single sensor data alone. Multi-sensor image fusion is widely recognized as an efficient tool for improving overall performance in image-based applications. Mitchell *et al.* (2010) and Zheng (2011) consider image fusion as the best option for the integration of information collected from different imaging sensors at varying spectral, spatial and temporal resolutions. Sentinel-1 and Sentinel-2 imagery provide a unique opportunity to investigate the synergistic potential of new age optical imagery fused with SAR imagery for invasive alien species detection and mapping. The freely available nature of S1 and S2 imagery, coupled with their large swath widths, short re-visit time and unprecedented spectral and spatial resolutions offers valuable cost-effective data for invasive alien species detection at both local and regional spatial extents.

## **1.2 Aim and objectives**

The aim of this study was to investigate the potential of image fusion between medium resolution optical remote sensing and Synthetic Aperture Radar imagery to reliably detect and map Bramble invasions within the uKhahlamba Drakensberg Park (UDP), KwaZulu-Natal, South Africa.

The objectives of the study were:

1. To evaluate the potential of freely available multispectral remote sensing imagery for detecting and mapping American Bramble (*Rubus cuneifolius*)
2. To determine the potential of fusing optical imagery and Synthetic Aperture Radar (SAR) imagery for American Bramble (*Rubus cuneifolius*) detection and mapping.
3. To investigate the capability of fused optical imagery and SAR polarization combinations and ratios to improve American Bramble (*Rubus cuneifolius*) detection and mapping
4. To determine the synergistic potential of Sentinel-2 optical imagery and S2 Vegetation Indices (VIs) in detecting and mapping the American Bramble (*Rubus cuneifolius*)

5. To determine the value of fusing Sentinel-2 Vegetation Indices (VIs) and Sentinel-1 Synthetic Aperture Radar (SAR) in detecting and mapping the American Bramble (*Rubus cuneifolius*), and
6. To determine the value of dual-polarized Sentinel-1 Synthetic Aperture Radar (SAR) fused with Sentinel-2 optical imagery for the American Bramble (*Rubus cuneifolius*) detection and mapping

### **1.3 Study area description**

The uKhahlamba-Drakensberg Park (UDP) covers approximately 2 428.13 km<sup>2</sup> within the KwaZulu-Natal (KZN) Province and is located at 29°12' 44" S; 29° 29' 11" E (Figure 1.2). Situated along the border of western Lesotho and eastern KZN, the UDP is predominantly a natural grassland with patches of bushland, native scrub vegetation and indigenous forests. Mean annual temperature in the area is approximately 16°C and annual precipitation ranges between 1000mm in the foothills and 1800mm at the escarpment (Tyson *et al.*, 1976). Annual average rainfall ranges from 990 mm to 1130 mm, with the area experiencing dry and cold winters and wet and humid summers (Nel *et al.*, 2004). The widespread distribution and infestation of American bramble (*Rubus cuneifolius*) has caused serious concerns on local biodiversity, land degradation and overall ecosystem functioning. Bramble has naturalized in localized patches of low to high cover while noticeable weed stands occupy vast areas within UDP natural grassland environment.

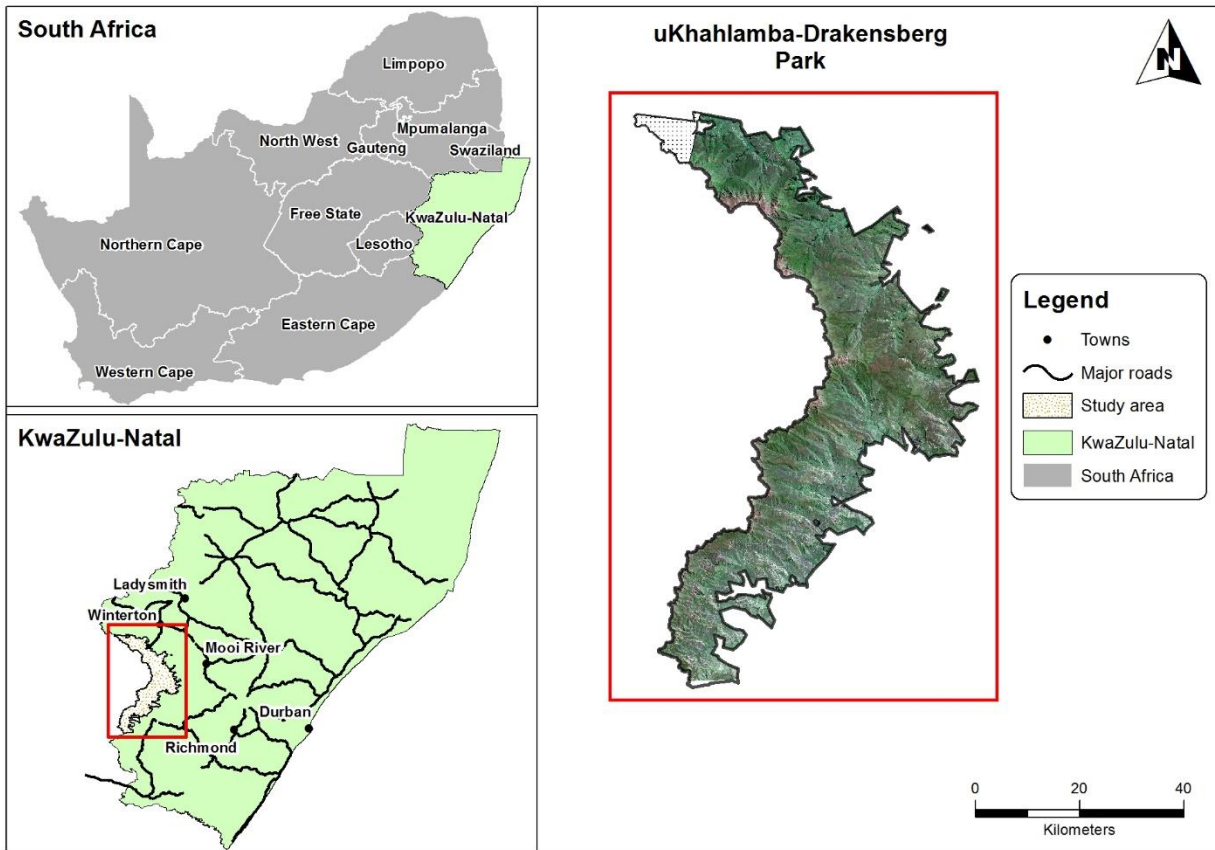


Figure 1.2: Location of the study area. The uKhahlamba-Drakensberg Park (UDP) is located within the KwaZulu-Natal midlands area, South Africa.

#### 1.4 Outline of the thesis

This thesis is presented as a set of research papers addressing each of the objectives listed in section 1.2. Two research papers have been published in peer-reviewed scientific journals while the remaining four papers are either in preparation or under review. Including the introduction and synthesis, this thesis consists of eight chapters.

Chapter Two assess the potential of freely available multispectral remote sensing imagery to detect and map the American Bramble from surrounding native vegetation. A comparison of classification accuracies was made between conventional Landsat 8 multispectral optical imagery and new-age Sentinel-2 multispectral optical imagery.

Chapter Three evaluates the potential of Sentinel-2 optical imagery fused with Sentinel-1 Synthetic Aperture Radar (SAR) imagery for Bramble detection and mapping. Feature level

image fusion in concert with the Support Vector Machine (SVM) algorithm are adopted to map Bramble infested areas.

Chapter Four uses the observations and conclusion in chapter three to test the synergistic potential of Sentinel-2 imagery and varying Sentinel-1 Synthetic Aperture Radar (SAR) polarizations. The concept of SAR polarization combinations/ratios is introduced, and the SVM algorithm used for multi-class classification. A comparison across fused S2 and S1 SAR band polarization combinations/ratios is used to select the optimum fusion between S2 and S1 polarizations.

Chapter Five assesses the synergistic potential of S2 optical bands and S2 derived Vegetation Indices (VIs). Using Variable Importance in the Projection (VIP), only the most influential S2 bands and VIs was selected for image fusion. Multi-class SVM was implemented in order to produce comparable seasonal confusion matrices. A comparison of seasonal results was conducted in order establish the optimum season for Bramble detection and mapping.

Chapter Six uses the observations and conclusion of Chapter Four to evaluate the utility of fused Sentinel-2 Vegetation Indices (VIs) and Sentinel-1 Synthetic Aperture Radar (SAR). This is done to determine if the synergistic power of S2 VIs and S1 SAR could increase overall detection and mapping accuracies of Bramble from surrounding native vegetation.

Chapter Seven introduces the concept of dual-polarized S1 Synthetic Aperture Radar (SAR) imagery. This chapter seeks to understand if S2 optical imagery fused with dual-polarized S1 SAR has the potential to increase detection and mapping accuracies of Bramble. Two combinations of dual-polarized imagery was used for separate fusion products and compared to conventional Sentinel-2 optical bands.

Finally, a synthesis of the study is given in Chapter Eight, where all findings and conclusions from the preceding chapters are summarized.

## Chapter Two

### Evaluating the potential of freely available multispectral remotely sensed imagery in mapping American bramble (*Rubus cuneifolius*)

This chapter is based on: Rajah, P., Odindi, J. and Mutanga, O., 2018: Evaluating the potential of freely available multispectral remotely sensed imagery in mapping American bramble (*Rubus cuneifolius*), *South African Geographical Journal*, 100,1-17.

#### Abstract

Globally, alien invasive plant species are considered a serious threat to native flora and fauna. In the eastern parts of South Africa, the American bramble (*Rubus cuneifolius*) has been identified as one of the major threats to social and ecological systems. Optimal management and mitigation of American bramble spread requires reliable and cost effective approaches to determine invaded spatial extents. In this study, we test the value of the recently launched, freely available Sentinel-2 (S2), as opposed to conventional Landsat 8 imagery in mapping the American bramble. Using the Support Vector Machine classification algorithm, we seek to identify the optimal season for mapping the American bramble as well as the most influential bands in the classification process. Results show that Sentinel-2 out-performed Landsat 8 in all seasons, with summer providing the highest classification accuracy (77% accuracy). The study also shows that strategically placed Sentinel-2 bands of Near Infrared, Red edge and Short Wave Infrared significantly contribute to an increase in overall bramble mapping accuracy. This study demonstrates the value of freely available multispectral imagery in mapping American bramble at large spatial extents, hence valuable for cost-effective operational use.

**Key words:** Support Vector Machine (SVM), American bramble, Multi-spectral remote sensing, Sentinel-2, Landsat 8, *Rubus cuneifolius*



## 2.1 Introduction

Alien plant invasions influence environmental change by adversely impacting ecological and socio-economic environments (Davies and Johnson, 2011; Rocchini *et al.*, 2015). Invasive alien plant species are detrimental to natural ecosystems by depleting natural capital and ecosystem services and often require significant resources for mitigation and restoration (Richardson and van Wilgen, 2004; Davies and Johnson, 2011). In South Africa, approximately ten million hectares have been invaded by alien invasive plants, threatening ecological resources and livelihoods (Nel *et al.*, 2005). Hence, methods that facilitate determination of their spatial extents are critical for mitigation of their spread and rehabilitation of invaded landscapes (Malanson and Walsh, 2013). Specifically, timely and cost-effective mapping of invasive species is valuable for the design and implementation of species-specific management and eradication strategies (Odindi *et al.*, 2016). Furthermore, reliable mapping of plant invasions can be useful for allocation of resources for management and rehabilitation (Masocha and Skidmore, 2011).

The American bramble (*Rubus cuneifolius*), a well-established alien invasive species in South Africa, has been identified as a major threat to native flora and fauna. The American bramble (hereafter referred to as Bramble) is a sprawling shrub species of the *Rosaceae* family found in diverse global climatic regions (Bromilow, 2010). Originating from North America, young Bramble canes (stems) are erect, but can bend over time with increased height. Bramble canes are characterised by downward curving thorns and trifoliolate leaves. Majority of these leaves are shed during autumn and winter. New leaves and lateral branches grow from canes during spring. The latter are vegetative and give rise to approximately 2-5 white flowers at the end of short leafy shoots, flowering from September to January annually (ATLAS, 2014). The species is believed to be one of the most devastating invasive plants in South Africa, particularly in the cool and moist KwaZulu-Natal mist-belt region (Erasmus, 1984). Bramble has significant adverse direct and indirect impacts on biodiversity, which include changes in nutrient cycling, increase in soil erosion, reduction in rangeland carrying capacity and viability, natural plant succession, fire patterns and behaviour and hydrological processes (Henderson, 2001).

Determination of an invasive species spatial extent is valuable for mitigation and rehabilitation of the invaded landscapes, as invasive alien species often degrade and compromise the natural state of landscapes (Bradley, 2014). Remote sensing technology provides an ideal opportunity to reliably detect, spatially monitor and map Bramble from surrounding native vegetation. Whereas the use of hyperspectral remotely sensed data for alien invasive detection and

mapping has been relatively successful in recent years (Ustin *et al.*, 2002; Underwood *et al.*, 2003; Tsai *et al.*, 2007 Kimothi *et al.*, 2010; Müllerova *et al.*, 2013; Nagendra *et al.*, 2013), adoption of hyperspectral imagery for regional mapping of alien invasive species remains a challenge. The reduced spatial extent (swath width) that characterises hyperspectral images require laborious mosaicking of multiple images for large-scale applications, which requires increased image pre-processing time as well as hardware and software capabilities. Furthermore, hyperspectral imagery is often not economically feasible, due to high cost per square kilometre and are characterised by high data dimensionality that require extensive processing and analytical skills. Similarly, whereas the application of new generation multispectral remotely sensed data (eg. World-View, Rapid Eye, IKONOS) for large scale alien invasive mapping has also been relatively successful (Kandwal *et al.*, 2009; Gil *et al.*, 2013; Robinson *et al.*, 2016), their high cost per unit area remains a major constraint.

To overcome the above-mentioned limitations, there has been an emergence of improved and freely available multispectral imagery for landscape mapping. The recently launched European Union's Sentinel-2 (S2) sensor under the Copernicus programme for instance, aims to provide freely available imagery for the entire globe as a continuation of the SPOT and Landsat missions' legacy (Hojas-Gascón *et al.*, 2015; Frampton *et al.*, 2013). The S2 carries a wide-swath (290km), medium to high resolution (10-20m), multi-spectral imager with 13 bands. These specifications are unprecedented and present a unique opportunity to gain new perspectives on medium to large-scale vegetation mapping (Immitzer *et al.*, 2016). The 13 spectral bands include three within the red-edge region, and two within the short-wave infrared region, strategically positioned for species level vegetation mapping (Cho *et al.*, 2012; Hedley *et al.*, 2012). However, whereas S2s relatively high spatial resolution, unique spectral configurations, wide swath width and five-day temporal resolution offer great potential in vegetation mapping (Ramoelo *et al.*, 2015; Hojas-Gascón *et al.*, 2015), S2s value in alien invasive plant mapping vis-à-vis the freely available Landsat 8 series has not been suitably examined.

The moderate temporal resolution that characterise freely available imagery such as S2 and traditional Landsat 8 (L8) facilitate multi-season analysis. According to Bradley (2014) and Haug and Asner (2009) the varying invasive species seasonal phenologies provide opportunities for reliable mapping. Denny (1990) notes that Bramble is characterised by varying phenological characteristics during its 18-month life cycle. Typically, new stems appear in October and grow rapidly until March, after which growth stops, with few leaves remaining until

the end of July. New leaves then appear in August, followed by flowers in September and fruiting development and ripening by January (Denny, 1990). This seasonal variability offers great potential for determination of the optimum season for Bramble detection and mapping.

Recently, robust machine learning algorithms like the Support Vector Machines (SVMs) have become popular within the remote sensing community. SVM is a supervised statistical learning technique first developed by Vapnik (1979) to deal with binary classifications and aims to find a hyper plane that divides the dataset into a discrete predefined number of classes consistent with training data (Mountrakis and Ogole, 2011). An optimum hyper plane is developed using training data sets and its generalisation capability is corroborated with test data sets (Kavzoglu and Colkesen, 2009). The overall performance of SVMs differs depending on the choice of kernel function and its parameters. Kernel functions act as an optimiser of the non-linear procedure to map the input data into high dimensional feature space while minimising over-fitting and other multi-dimensional problems commonly experienced with remote sensing data (Ramoelo *et al.*, 2015). Recent literature has shown that SVMs are capable of classifying numerous classes using limited support vectors as training samples, without compromising overall accuracies (Foody and Mathur, 2004; Mantero *et al.*, 2005; Bruzzone *et al.*, 2006; Shao and Lunetta, 2012; Zheng *et al.*, 2015). The characteristic thorny and thicket nature of the Bramble and prevalence on un-even mountainous terrain makes collection of training and validation data challenging. Hence, the insensitivity of SVM to training sample makes it ideal for the location chosen as the study area (Figure 2.1).

The launch of S2 provides an ideal platform for comparison with existing freely available, medium spatial resolution, wide swath-width imagery such as L8. We hypothesise that improvements in freely available S2 imagery could improve Bramble mapping, due to the collective effects of several strategically placed spectral bands and superior spatial resolution. Hence, this study aims to compare the performance of multi-seasonal L8 and S2 in discriminating and mapping the distribution the Bramble within a conserved environment.

## **2.2 Methodology**

### **2.2.1 Study area**

The study was conducted at the uKhahlamba Drakensberg Park (UDP), an official UNESCO world heritage site (GPS co-ordinates: -29.380018°S; 29.539746°E) along the western border of the KwaZulu-Natal province of South Africa (Figure 2.1). The UDP is considered one of the

most significant natural grasslands of South Africa (Everson and Everson, 2016). The UDP is managed by Ezemvelo KwaZulu-Natal Wildlife (EKZNW), a provincial conservation authority. Wet and humid conditions are experienced during summer (November to March) (Nel *et al.*, 2004), where rainfall ranges from 990-1130mm (Dollar and Goudy, 1999). Winters are dry and cold (May to August) with regular occurrences of snowfall and frost (Mansour *et al.*, 2012). Mean annual temperature in the area is approximately 16°C and annual precipitation ranges between 1000mm in the foothills and 1800mm at the escarpment (Tyson *et al.*, 1976). The landscape is predominantly natural grassland (wire grass (*Aristida purpurea*), weeping lovegrass (*Eragrostis curvula*) and common thatch grass (*Hyparrhenia hirta*) with patches of natural shrubs (*Erica spp.*) and thicket. Bramble is an emerging alien invasive plant species within the UDP and has already invaded a significant portion of the landscape (Bromilow, 2010). UDP climate provides adequate conditions for Bramble to thrive and spread.

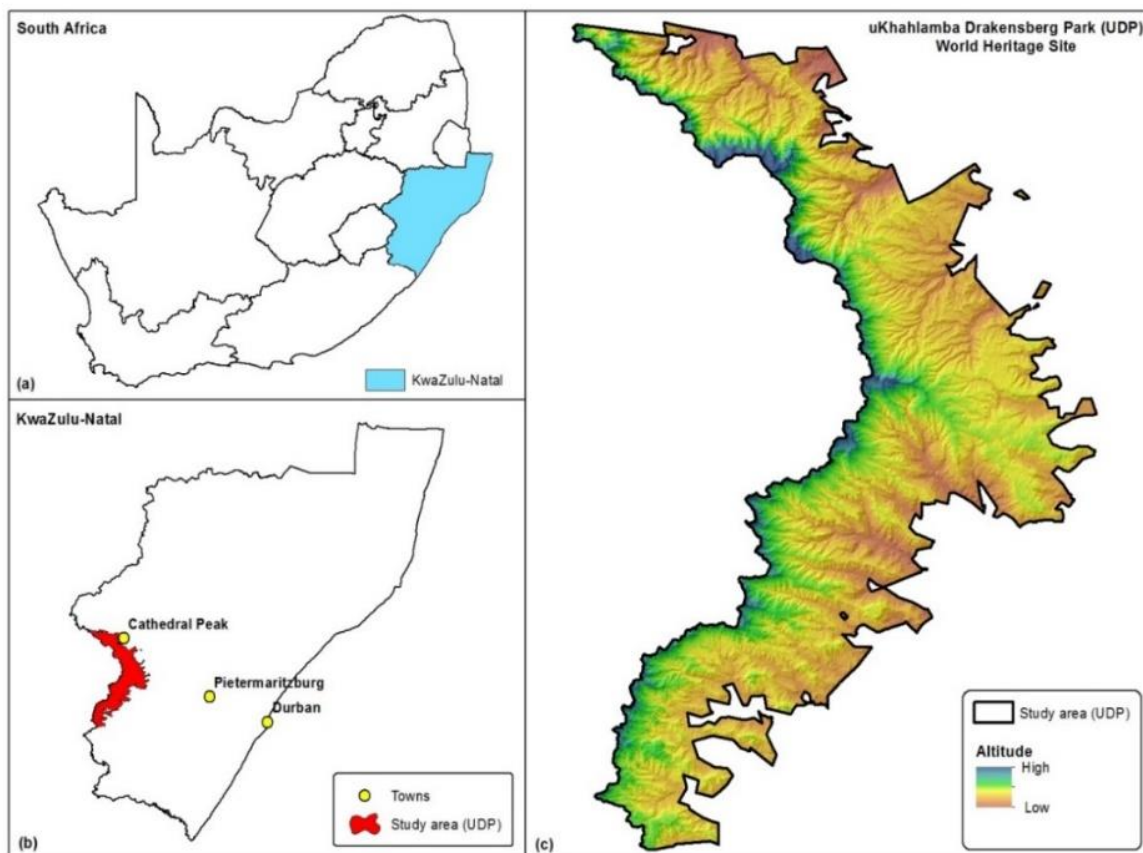


Figure 2.1: The study area (a and b) and the uKhahlamba Drakensberg Park (UDP) boundary (c).

## 2.2 Field data collection

Using a Trimble differentially corrected GeoXT handheld GPS receiver, field data points were collected based on purposive sampling (Wang *et al.*, 2012) during spring and summer, which coincides with Brambles flowering phenological stage (Table 2.1). Purposive sampling is the deliberate choice of a target species unique qualities. The technique is non-random and chosen individuals (ground truth points) are at the researcher's discretion. The approach was considered ideal due to the area's steep and mountainous terrain, hence restricted accessibility. Ground control points were collected as close as possible to the centre of Bramble patches. Patches of Bramble ranged from 15m x 15m to 50m x 50m (Figure 2.2),

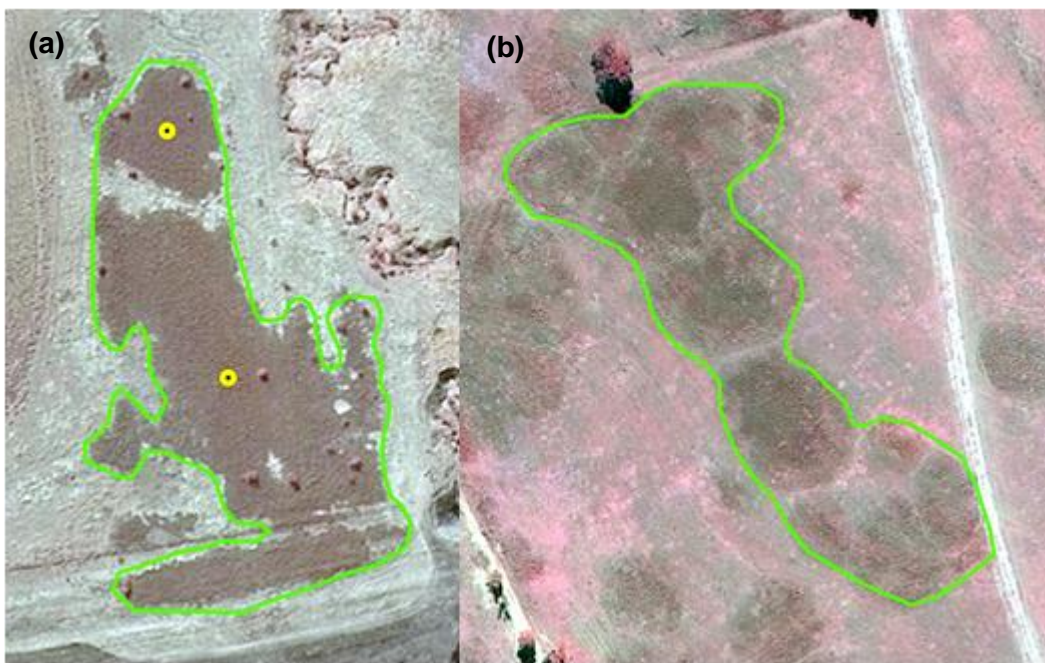


Figure 2.2: Examples of ground control Bramble patches collected via physical field work (a) and high resolution aerial photographs (b).

Ground control point data collected from Bramble patches were spatially independent, so as to compensate for the images spatial resolution. Spatial independence of ground control data ensured that each Bramble patch fell within a single image pixel and was associated with the unique spectral reflectance of that specific pixel. In addition, aerial photograph imagery collected in 2016, at a 0.5m spatial resolution was used to supplement and verify selected ground truth points.

Table 2.1: Life-cycle phenology of American bramble (*Rubus cuneifolius*).

	Jun	Jul	Aug	Sept	Oct	Nov	Dec	Jan	Feb	Mar	Apr	May	
	Winter		Spring			Summer			Autumn				
<b>Germination</b>				Green			Blue						
<b>Flowering (2-y-o)</b>						Blue		Green		Blue			
<b>Fruiting (1-y-o)</b>							Blue		Green		Blue		
<b>Tip rooting (1-y-o)</b>	Blue									Green			
<b>Dormancy</b>	Green												

\* Green shading indicates most common time frame for stage of life-cycle, however, each stage may still occur during blue shaded phases.

### 2.2.2 SVM classification

Cloud free L8 and S2 images were acquired for each season (summer, spring, autumn and winter). Landsat 8 imagery was converted from digital number (DN) to surface reflectance using the ArcMap 10.4 Landsat 8 DN to reflectance toolbox (Dilts, 2015). The Landsat 8 toolbox provides several basic pre-processing tools that allow functionality of remote sensing data within an ArcMap environment. One of the basic tools is the DN to reflectance tool, which converts raw Digital Number (DN) values to surface reflectance values. S2 imagery was converted from level-1C raw products (radiance) to level-2A products (surface reflectance) using the Sen2Cor plugin within the ESA SNAP toolbox 3.0 (SNAP - ESA Sentinel Application Platform). All images were corrected for topographic effects of shadow associated with mountainous areas using the SAGA (2.1.2) terrain analysis lighting tool within the Quantum GIS (QGIS) environment on a band by band basis. QGIS is GIS freeware and is the equivalent of ESRI ArcMap commercial GIS software. The System for Automated Geoscientific Analyses (SAGA) is a plugin that works in conjunction with QGIS and has numerous tools that automate analytical and pre-processing spatial algorithms (QGIS Development Team, 2016). The correction of topographic effects is one such tool, and was used to mitigate the topographic effects of shadow within the study area. Collected ground truth points ( $\approx 1000$ ) were used to extract spectra for the four land cover classes (Bare rock, Bramble, Forest and Grassland) considered in this study. Spectral reflectance values were extracted from L8 (30m resolution) and S2 (20m resolution) imagery using the ArcMap extract multi-values to points tool. In L8 images, spectra from the red, green, blue, near infrared (NIR), short wave infrared 1 (SWIR1) and shortwave infrared 2 (SWIR2),

were extracted while red, green, blue, near infrared (NIR), red edge 1 (RE1), red edge 2 (RE2), red edge 3 (RE3), shortwave infrared 1 (SWIR1) and shortwave infrared 2 (SWIR2) bands were extracted from the S2 images.

An optimal set of spectral bands, also known as band optimisation was determined for Bramble classification. Feature selection which recognised each spectral band as a feature which contributed to the overall accuracy of SVM classification accuracy was implemented using python to determine overall accuracy on a band by band basis. Overall accuracies for cumulative spectral bands were produced and the highest resulting accuracy was used for classification of the specific dataset. To optimise the SVM classification algorithm, a model tuning process was implemented within python to determine the best hyper-parameters for each season. The gamma range was 0.01 to 100, C range was 0.001 to 1000 and with four (linear, sigmoid, poly and rbf) kernel options. Optimum hyper-parameters derived from the SVM tuning process were then applied to the entire image based on results produced by the ground truth training spectra. Python 2.7.13 (van Rossum and Drake, 2012) was used to implement the SVM classification on all imagery and a one against all approach used to implement a multi-class classifier. A one against all approach isolates each class and is designed to separate the target class from the remaining classes. Ground control data were split into test (30%) and training data (70%) sets for SVM multi-class analysis. Pixels were classified into the areas dominant land-use-land-cover classes, i.e. Bare rock (1), Bramble (2), Forest (3), Grassland (4).

### 2.2.3 Mapping and map validation

Optimal hyper-parameters derived from tuning the SVM algorithm were used in conjunction with Python 2.7.13 to spatially determine the major land-use-land-cover classes within the study area. Extracted training pixel spectra (70%) of the four classes served as the input for seasonal Bramble spatial distribution maps, in relation to other land-use-land-covers for the two sensors. Seasonal SVM classification accuracy was assessed using respective test pixel spectra (30%) that produced a single confusion matrix for each satellite at each season.

## 2.3 Results

### 2.3.1 Optimum band selection and band identification

Optimum number of selected bands varied between L8 and S2, across all seasons. Winter L8 band selection produced the lowest (2) band selection across L8 seasonal imagery. Spring S2 imagery produced the lowest optimum band selection (4), while autumn had the highest (9). All seasons except winter resulted in consistent optimum bands of NIR, SWIR1 and SWIR2 for L8 imagery, with only winter analysis excluding the NIR as one of the influential bands (Table 2.2). Similarly, S2 placed importance on the NIR, SWIR1 and SWIR2 in all seasons. Additionally, S2 placed importance on the RE1, RE2 and RE3 bands in all seasons, except spring (Table 2.2).

Table 2.2: Bands identified for discrimination analysis (NIR = Near infrared; SWIR1= Shortwave infrared1, SWIR2= Shortwave infrared 2, RE1= Red edge 1, RE2= Red edge 2 and RE3= Red edge 3.

<b>Selected optimum bands</b>	
<b>Landsat 8</b>	
Summer	Blue, NIR, SWIR1, SWIR2
Spring	Green, Blue, NIR, SWIR1, SWIR2
Autumn	Green, Blue, NIR, SWIR1, SWIR2
Winter	SWIR1, SWIR2
<b>Sentinel-2</b>	
Summer	Green, Blue, NIR, RE1, RE2, RE3, SWIR1, SWIR2
Spring	NIR, RE3, SWIR1, SWIR2
Autumn	Red, Green, Blue, NIR, RE1, RE2, RE3, SWIR1, SWIR2
Winter	NIR, RE1, RE2, RE3, SWIR1, SWIR2

### 2.3.2 Multi-seasonal discrimination

Overfitting and over-estimation was observed for L8 spring imagery, as the SVM algorithm could not effectively discriminate between all classes (Table 2.3b). Similar to summer L8 results, users (45%) and producers (52%) accuracies were poor for Bramble, while Forest produced the highest users and producers accuracies (86% and 60%) (Table 2.3b). SVM optimal hyperparameters applied to the spring imagery over fitted for Bramble and under fitted for the Forest class (Figure 2.3c). Spring L8 SVM hyperparameters produced a lower overall accuracy (55%), as compared to summer (57%).



Table 2.3: Support vector machine confusion matrices showing users, producers and overall accuracy for all four seasons using Landsat 8 imagery. Where BR = Bare rock; BBL = Bramble; FR = Forest; GR = grassland; PA= Producers accuracy; OA= Overall accuracy and UA = Users Accuracy.

	BR	BBL	FR	GR	UA (%)	BR	BBL	FR	GR	UA (%)
	(a) Spring					(b) Summer				
<b>BR</b>	31	1	15	0	66	25	0	21	1	53
<b>BBL</b>	0	32	28	48	30	0	35	4	39	45
<b>FR</b>	1	4	73	0	94	11	0	67	0	86
<b>GR</b>	0	23	1	28	54	1	32	20	29	35
<b>PA (%)</b>	97	37	57	37		68	52	60	43	
<b>OA (%)</b>	<b>57</b>					<b>55</b>				
	(c) Autumn					(d) Winter				
<b>BR</b>	36	0	9	2	77	32	0	3	12	68
<b>BBL</b>	0	23	25	5	43	0	16	10	43	23
<b>FR</b>	0	0	77	1	99	7	0	49	2	84
<b>GR</b>	2	25	51	29	27	3	15	33	60	68
<b>PA (%)</b>	95	48	48	78		76	52	61	57	
<b>OA (%)</b>	<b>50</b>					<b>55</b>				

Spring S2 results produced improved overall classification accuracy (70%) (Table 2.4a), compared to L8 spring results (Table 2.3a). Bramble achieved the lowest users accuracy of all land cover classes (39%) and the second lowest producers accuracy of all land cover classes (68%) (Table 2.4a). Application of optimal spring hyper-parameters to spring S2 imagery resulted in a spatial distribution map which proved to satisfactorily (70%) predict all classes involved with minimal over-fitting of classes (Figure 2.3d).

Table 2.4: Support vector machine confusion matrices showing users, producers and overall accuracy for all four seasons using Landsat 8 imagery. Where BR = Bare rock; BBL = Bramble; FR = Forest; GR = grassland; PA= Producers accuracy; OA= Overall accuracy and UA = Users Accuracy

	BR	BBL	FR	GR	UA (%)	BR	BBL	FR	GR	UA (%)
	(a) Spring					(b) Summer				
<b>BR</b>	31	0	0	15	67	32	2	0	12	69
<b>BBL</b>	0	28	0	44	39	0	24	0	29	45
<b>FR</b>	0	0	56	3	94	1	1	54	3	91
<b>GR</b>	1	13	3	70	80	2	3	7	94	88
<b>PA (%)</b>	96	68	94	53		91	80	88	68	
<b>OA (%)</b>	<b>70</b>					<b>77</b>				
	(c) Autumn					(d) Winter				
<b>BR</b>	30	0	0	16	66	34	0	0	12	73
<b>BBL</b>	0	20	1	47	30	0	22	1	69	24
<b>FR</b>	1	0	55	3	93	1	0	53	5	89
<b>GR</b>	1	30	0	60	66	0	15	1	51	76
<b>PA (%)</b>	93	39	98	48		97	59	96	37	
<b>OA (%)</b>	<b>63</b>					<b>61</b>				

Summer L8 results showed unsatisfactory discrimination in all classes (Table 2.3a). The lowest producers accuracy was recorded for Bramble and Grassland classes while the highest producers accuracy was recorded for Bare rock (Table 2.3a). Overall summer classification accuracy was 57% and had the least overfitting and over-estimation, compared to other L8 seasons. Bramble spatial distribution was over estimated once the optimal summer SVM hyper-parameters were applied to the image, conversely, spatial distribution of grassland was under estimated (Figure 2.3a). Summer S2 classification accuracies were superior to L8 summer imagery (Table 2.2a and 2.3a). The use of optimal summer hyper-parameters on summer

imagery produced the highest overall accuracy (77%) for S2 across all seasonal imagery, with minimal over-overfitting (Figure 2.3b).

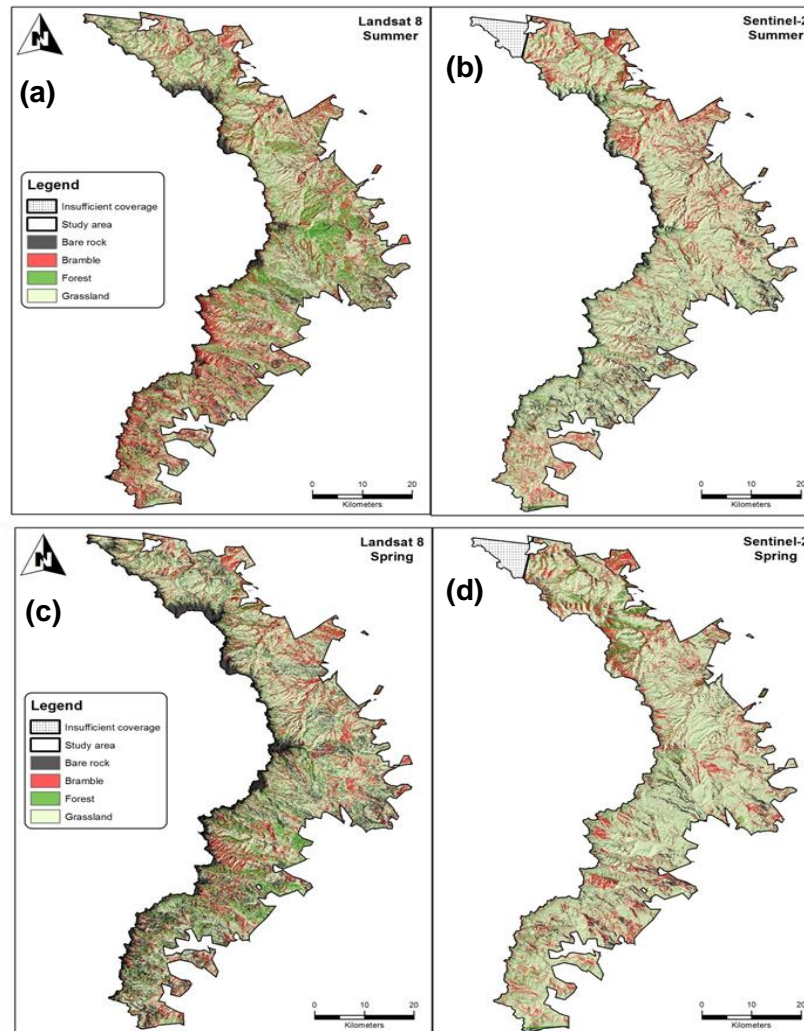


Figure 2.3: Summer and spring classification maps from Landsat 8 and Sentinel-2 imagery. Where (a) = Landsat 8 summer; (b) = Sentinel-2 summer; (c) = Landsat 8 spring and (d) = Sentinel-2 Spring.

Landsat 8 autumn results provided the lowest overall classification accuracy (50%) across all seasonal L8 imagery (Table 2.3c). Low producer accuracies were observed for Bramble (48%) and Forest (48%) (Table 2.3c). Autumn imagery resulted in the most over-fitted L8 spatial distribution map across all seasons, with Bramble being the most over-estimated class and Grassland being the most under-estimated class (Figure 2.4a). Sentinel-2 autumn results yielded the third highest overall accuracy across all seasonal imagery (Table 2.4c). Bramble

achieved the lowest users and producers accuracies. Although Sentinel-2 autumn imagery provided an overall accuracy of 63%, the classification and spatial distribution of Bramble and other surrounding classes were unsatisfactory.

Winter L8 results did not satisfactorily discriminate between Bramble and other land classes (Table 2.3d). Bramble achieved the lowest users and producers accuracies, whilst Bare rock achieved the highest producers accuracy and forest the highest users accuracy. Application of optimal SVM hyper-parameters to winter imagery resulted in overfitting (Figure 2.4c) and an over-estimation in the prediction of the spatial distribution of the Bramble and Forest classes. S2 winter imagery provided unsatisfactory discrimination between Bramble and Grassland classes (Table 2.4d). Application of optimal SVM winter hyper-parameters to S2 winter imagery resulted in an over-estimation of Bramble and underestimation of Grassland (Figure 2.4d), despite a 61% overall accuracy for winter SVM classification.

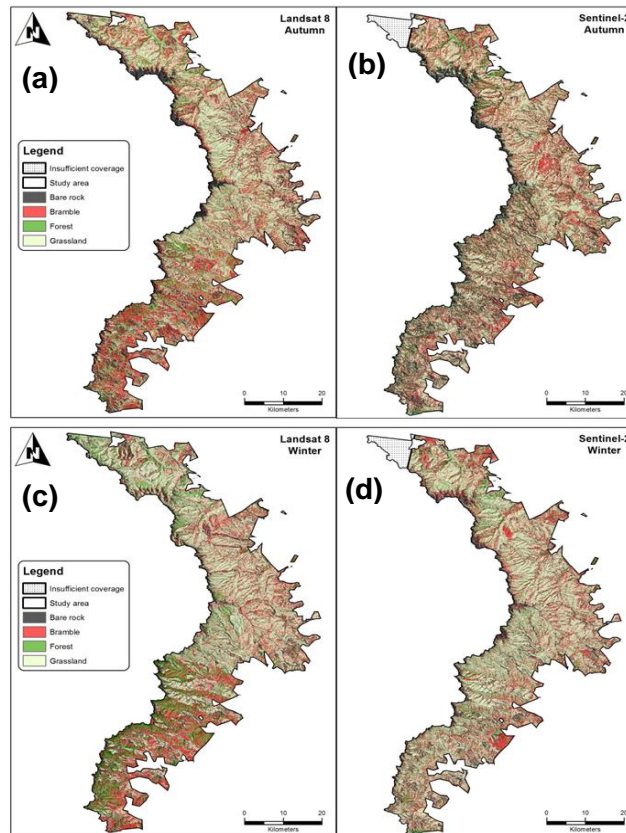


Figure 2.4: Autumn and Winter classification maps from Landsat 8 and Sentinel-2 imagery. Where (a) = Landsat 8 summer; (b) = Sentinel-2 summer; (c) = Landsat 8 spring and (d) = Sentinel-2 Spring.

## 2.4. Discussion

Generally, spatial distribution maps using L8 imagery resulted in inferior overall classification accuracies for Bramble. This can be attributed to overfitting when optimal SVM hyper-parameters were used on seasonal L8 imagery, likely due to L8s lower spatial resolution. The 30 meter L8 pixel is prone to the mixed pixel problem, as the dominant class has a major influence in the overall reflectance captured by the sensor. Consequently, smaller Bramble patches (less than 20m) were not easily distinguished as reflectance from the surrounding vegetation masked Bramble reflectance. This limitation is prevalent during the dry season, when both the Bramble and the surrounding vegetation senesce. The low Bramble classification accuracy using L8 could also be attributed to the sensors inability to differentiate the subtle spectral differences between Bramble and related land cover types like forest and grassland. However, despite these limitations, Bradley (2014) notes that results generated from medium resolution imagery such as L8 are useful in providing a preliminary understanding of a generalised landscape and regional invasion status and risk.

Despite the lower Bramble classification accuracies, the L8 summer imagery produced the highest classification accuracies, compared to spring, autumn and winter L8 imagery. According to Bradley (2014), this arises from the high variability in energy absorption or reflectance between target classes. The higher classification accuracy during spring can also be attributed to Bramble's distinct white inflorescence during the season (Denny, 1990), facilitating spectral discrimination from surrounding species. Autumn and winter produced the lowest classification accuracies. This finding is consistent with Shezi and Poona (2010), who found poor Bramble classification accuracies using SPOT 5 autumn and winter image data. Bramble and surrounding vegetation begin to senesce simultaneously during late autumn and winter (ATLAS, 2014), impeding their reliable delineation. Furthermore, this relative homogeneity compromises SVM performance by over-fitting when using autumn and winter imagery. According to Melgani and Bruzzone (2004), SVM was originally developed for binary classifications, Karimi *et al* (2006) notes that this reduces the complexity of the classification problem. Consequently, a binary classification of Bramble from surrounding native vegetation may have achieved better results than those achieved using multi-class SVM.

The S2 imagery produced improved Bramble discrimination results when compared to L8. The best seasons for discriminating Bramble from surrounding native vegetation were summer and spring. Several studies (e.g. Andrew and Ustin, 2008; Somodi *et al.*, 2012; Mirik *et al.*, 2013)

have attributed such increased discrimination capability to invasive plant species inflorescence during summer and spring. Within the study area, Bramble is predominantly surrounded by grassland vegetation such as wire grass (*Aristida purpurea*), weeping lovegrass (*Eragrostis curvula*) and common thatch grass (*Hyparrhenia hirta*) and several other native grass species which decreases potential spectral discrimination. In comparison to L8, S2's higher spatial resolution (20 meters) reduces the mixed pixel problem. Therefore, the adoption of S2 facilitated the detection and mapping of smaller Bramble patches that were otherwise undetectable due to the coarser spatial resolution of L8.

The S2's superior spectral resolution could be used to account for the improved classification accuracies. The red edge spectral region is widely recognised for vegetation discrimination (Cho and Skidmore, 2006). In consistency with Cho *et al* (2012) and Gilmore *et al* (2008), optimum band analysis in this study identified S2 red edge bands to be the most influential bands across all four seasons. This discriminatory power can be attributed to the region's sensitivity to Bramble's leaf chlorophyll, leaf structure and water content (Slaton *et al.*, 2001; Sims and Gamon, 2002; Shafri *et al.*, 2006; Gilmore *et al.* 2008). Unlike L8, S2 is characterised by three red edge bands, which could have contributed to the improved classification accuracy. These findings are consistent with Adelabu *et al* (2014), who noted a significant reduction in classification accuracy when red edge bands were excluded from classification.

Bramble is known to thrive in cool and moist conditions such as riparian zones (Erasmus, 1984). In addition to the value of the red edge section in vegetation mapping, the short wave infrared (SWIR) reflectance has been associated with foliar water content (Trombetti *et al.*, 2008; Yilmaz *et al.*, 2008). The increased number of S2 SWIR bands could explain the improved classification accuracy within the study area, as SWIR bands were important across all seasons. Numerous studies (e.g. Hauglin and Ørka, 2016; Gil *et al.*, 2013; Kimothi and Dasari, 2010) have validated the effectiveness of multispectral sensors for discriminating alien invasive species at a small scale. Results from this study indicate that applicable wide swath-width, new age multispectral imagery has the potential to provide an economically viable option for invasive alien detection and mapping at a large scale. This research targeted and mapped areas that were already heavily infested by Bramble, hence results are useful for implementing mitigation strategies as well as growing the knowledge base surrounding temporal and spatial patterns associated with Bramble infestations.

## 2.5. Conclusion

The aim of this study was to determine the potential of freely available satellite imagery to discriminate and map the spatial distribution of American bramble (*Rubus cuneifolius*) in UDP. Results from this study indicate that S2 imagery, characterised by more strategically positioned bands like the NIR, Red edge and SWIR bands, provides a cost effective means of determining Bramble's spatial distribution. Sentinel-2 outperformed L8 in discriminating and mapping Bramble spatial distribution within the UDP. Multi-season analysis of satellite imagery indicated that the optimum season for Bramble detection and mapping is either spring or summer. The superior performance of S2 over L8 can be attributed to its increased spectral resolution and strategically placed bands as well as its increased spatial resolution. This finding promotes S2 imagery as a viable option to existing freely available wide-swath multispectral imagery for invasive species mapping.

## Chapter Three

### Feature level image fusion of optical imagery and Synthetic Aperture Radar (SAR) for invasive alien plant species detection and mapping

**This chapter is based on:** Rajah, P., Odindi, J. and Mutanga, O., 2018. Feature level image fusion of optical imagery and Synthetic Aperture Radar (SAR) for invasive alien plant species detection and mapping. *Remote Sensing Applications: Society and Environment*, 10, 198-208.

#### Abstract

Invasive alien plant species are regarded as a major threat to among others socio-economic systems, global biodiversity and conservation initiatives. A reliable understanding of their spatial and temporal distribution is paramount for understanding their impact on co-existing landscapes and ecosystems. While traditional passive remote sensing methods have been successful in assessing invasion of such species, limiting factors such as cost, restricted coverage, image availability, terrain and inadequate resolutions hamper mapping and detection at large spatial extents. To date, the adoption of active remote sensing techniques as complimentary data to invasive alien plant mapping has been limited. In this study, we fuse two commonly used medium spatial and spectral resolution imagery (Sentinel-2 and Landsat 8) with active remote sensing data (Synthetic Aperture Radar imagery) in determining the optimal season for detecting and mapping the American Bramble (*Rubus cuneifolius*). Feature level image fusion was adopted to integrate passive and active remote sensing imagery and Support Vector Machine (SVM) supervised classification algorithm used to discriminate the American Bramble from surrounding native vegetation. Seasonal results showed that Sentinel-2 data, fused with SAR data generated the highest classification accuracy during summer (76%), while Landsat 8 imagery fused with SAR data performed best in winter (72%). These findings demonstrate that fusion of SAR with traditional optical imagery can be used to detect and map the American Bramble at a regional scale. We conclude that SAR data can be used synergistically with optical remote sensing to improve discrimination and mapping of the American Bramble.

Key words: Invasive alien plant species; Remote sensing; Synthetic Aperture Radar (SAR); Sentinel-2; American Bramble, Multisensor image fusion



### 3.1 Introduction

The range and spatial extent of invasive alien plant species are important variables influencing ecosystem health and biodiversity. According to Ghulam *et al* (2011), the robust natures of invasive alien plant species provide a competitive advantage for already limited resources. Commonly, absence of limiting factors leads to abundant growth and increase in spatial extent, which negatively affects local and regional landscape productivity and biodiversity (Dornelas, 2010). Understanding the severity and extent of invasion is crucial for assessment of potential impacts on the landscape, ecosystem services and mitigation (Bourgeau-Chavez *et al.*, 2013). Traditional field based methods of monitoring the extent and spread of invasive alien plant species are limited by their time consuming and laborious data collection, hence limited to small scale studies. Adoption of these approaches are also limited by their high cost and physical barriers that constrain accessibility (Bradley, 2014; Müllerová *et al.*, 2013). Other approaches like use of aerial photographs have a high cost per unit area and are unsuitable for digital analysis.

To date, the adoption of passive remote sensing imagery for invasive alien plant species mapping has significantly become popular (Gil *et al.*, 2013; Müllerová *et al.*, 2013; Bradley, 2014; Kandwal *et al.*, 2009; Tsai *et al.*, 2007). Although such imagery are known to yield reliable spatial distribution maps (Walsh, 2018; Niphadkar *et al.*, 2017; Bradley, 2014), their cost are of a major concern particularly for regional scale mapping. Furthermore, their limited swath width, cloud cover and spatial resolution remain key limiting factors for invasive alien plant species mapping. The advent of freely available sensors, with large swath widths and higher temporal resolutions (e.g. Landsat 8 and Sentinel-2) present unique opportunities for cost-effective and practical multi-season invasive alien plant species mapping at large spatial extents.

In addition to exploitation of improved spatial and spectral resolution in vegetation mapping, Oldeland *et al* (2010) and Zhang *et al* (2008) noted that recent studies have sought to exploit additional factors such as species specific reflectance variability resulting from multi-temporal phenological evolution. Generally, multi-season invasive alien plant species mapping depends on a combination of factors that include biophysical and biochemical properties of target invaders relative to indigenous species, their spatial extent and pattern of dispersal and spatial resolution of imagery used (Dorigo *et al.*, 2012). Invaders have often distinct phenological characteristics from resident species, which enables them to exploit ecological niches better within their invasive range. According to McNairn *et al* (2009), seasonal phenological

fluctuations in leaf pigmentation, water content and structure impact reflectance and backscatter measurements. Such variabilities offer great potential for detecting and mapping invasive alien plant species using remotely sensed data (Bradley, 2014). These characteristics, in addition to Landsat 8 and Sentinel-2's shorter re-visit times, allow for repeat image acquisition, valuable for multi-season analysis.

Recently, active remote sensing has shown great potential as a complementary data source to optical remotely sensed imagery. Synthetic Aperture Radar (SAR) in particular offers detailed information on the often difficult to detect characteristics of the surface target such as shape, moisture and roughness (Chen *et al.*, 2010). However, despite this potential previous adoption of SAR imagery in invasive alien plant species, mapping has been limited by high acquisition cost, limited area coverages and complex data pre-processing and processing (McNairn *et al.*, 2009). The recent launch of Sentinel-1, a joint initiative between the European Commission (EC) and the European Space Agency (ESA) and the subsequent provision of its free SAR data provides new opportunities for mapping invasive alien plant species. Sentinel-1 has up to 400kms swath-width and is equipped with a C-band SAR sensor operating in four exclusive imaging modes (Sentinel-1 User handbook, 2013). SAR data can operate at wavelengths regardless of cloud conditions or lack of illumination and is capable of acquiring data during day and night (Sentinel-1 User handbook, 2013).

The complementarity between SAR and optical multi-spectral imagery has great potential in remote sensing applications. For example, multispectral images possess surface information on reflectance and emissivity characteristics, while SAR images capture the structure and backscatter dielectric properties of earth surface materials (Zhu *et al.*, 2012). According to Zhang (2010) such complementarity, achieved through data fusion can be used to improve interpretation of source data. Additional data fusion benefits include improved output reliability, decreased uncertainty surrounding target features with similar spectral reflectance and improved delineation classification performance (Gharbia *et al.*, 2014). According to Le Hegarat-Masclé *et al* (2000), both optical and SAR imagery use their complementarities to reduce confusion through their description of target features, reducing imprecision and classification errors.

Despite these potential benefits, very few studies have used multispectral imagery fused with SAR imagery to map alien invasive plant species. In a recent review for instance, Peerbhay *et al* (2016) identified a gap in literature on the use of fused SAR and optical imagery in invasive

alien plant mapping. As aforementioned, combining optical and SAR imagery allows for the measurement of reflectance of both canopy layer (optical imagery) and geometric information (SAR imagery) of vegetation cover (Vaglio *et al.*, 2013). SAR sensors collect backscatter measurements in Decibels (dB), which are dependent on the roughness, geometry and content of the target object (Hong *et al.*, 2014). Optical imagery on the other hand provides suitable and interpretable imagery for classification of broad vegetation classes. Complementarity of the two datasets increases the delineation variables, allowing for a more detailed vegetation characterisation (Sameen *et al.*, 2016; McNairn *et al.*, 2009; Hong *et al.*, 2014). It is this complementary nature of optical and SAR imagery that could serve to better discriminate bramble from surrounding native vegetation upon image fusion.

Image integration, based on fusion levels, can be broadly grouped into three; pixel-level, feature level and decision level (Hong *et al.*, 2014). In this study, feature level fusion was adopted. The approach is an intermediate of image fusion, referring to the merging of measured physical parameters, but ensures minimal loss of information in the fused images (Pandit and Bhiwani, 2015). Feature level fusion involves observation of an object and feature extraction to yield a feature vector for respective sensor (Zeng *et al.*, 2006). Feature level fusion was adopted in this study as it is less stringent to sensor alignment compared to other fusion techniques. Additionally, feature level fusion achieves a considerable compression of information and is highly conducive to efficient real-time remote sensing imagery processing (Joshi *et al.*, 2016; Solberg, 2006). Feature vectors are then fused and identification is made based on the combined joint feature vector received from combined optical and SAR imagery. Accordingly, this study sought to determine the efficacy of multi-source remote sensing data fusion by utilizing Landsat 8 and Sentinel-2 (S2) optical imagery fused with Sentinel-1 Synthetic Aperture Radar (SAR) imagery to detect and map the spatial distribution of the American Bramble (hereafter referred to as Bramble)

## **3.2 Methodology**

### **3.2.1 Study area**

This study was conducted at the uKhahlamba Drakensberg Park (UDP) (Figure 3.1), considered one of the most important natural grasslands of South Africa (Everson and Everson, 2016). The UDP is a UNESCO world heritage site located on the western border of the KwaZulu-Natal

province of South Africa. The landscape is dominated by natural grassland with patches of natural shrubs and thicket. Winters are cold and dry with frost and snow experienced regularly (Mansour *et al.*, 2012). Summers are humid and wet, with rainfall ranging from 990-1130mm (Dollar and Goudy, 1999).

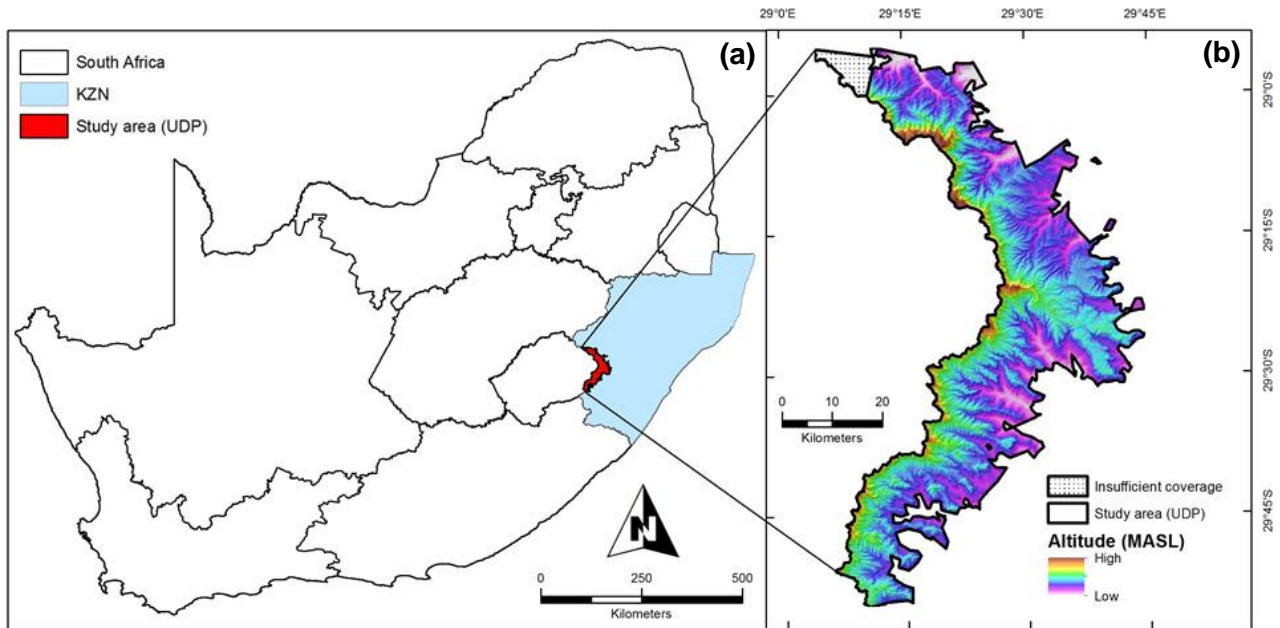


Figure 3.1: The location of the Kwazulu-Natal (KZN) province within South Africa (a). Extent of the uKhahlamba Drakensberg Park (UDP), illustrating altitude as meters above sea level (b).

### 3.2.2 Target species

American Bramble (*Rubus cuneifolius*) has been identified as a major threat to native flora and fauna. A sprawling shrub species belonging to the *Rosaceae* family, Bramble is known to thrive in a diverse range of habitats (Bromilow, 2010). Originally from North America, it is believed to be one of the most harmful invasive alien plants in South Africa, particularly within the Kwazulu-Natal (KZN) province, where the cool and moist climatic conditions favour its proliferation (Erasmus, 1984). Bramble's thorny stems and growth in bush clumps are directly responsible for adverse effects on biodiversity. Henderson *et al* (2001) identified reduction in a landscape's carrying capacity, alterations in nutrient cycling, increased soil erosion, changes in fire regimes and behaviour and the disruption of hydrological process as some of the specie's adverse effects. Hence, Bramble's effective management or eradication is of paramount importance to landscape productivity and sustainability.

### 3.2.3 Field data collection

Purposive sampling technique was used to collect ground truth land-cover data during spring and summer of 2016. These seasons were chosen as Bramble patches are easily discernible from surrounding vegetation during these periods. A Trimble differentially corrected GeoXT GPS was used to record Bramble patches and surrounding vegetation classes. Bramble ground control points were recorded as close to the centroid of Bramble patches as possible. In order to compensate for spatial resolution of satellite imagery, and to ensure that Bramble patches fell within image pixels and could be associated with the unique spectral reflectance, spatially independent ground truth Bramble patches ranging from 15m x 15m to 50m x 50m were collected. In this regard, a Bramble ground truth point was only collected if it was located more than one-pixel space away from the next Bramble patch, hence ensuring spatial independence. Due to the area's steep and mountainous terrain, hence restricted accessibility, only Bramble patches that could be accessed by foot were considered for the study. Aerial photographs of 0.5m spatial resolution captured in 2016 were also used to supplement and verify selected land-cover ground truth points. A total of 1000 ground truth points were collected and used in the study.

### 3.2.4 Image acquisition

#### 3.2.4.1 Optical imagery

Multi-season (summer, autumn, winter and spring) Landsat 8 imagery (Table 3.1) was acquired and converted from digital number (DN) to surface reflectance using the ArcMap 10.4 Landsat 8 DN to reflectance toolbox. The Landsat 8 toolbox provides several basic pre-processing tools that allow processing of remote sensing data within an ArcMap environment. The DN to reflectance tool converted raw Digital Number (DN) values to surface reflectance using Dark Object Subtraction 1 (DOS1) atmospheric correction. The ESA SNAP toolbox 3.0 was used to convert seasonal Sentinel-2 level-1C raw products (Table 3.1) to surface reflectance via the Sen2Cor plugin. Sen2Cor implements Sentinel-2 Atmospheric Correction (S2AC), which performs atmospheric correction based on the LIBRADTRAN radiative transfer model (Richter *et al.*, 2011; Mayer and Kyling, 2000). Both Landsat 8 and Sentinel-2 images were corrected for topographic effects of shadow associated with mountainous areas. Topographic correction was performed using the System for Automated Geoscientific Analyses SAGA (2.1.2) terrain analysis lightening tool within a Quantum GIS (QGIS) environment. The terrain analysis lightening tool topographically corrected all images using the Minnaert Correction method, a

method which considers satellite azimuth and height. QGIS is GIS freeware and is comparable to ESRI ArcMap commercial GIS software. SAGA is a plugin that works in conjunction with QGIS.

Table 3.1: Image acquisition dates for individual optical and SAR imagery

<b>Season</b>	<b>*Landsat 8 image acquisition date</b>	<b>*Sentinel-2 image acquisition date</b>	<b>*Sentinel-1 (SAR) image acquisition date</b>
<b>Summer</b>	01/01/2017	19/01/2017	06/01/2017
<b>Autumn</b>	06/05/2016	14/04/2016	11/05/2016
<b>Winter</b>	09/07/2016	23/06/2016	22/07/2016
<b>Spring</b>	30/11/2016	01/09/2016	07/11/2016

\*Image acquisition dates based on southern hemisphere seasonal variability

#### 3.2.4.2 SAR imagery

Sentinel-1 is a phase-preserving dual polarisation SAR system. It can transmit a signal in either horizontal (H) or vertical (V) polarisation, and then receive in both H and V polarisations. Dual polarisation Level-1 Single Look Complex (SLC) products contain complex values. In addition to the backscatter intensity that can be measured from each single polarisation, the inter-channel phase information allows for analysis of backscattering properties. Hence, the inclusion of polarisation acquisition modes in Sentinel-1 SAR data allows for additional variables to be evaluated (Beyer, 2015; Vyjayanthia and Nizalapur, 2010). As backscatter is heavily dependent on the geometric structure of the target object, varying polarisations of SAR imagery fused with optical imagery could improve alien invasive plant mapping. Cross-polarised SAR backscatter measurements differ from co-polarised measurements as the former is more sensitive to vegetation volume (Srivastava *et al.*, 2009). Consequently, Huang *et al* (2015) notes that cross polarised SAR data is better adapted to detect sparse vegetation, as compared to shorter wavelength co-polarised SAR data.

Multi-season Synthetic Aperture Radar (SAR) images were downloaded from the Sentinel-1 data hub. Sentinel-1 level-1 Ground Range Detected (GRD) products were utilised for this study. Level-1 GRD products were multi-looked and projected to ground range using an earth ellipsoid model. The products were acquired using the Interferometric Wide Swath (IW) mode, and had a spatial resolution of 20 meters with a 250km<sup>2</sup> swath width. SAR imagery was pre-

processed using the ESA SNAP toolbox following the methodology outlined in Bevington (2016). The Bevington (2016) SAR image processing chain consisted of five steps: (1) Application of orbit file to SAR image; (2) Radiometric calibration; (3) Terrain correction; (4) Application of speckle filter; (5) Convert SAR DN to Gamma backscatter values. SAR imagery in both Vertical Horizontal (VH) and Vertical Vertical (VV) polarisation modes were fused with optical imagery to determine the influence of SAR cross-polarisation on overall seasonal discrimination accuracies, in comparison to co-polarised SAR.

### 3.2.5 Data fusion

As aforementioned, the feature level approach was used to fuse optical and SAR imagery. Multi-season SAR images were resampled to 30 meter (Landsat 8) and 20-meter spatial resolution (Sentinel-2). An illustration of the steps followed to ensure feature level data fusion is shown in Figure 3.2.

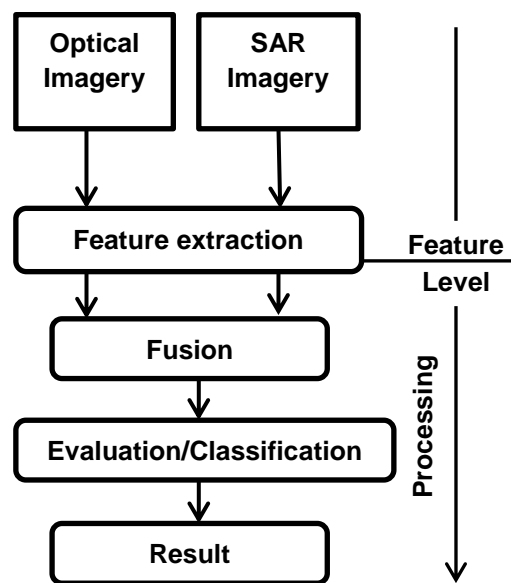


Figure 3.2: Feature level fusion processing chain.

Extraction of features (ground truth points) were done separately for optical imagery (spectral reflectance measurements) and SAR imagery (backscatter measurement). Corresponding backscatter measurements were assigned to the corresponding extracted spectral reflectance measurement. The composite band tool was used to fuse optical and SAR imagery at a feature level within an ArcMap 10.4 environment. This was achieved by stacking optical and SAR imagery on a band by band basis, creating a composite (fused) image containing both spectral

reflectance and backscatter measurements. The fused spectral measurement and backscatter data was then used for image classification analysis.

### 3.2.6 Image classification

Fused spectral reflectance with SAR backscatter measurements were extracted and classified using SVM algorithm. SVM is a supervised statistical learning technique first developed by Vapnik (1979) to deal with binary classifications. The algorithm aims to find a hyper-plane that divides the dataset into a discrete predefined number of classes consistent with training data (Mountrakis *et al.*, 2010). Studies have demonstrated that SVMs are proficient in classifying several classes using limited support vectors as training samples, without compromising overall accuracies (Foody and Mathur, 2004; Mantero *et al.*, 2005; Bruzzone *et al.*, 2006; Shao *et al.*, 2012; Zheng *et al.*, 2015). Collected ground truth points were used to extract spectra for the four major land cover classes (Bare rock, Bramble, Forest and Grassland) in the study area.

### 3.2.7 Spatial distribution maps and validation

Python 2.7.13 was used to generate a SVM classification map of the four major land cover classes considered in this study. Fused (optical and SAR) training pixel spectra (70%) of all four classes served as the input for multi-season Bramble spatial distribution maps. Multi-season classification accuracy was assessed using the respective fused test pixel spectra (30%).

## 3.3 Results

### 3.3.1 Seasonal comparisons of Bramble infestations in relation to other landcovers

#### 3.3.1.1 Summer

Summer L8 results for VH and VV SAR polarisations (Figure 3.3a and b) overall accuracies were 65% and 68% respectively (Table 3.2a and b). Users and producer's accuracies for fused L8 and VH SAR imagery were low for Bramble (53% and 55%, respectively). The Summer L8 VV fused imagery resulted in a 64% producers and a 57% user's accuracy for Bramble. Sentinel-2 results for VH and VV SAR polarisations (Figure 2.3c and d) had overall accuracies of 76% (Table 3.2c and d). Bramble users and producer's accuracies improved for both S2 VH (from 70% and 71%) and S2 VV (from 72% to 73%) fused imagery as compared to L8 fused imagery. Summer analysis between SAR polarisations resulted in L8 VV outperforming L8 VH



by 3%. There was however no difference in the overall accuracy achieved using fused L8 VH and L8 VV images.

Table 3.2: Summer confusion matrices of VH and VV fused polarisation for Landsat 8 and Sentinel-2. Where BR = Bare rock; BBL = Bramble; FR = Forest; GR = grassland; PA= Producers accuracy; OA= Overall accuracy and UA = Users accuracy

<b>L8 Summer</b>	<b>BR</b>	<b>BBL</b>	<b>FR</b>	<b>GR</b>	<b>UA (%)</b>	<b>BR</b>	<b>BBL</b>	<b>FR</b>	<b>GR</b>	<b>UA (%)</b>
	(a) VH					(b) VV				
<b>BR</b>	28	0	7	9	64	25	3	6	10	57
<b>BBL</b>	0	28	13	12	53	0	30	9	14	57
<b>FR</b>	0	8	38	3	78	0	4	40	5	82
<b>GR</b>	0	15	7	46	68	0	10	7	50	75
<b>PA (%)</b>	100	55	58	66		100	64	65	63	
<b>OA (%)</b>	<b>65</b>					<b>68</b>				
<b>S2 Summer</b>	(c) VH					(d) VV				
<b>BR</b>	33	0	4	9	72	31	0	5	10	67
<b>BBL</b>	0	37	3	13	70	0	38	3	12	72
<b>FR</b>	1	2	42	4	88	0	1	43	5	88
<b>GR</b>	0	13	3	52	76	0	13	2	53	78
<b>PA (%)</b>	97	71	81	67		100	73	81	66	
<b>OA (%)</b>	<b>76</b>					<b>68</b>				

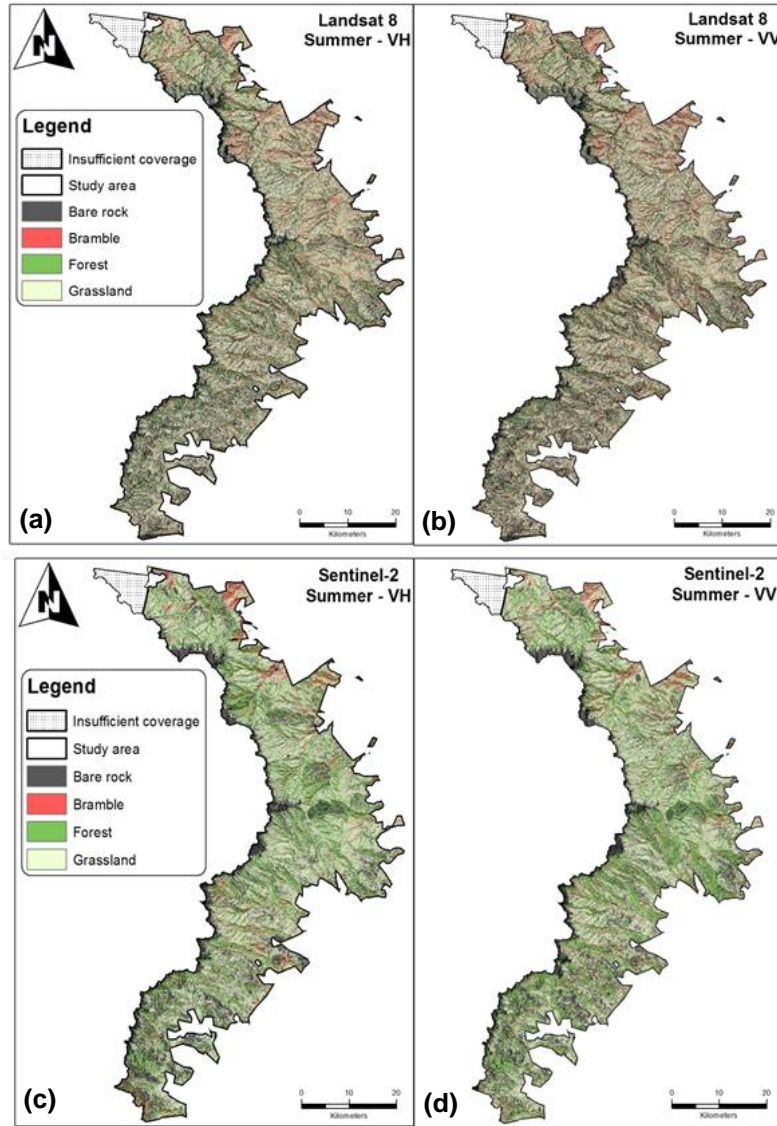


Figure 3.3: Summer spatial distribution maps for fused Landsat 8 and Sentinel-2 VH and VV polarisations. Where (a) = Landsat 8 (VH); (b) = Landsat 8 (VV); (c) = Sentinel-2 (VH) and (d) = Sentinel-2 (VV).

### 3.3.1.2 Autumn

Fused L8 autumn overall accuracies ranged from 71% (VH) to 66% (VV) (Figure 3.4a and b). However, user's and producer's accuracies for autumn L8 VH and L8 VV resulting from Bramble were the lowest across all land-cover classes (Table 3.3a and b). S2 VH and S2 VV fused imagery achieved superior overall accuracies as compared to L8 VV imagery (Figure 3.4c and d), while S2 VH imagery achieved similar overall accuracy to L8 VH imagery (Table 3.3a, b, c

and d). Bramble user's and producer's accuracies S2 VH (57% and 63%) and S2 VV (58% and 60%) imagery surpassed those achieved using L8 fused imagery (Table 3.3a, b, c and d).

Table 3.3: Autumn confusion matrices for VH and VV fused polarisation for Landsat 8 and Sentinel-2. Where BR = Bare rock; BBL = Bramble; FR = Forest; GR = grassland; PA= Producers accuracy; OA= Overall accuracy and UA = Users accuracy.

<b>L8 Autumn</b>	<b>BR</b>	<b>BBL</b>	<b>FR</b>	<b>GR</b>	<b>UA (%)</b>	<b>BR</b>	<b>BBL</b>	<b>FR</b>	<b>GR</b>	<b>UA (%)</b>
	(a) VH					(b) VV				
<b>BR</b>	34	3	1	7	76	33	0	5	6	75
<b>BBL</b>	0	28	10	15	53	0	18	19	16	34
<b>FR</b>	1	3	44	1	90	1	2	43	3	88
<b>GR</b>	0	15	5	48	71	0	10	10	48	71
<b>PA (%)</b>	97	57	73	68		97	60	56	66	
<b>OA (%)</b>	<b>71</b>					<b>66</b>				
<b>S2 Autumn</b>	(c) VH					(d) VV				
<b>BR</b>	30	3	1	12	65	30	4	2	10	65
<b>BBL</b>	0	30	8	15	57	0	31	7	15	58
<b>FR</b>	1	2	45	1	92	1	2	42	4	86
<b>GR</b>	1	13	4	50	74	1	15	4	48	71
<b>PA (%)</b>	94	63	78	64		94	60	76	62	
<b>OA (%)</b>	<b>71</b>					<b>70</b>				

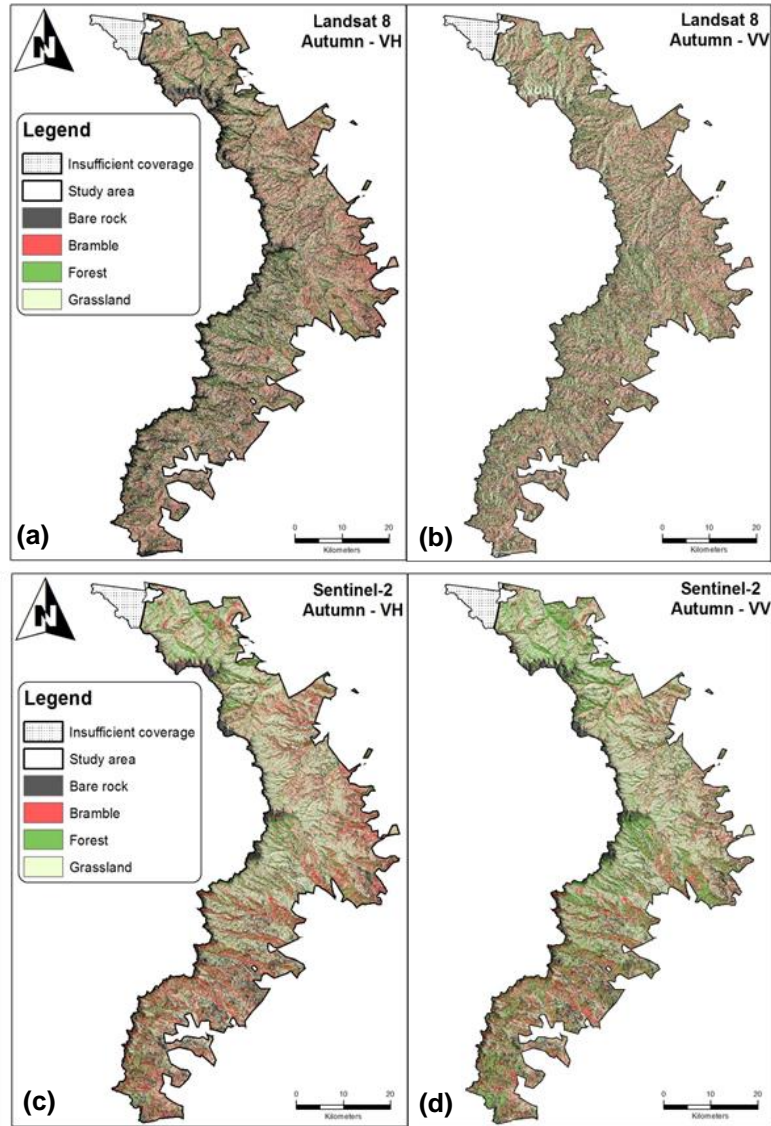


Figure 3.4: Autumn spatial distribution maps for fused Landsat 8 and Sentinel-2 VH and VV polarisations. Where (a) = Landsat 8 (VH); (b) = Landsat 8 (VV); (c) = Sentinel-2 (VH) and (d) = Sentinel-2 (VV).

### 3.3.1.3 Winter

L8 VH fused imagery produced an overall accuracy of 72%, hence outperformed L8 VV fused imagery (Figure 3.5a and b) (overall accuracy of 64%) (Table 3.4a and b). Bramble user's and producer's accuracies were among the lowest of all the land cover classes (Table 3.4a and b) using L8 fused imagery. S2 fused imagery across both polarisations achieved higher overall accuracies (Figure 3.5c and d) as compared to L8 fused images. Sentinel-2 VH fused imagery produced an overall accuracy of 76%, while S2 VV fused imagery produced an overall accuracy

of 71% (Table 3.4c and d). S2 VH and S2 VV Bramble users and producer's accuracies were higher than those recorded by L8 fused imagery.

Table 3.4: Winter confusion matrices for VH and VV fused polarisation for Landsat 8 and Sentinel-2. Where BR = Bare rock; BBL = Bramble; FR = Forest; GR = grassland; PA= Producers accuracy; OA= Overall accuracy and UA = Users accuracy.

<b>L8 Winter</b>	<b>BR</b>	<b>BBL</b>	<b>FR</b>	<b>GR</b>	<b>UA (%)</b>	<b>BR</b>	<b>BBL</b>	<b>FR</b>	<b>GR</b>	<b>UA (%)</b>
	(a) VH					(b) VV				
<b>BR</b>	29	6	2	9	63	27	4	5	8	61
<b>BBL</b>	1	34	2	16	64	3	20	88	22	38
<b>FR</b>	0	3	45	1	92	0	4	44	1	90
<b>GR</b>	3	14	2	45	70	3	10	9	46	68
<b>PA (%)</b>	88	60	88	63		82	29	67	60	
<b>OA (%)</b>	<b>72</b>					<b>64</b>				
<b>S2 Winter</b>	(c) VH					(d) VV				
<b>BR</b>	35	4	1	6	76	35	2	2	6	78
<b>BBL</b>	1	35	2	15	66	1	25	8	17	49
<b>FR</b>	1	3	45	0	92	1	4	43	1	88
<b>GR</b>	7	9	2	48	73	5	8	6	48	72
<b>PA (%)</b>	80	69	90	70		83	64	73	67	
<b>OA (%)</b>	<b>76</b>					<b>71</b>				

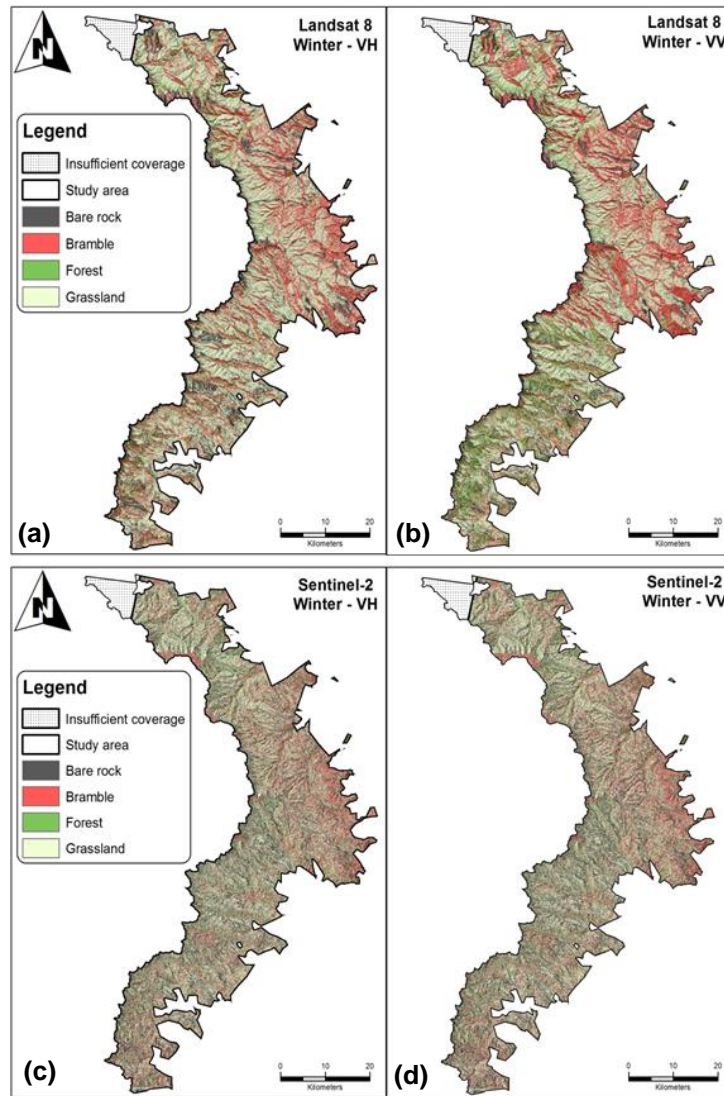


Figure 3.5: Winter spatial distribution maps for fused Landsat 8 and Sentinel-2 VH and VV polarisations. Where (a) = Landsat 8 (VH); (b) = Landsat 8 (VV); (c) = Sentinel-2 (VH) and (d) = Sentinel-2 (VV).

### 3.3.1.4 Spring

Spring L8 results showed a decrease in overall accuracies for both VH and VV fused images (Figure 3.6a and b), both producing overall accuracies of 64% (Table 3.5a and b). A decrease in Bramble user's accuracy (32%) and an increase in Bramble producer's accuracy (71%) was realised for L8 VH and L8 VV fused imagery as compared to summer L8 fused results (Table 3.5a and b). S2 overall accuracies for VH and VV fused images improved when compared to L8 (Figure 3.6c and d), with overall accuracies ranging from 67% (VH) to 72% (VV) (Table 3.5c and d). Bramble user's accuracy increased for VH and VV S2 fused images, while Bramble

producer's accuracy decreased with the fusion of VH and VV SAR data and Sentinel-2 (Table 3.5c and d).

Table 3.5: Spring confusion matrices of VH and VV fused polarisation for Landsat 8 and Sentinel-2. Where BR = Bare rock; BBL = Bramble; FR = Forest; GR = grassland; PA= Producers accuracy; OA= Overall accuracy and UA = Users accuracy.

<b>L8 Spring</b>	<b>BR</b>	<b>BBL</b>	<b>FR</b>	<b>GR</b>	<b>UA (%)</b>	<b>BR</b>	<b>BBL</b>	<b>FR</b>	<b>GR</b>	<b>UA (%)</b>
	(a) VH					(b) VV				
<b>BR</b>	27	2	4	12	60	25	0	9	10	57
<b>BBL</b>	0	21	8	24	40	0	17	15	21	32
<b>FR</b>	1	1	44	3	90	1	3	43	2	94
<b>GR</b>	0	10	8	50	74	0	7	8	52	78
<b>PA (%)</b>	96	62	69	56		96	71	57	61	
<b>OA (%)</b>	<b>64</b>					<b>64</b>				
<b>S2 Spring</b>	(c) VH				(d) VV					
<b>BR</b>	29	5	1	11		26	9	1	10	57
<b>BBL</b>	0	30	0	23		1	33	3	16	62
<b>FR</b>	1	1	44	3		0	1	46	2	94
<b>GR</b>	9	14	4	41		4	11	2	51	75
<b>PA (%)</b>	76	60	90	53		84	61	88	66	
<b>OA (%)</b>	<b>67</b>					<b>72</b>				



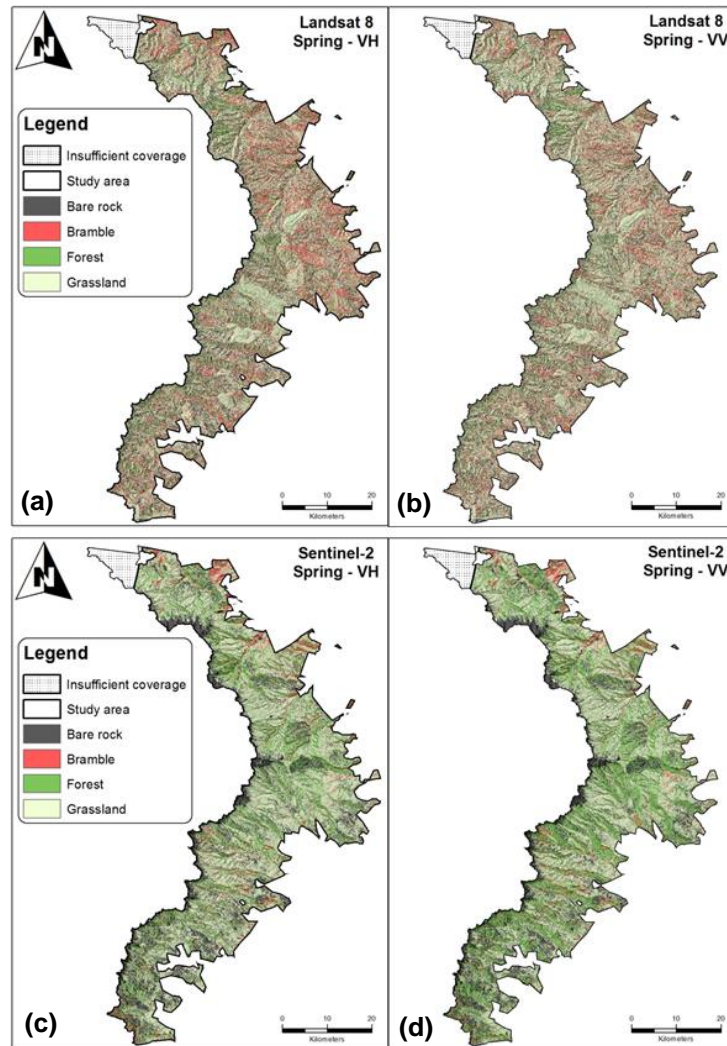


Figure 3.6: Spring spatial distribution maps for fused Landsat 8 and Sentinel-2 VH and VV polarisations. Where (a) = Landsat 8 (VH); (b) = Landsat 8 (VV); (c) = Sentinel-2 (VH) and (d) = Sentinel-2 (VV).

### 3.4 Discussion

This study sought to determine the value of fusing optical and SAR imagery at a feature level in discriminating Bramble from surrounding native vegetation and other land cover types. Generally, overall accuracies of multi-season SAR fused Sentinel-2 data outperformed SAR fused multi-season Landsat 8 imagery. Summer Sentinel-2 fused data produced the highest accuracy (76%) across all seasons and SAR polarisations. This finding is in agreement with van Beijma *et al* (2014) who suggests that the fusion of SAR with optical imagery could be reliably used to map vegetation at a species level. However, our results contradict Hong *et al* (2014), who noted that basic integration of SAR and optical imagery using feature level fusion may not



significantly improve the detection and mapping of land cover types. In our study, we hypothesise that timeous acquisition and seasonal alignment of SAR and optical imagery used for data fusion could have assisted in achieving improved Bramble classification accuracies. The broad-leafed nature of Bramble plants makes it easier to discriminate, in comparison to grassland and alfalfa considered in Hong *et al* (2014). This variability in phenology characteristic could be used to explain the contradictory results. According to Bradley (2014), no sensor can achieve high spatial, spectral and temporal coverage collectively over an expansive spatial extent. Consequently, the choice of remote sensing approach will always be limited by the above-mentioned sensor characteristics. Sentinel-2's strategically placed bands, coupled with its superior spatial resolution, when compared to Landsat 8, is an example of trade-offs that can affect overall mapping accuracies.

The summer results showed that simple feature level fusion can be used to reliably detect and map Bramble, in comparison to single source active or passive remote sensing imagery. McNairn *et al* (2009) demonstrated superior classification performance during summer, where seasonal changes in vegetation pigmentation, water content and structure are known to affect reflectance and SAR backscatter. Exploitation of these changes using the synergistic power of optical and SAR imagery, which is particularly sensitive to vegetation moisture content, could be responsible for summer's best classification results, in comparison to other seasons. Studies into the behaviour of active remote sensing signals, as a function of leaf area index (LAI) has related decreased backscatter measurements with an increase in LAI for narrow vegetation (such as grassland), and an increase in backscatter measurements for broad leaf vegetation (Macelloni *et al.*, 2001; Fontanelli *et al.*, 2013). The relationship between LAI and the intensity of backscatter measurements could account for summer accuracies, as broad leaf Bramble patches would be more discernible from narrow leaf surrounding grassland.

In fusing SAR data with optical imagery, Hong *et al* (2014) demonstrated that cross-polarised SAR performed slightly better than co-polarised SAR. These findings support results from this study for Sentinel-2 and Landsat 8 in winter and autumn and for Landsat 8 in spring. Additionally, the alignment of SAR data and optical data acquisition could further serve to explain suitable accuracies for Bramble discrimination and mapping, as seasonal differences in backscatter measurements combined with those of spectral reflectance could have improved classification accuracies. The superior performance of cross-polarised fused SAR data is attributed to sensitivity of scattering from the surface, relating to vegetation water content (Ghulam *et al.*, 2011). This explains the increased accuracies resulting from cross-polarised

fusion during the drier autumn and winter seasons. Bramble is known to thrive in wet and moist habitats, hence out-compete native vegetation for water resources during these seasons.

Summer was the only season where co-polarised fused SAR data outperformed or equalled cross-polarised fused SAR data. Similar findings were achieved by Naidoo *et al* (2013) within the study area. The relatively moderate classification accuracies achieved during autumn and winter as compared to spring also followed a similar trend to those achieved by Naidoo *et al* (2013). The better performance of winter and autumn fused imagery compared to spring fused imagery is also consistent with existing literature (Santoro *et al.*, 2014 and Mathieu *et al.*, 2013). Santoro *et al* (2014) attributes decreased classification accuracies to increased transparency within vegetation canopy due to senescence, which allows SAR penetration as well as an increased influence of exposed soil.

Depending on the frequency or wavelength of the sensor in use, target vegetation content and structure can be sensed in different ways using SAR data. The C-band SAR wavelengths, for instance, interact with surface structures such as fine leaf and branch elements, which in turn results in canopy level backscattering. According to Naidoo *et al* (2013), polarisation of SAR data can significantly improve the sensing of vegetation structure. For example, VH polarisation is better linked to canopy structure due to volumetric water content within the canopy architecture (Schmullius and Evans, 1997). This study accordingly contributes to the existing literature by quantifying the impacts of both seasonality and polarisation information on classification accuracy.

### **3.5 Conclusion**

This study sought to fuse wide swath optical remotely sensed data with wide swath Synthetic Aperture Radar (SAR) data to detect and map the American Bramble (*Rubus cuneifolius*). Although numerous studies have outlined the complementary nature of SAR to optical imagery (Gomez, 2017; Naidoo *et al.*, 2015; Baghdadi *et al.*, 2015; Hong *et al.*, 2014), only few studies have been undertaken on a possible operational scale. Seasonal analysis of fused imagery indicated that feature level image fusion has the potential to accurately detect and map Bramble from surrounding native vegetation. Sentinel-2 fused imagery outperformed Landsat 8 fused imagery across all seasons, with the exception of autumn. Cross-polarised SAR data (VH), when fused with optical imagery, showed increased classification accuracies as compared to co-polarised SAR data (VV) during autumn and winter. The optimum season for Bramble

detection was in winter using Sentinel-2 co-polarised fused imagery. This study demonstrates that optical imagery can be used in conjunction with SAR imagery to provide a synergistic approach to invasive alien plant detection and mapping at a large scale.

## Chapter Four

### The fusion of optical imagery and SAR polarization combinations and ratios for invasive alien plant detection and mapping

**This chapter is based on:** Rajah, P., Odindi, J. and Mutanga, O., and Kiala, S., (*Under review: Resubmission - Journal of Applied Remote Sensing*): The fusion of optical imagery and SAR polarization combinations and ratios for invasive alien plant detection and mapping.

#### Abstract

Grassland is the largest biome on earth. The biome has great socio-economic and environmental value that includes carbon reservoir, biodiversity, source of pasture for livestock and wildlife and provision of a range of ecosystem goods and services. However, invasion by alien plant species has increasingly become a severe threat to the biome. Optimal and cost-effective mitigation of effects of invasive species on the grassland biome requires an understanding of the extents and distribution of invasive alien species within the landscape. Whereas studies on the adoption of optical remote sensing for invasive alien plant detection and mapping are abundant, there is paucity in literature on the use of Synthetic Aperture Radar (SAR) remotely sensed data on invasive species mapping. The inherent ability of SAR to acquire data in all weather conditions, during day or night, at varying polarizations could be valuable in complimenting optical imagery and consequently improving classification accuracies. Hence, this study sought to determine the synergistic potential of fusing Sentinel-2 (S2) optical imagery with Sentinel-1 (S1) SAR band ratios in detecting and mapping the American bramble (*Rubus cuneifolius*) within a grassland environment. SAR dual polarization bands and indices were developed for feature level image fusion, and the Support Vector Machine (SVM) learning algorithm used to discriminate the American bramble from native vegetation. Results showed that S2 optical imagery fused with S1 SAR indices that measured the difference between polarizations (Vertical-Horizontal (VH) – Vertical-Vertical (VV) and Vertical-Vertical (VV) – Vertical-Horizontal (VH)) achieved the highest classification accuracies, with overall accuracies of 72% and 74%, respectively. These findings demonstrate the value of dual polarized SAR indices synergistic properties, fused with conventional optical imagery for mapping the American bramble within a grassland environment.

**Key words:** Synthetic Aperture Radar (SAR); Support Vector Machine (SVM); Polarization; Synergistic; American Bramble.

## 4.1 Introduction

The grassland biome is one of the most dominant land-cover types on earth, covering approximately 40.5% of global terrestrial landscape (Carlier *et al.*, 2009; World Resources Institute, 2000). Globally, natural grasslands are valuable socio-economic and environmental resources. However, in South Africa, like many other parts of the world, the grassland biome is under severe threat from different forms of degradation. According to Fourie *et al.* (2015) approximately 45% of the grassland biome in the country has been transformed. Invasive alien plant species have particularly become a major threat to the grassland biome (Te Beest *et al.*, 2012). These threats include enhanced fire frequency, which compromise ecosystem condition, nutrient depletions, changes in micro-climates, alteration in vegetation succession, and restriction in movement of grazing fauna (D'Antonio *et al.*, 1992; Bradley *et al.*, 2006, Foxcroft *et al.*, 2010; Chaneton *et al.*, 2012; Steidl *et al.*, 2013; Maron *et al.*, 2014). To mitigate these effects, objective and cost-effective approaches to identification and mapping of invasive species are paramount. Regular and timely detection and mapping of invasive alien species within the biome is particularly valuable in developing optimal eradication strategies and sustainable management of the biome (Hulme, 2009).

The value of conventional optical remotely sensed data for invasive alien species detection and mapping has been extensively investigated in the recent past (Huang and Asner, 2009; Kimothi and Dasari, 2010; Van den Berg *et al.*, 2013; Gil *et al.*, 2013; Singh *et al.*, 2013). Whereas the adoption of higher spatial and spectral resolution remotely sensed imagery are known to yield reliable results, use of such datasets are limited to smaller spatial extents due to high cost per unit area. On the other hand, lower spatial resolution sensors such as Moderate-Resolution Imaging Spectro-radiometer (MODIS) and the Landsat series cannot be used to reliably delineate invasive species as their utility is hindered by the common mixed pixel problem. Other commonly used sensors like SPOT have limited spectral discriminatory power. New generation moderate resolution sensors have recently emerged, with the Sentinel constellation (Sentinel-2 - optical and Sentinel-1 -Synthetic Aperture Radar - SAR) attracting significant interest. A product of the European Space Agency (ESA), Sentinel-2 (S2) and Sentinel-1 (S1) imagery are freely available and possess unique spatial and spectral characteristics valuable for landscape delineation. The sensors provide an opportunity to complement optical and SAR in invasive alien species detection and mapping.

According to Solberg (2006), surface features are characterized by specific spectral properties at different frequencies of the electromagnetic spectrum. Hence, sensors capturing different wavelengths provide complimentary information about the earth's surface. Therefore, merging multi-source remotely sensed data such as S1 and S2 offer great potential for delineating surface features, as compared to single source data Solberg (2006). SAR sensors such as S1 are also capable of recording SAR backscatter ( $\sigma_0$ ) measurements in various polarization modes. Polarization of SAR data refers to the orientation of the electric field vector of emitted and received signals. S1 has the ability to emit and receive electromagnetic waves across both horizontal and vertical planes. Hence, a Vertical Horizontal (VH) polarization would emit an electromagnetic wave vertically and receive backscatter measurements on a horizontal plane. SAR emitted and received across opposite planes (VH) is referred to as cross-polarized in nature. A Vertical Vertical (VV) polarization on the other hand would emit and receive backscatter measurements on the vertical plane. This type of SAR measurement is referred to as co-polarized SAR data. Vegetation volume and geometric structure are believed to be key variables that determine SAR backscatter (Srivastava *et al.*, 2009; Hong *et al.*, 2014). The suggestion that co-polarized SAR is subtly stronger at detecting variations across these variables (Vyjayanthia and Nizalapur, 2010), provides background for investigating the potential of SAR polarization combinations and ratios for fusion with optical imagery to exploit these polarization subtleties for invasive alien detection and mapping.

Merging remotely sensed imagery, a process referred to as image fusion, is most effective when intended to improve image reliability and subsequent image classification accuracies. Palubinskas (2012) notes that image fusion involves a combination of two or more images from sensors of different wavelengths, simultaneously viewing the same scene to form a composite image. According to Dong and Srivastava (2013), the composite image serves to improve image data content and facilitate determination of targets due to the synergistic properties of SAR and optical imagery. Currently, three image fusion approaches exist; pixel level, feature level and decision level (Sahu and Parsai, 2012). Feature level fusion was adopted in this study as it is less stringent to sensor alignment compared to other fusion techniques. Additionally, feature level fusion achieves a considerable compression of information and is highly conducive to efficient real-time remote sensing imagery processing (Malik *et al.*, 2013). The approach extracts features such as edges, textures and shapes from different images of the same geographic area by separate pre-processing (Schmitt and Zhu, 2016; Pandit and Bhiwani, 2015). Extracted features are then combined to form an optimal feature set that is further

classified using supervised or unsupervised classifiers. This process allows correlative feature information to be excavated, eliminates redundant features and establishes new compound features, increasing reliability of feature information (Zeng *et al.*, 2006; Pandit and Bhiwani, 2015).

Although optical imagery is considered a powerful resource for invasive alien discrimination, constraints associated with spectral resolution and surface reflectance measurements that only take into account the surface of canopy vegetation, limit its application to alien invasive detection and mapping (Joshi *et al.*, 2016). Hence, the unique ability of SAR to penetrate vegetation surface canopy has led to studies on relations between SAR backscatter and vegetation parameters such as leaf area index (LAI) and biomass (Ghasemi *et al.*, 2011; Inoue *et al.*, 2014). According to Dusseux *et al.* (2014), SAR's unique capabilities make it an ideal complement to optical data for grassland monitoring. The distinct invasive alien species characteristics such as LAI, canopy surface roughness and biomass present an ideal opportunity for the fusion of SAR and optical data for improved mapping accuracies. Consequently, this study sought to fuse different S1 SAR polarization ratios with new age S2 optical imagery to determine their synergist potential in detecting and mapping the American bramble (*Rubus cuneifolius*) within a protected grassland environment.

## **4.2 Methodology**

### **4.2.1 Study area**

This study was conducted within the uKhahlamba Drakensberg Park (UDP) in the Kwa-Zulu Natal (KZN) province, South Africa (Figure 4.1). The undulating terrain of the UDP is dominated by natural grassland and patches of thickets and natural shrubs. Summers are wet and humid, with a rainfall range of 990-1130mm (Dollar and Goudy, 1999). Winters are dry and cold with occasional snow and frost (Mansour *et al.*, 2012).

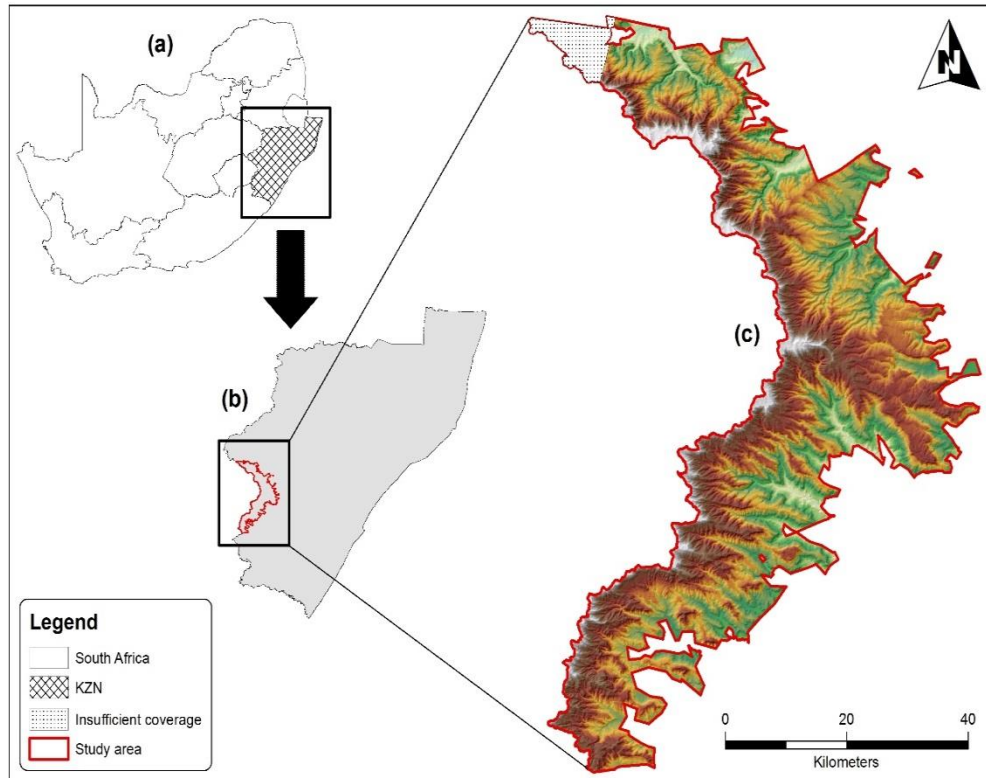


Figure 4.1: uKhahlamba Drakensberg Park (UDP) boundary (c), within the KZN province (b) of South Africa (a).

#### 4.2.1.1 Field data collection

Field data within the UDP was collected in September and December 2016. The stratified purposive non-random sampling technique was used to collect Bramble patches points using a handheld Trimble differentially corrected GeoXT geographical positioning system (GPS). The purposive non-random sampling approach ensured that an appropriate representative sample was achieved across all major land-cover classes within the study area (Bare rock, Bramble, Grassland and Forest). Field validation ground control points were collected as close as possible to the centroid of the respective land-cover class sampled. To ensure land-cover classes were associated with the unique spectral reflectance and backscatter of a single pixel, spatially independent ground control sample plots ranging from 15m x 15m to 50m x 50m were collected. The UDPs steep and mountainous terrain restricted accessibility to certain Bramble stands, hence only accessible Bramble stands were considered for this study. The 2015 UDP aerial photographs, at a 0.5m spatial resolution were used to collect additional Bramble and other land cover ground truth data for inaccessible areas and to verify land cover classes.



#### 4.2.2 Image acquisition

Summer S2 and S1 imageries were acquired from the Copernicus open access data hub (<https://scihub.copernicus.eu/>). The Sentinel Applications Platform (SNAP) toolbox version 3.0 was used to pre-and process both S2 and S1 imageries.

##### 4.2.2.1 Optical imagery

Level-1C S2 raw data products were acquired. S2 raw digital number (DN) values were converted to spectral surface reflectance values using the Sen2Cor plugin algorithm of SNAP. The System for Automated Geoscientific Analyses (SAGA 2.1.2) terrain analysis tool within a Quantum GIS (QGIS) environment was used to correct topographic effects of shadowing commonly associated with mountainous areas on a band by band basis. The following nine S2 optical bands were used in this study: Band 2 (blue); Band 3 (green), Band 4 (red), Band 5 (vegetation red edge 1), Band 6 (vegetation red edge 2), Band 7 (vegetation red edge 3), Band 8 (Near Infra-red); Band 11 (Short-wave Infra-red1) and Band 12 (Short-wave Infra-red2). A nine-band optical composite image was used for feature level fusion with respective SAR polarization ratio bands.

##### 4.2.2.2 SAR imagery

The S1 open access data-hub was used to download raw level-1 S1 level-1 Ground Range Detected (GRD) products. GRD products consist of focused SAR data that has been detected, multi-looked and projected to ground range using an Earth ellipsoid model were acquired. These S1 products were in Interferometric Wide Swath (IW) mode, with a spatial resolution of 10 meters and a swath width of 250km<sup>2</sup>. S1 image products was pre-processed using the methodology outlined in Bevington (2016). The Bevington (2016) SAR image processing chain consists of five steps: (1) Application of orbit file to SAR image; (2) Radiometric calibration; (3) Application of speckle filter; (4) Terrain correction; and (5) Conversion of SAR DN to Sigma0 backscatter values (dB) units using  $10 \times \log_{10}(\sigma_0)$  equation (Li *et al.*, 2011). S1 image products in dB units were then used to derive several S1 SAR dual polarized band indices.

##### 4.2.2.3 S1 SAR dual polarized indices

S1 SAR dual polarized bands and indices were individually fused with S2 optical imagery at a feature level. S1 SAR dual polarized indices were calculated as follows: (1) VH/VV; (2) VH – VV; (3) VH + VV; (4) VH x VV; (5) VV/VH and (6) VV – VH. SAR band indices were devised

using all possible realistic mathematical expressions in order to determine if the difference, additive, multiplicative or fractional products of VH and VV dual polarizations were optimal for discriminating Bramble from surrounding native vegetation.

#### 4.2.3 Data Fusion

Fusion of S2 optical imagery and S1 SAR dual polarized bands and indices was conducted at a feature level (Figure 4.2). S1 SAR imagery was resampled to a spatial resolution of 20 meters in order to coincide with the spatial resolution of S2 optical imagery.

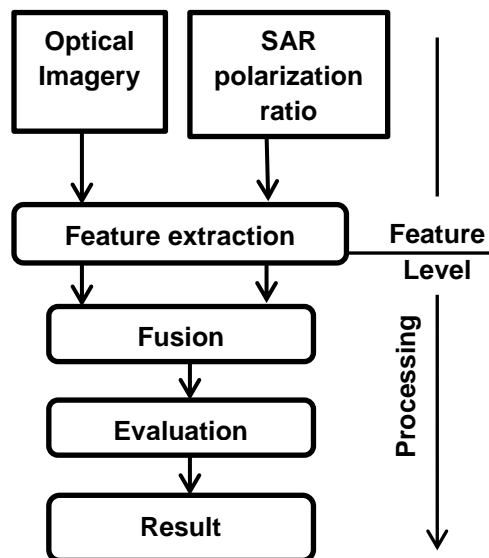


Figure 4.2: Feature level fusion processing chain

In the feature-level fusion, each sensor observes an object, and a feature extraction is performed to yield a feature vector from each sensor. After using an association process to sort feature vectors into meaningful groups, these feature vectors are then fused and an identity declaration is made based on the joint feature vector (Zeng *et al*, 2006). Extraction of field validated features was done on an individual basis for optical imagery and SAR index images. Corresponding spectral reflectance measurements were assigned to extracted SAR ratio backscatter features. Fused S2 optical imagery and S1 SAR backscatter data were then used for classifying and mapping American bramble.

#### 4.2.4 Image classification

Image classification was conducted post feature level image fusion using the Support Vector Machine (SVM) machine learning algorithm within a Python environment. SVM is a supervised statistical learning technique first developed by Vapnik (1979) to deal with binary classifications. The algorithm aims to find a hyper-plane that divides the dataset into a discrete predefined number of classes consistent with training data (Mountrakis and Ogole, 2011). Statistical evaluation has shown that SVM is proficient in classifying several classes using limited support vectors as training samples, without compromising the classification accuracies (Foody and Mathur, 2004; Mantero *et al.*, 2005, Bruzzone and Chi, 2006; Shao and Lunetta, 2012; Zheng *et al.*, 2015). The SVM classifier is trained using 70% of the collected ground truth data points for the four major land cover classes (Bare rock, Bramble, Forest and Grassland) in the study area.

#### 4.2.5 Map production and accuracy assessment

In a Python 2.7.13 environment, the SVM classifier was used to generate classification maps of the four land cover classes from fused data S2 optical and S1 SAR data. A random 30% of the ground data points were used as test data set to validate the classified maps. Confusion matrices for each of the six fused SAR ratios were produced on the test data set to evaluate user's and producer's accuracies of all four considered land cover classes.

### 4.3 Results

Generally, all S1 SAR dual polarized bands and indices fused with the S2 optical imagery produced above average classification accuracies, with values ranging from 64% to 74% (Tables 4.1 - 4.3). The VV – VH S1 SAR index achieved the highest overall classification accuracy across all S1 SAR dual polarized and S2 optical fused imagery (74%) (Table 4.1a). The VH – VV S1 SAR dual polarized index fused with S2 optical imagery produced the second highest overall classification accuracy (72%) (Table 4.1b). Bramble achieved the lowest user's accuracy (47%) and Grassland the highest (88%) (Table 4.1b).

Table 4.1: Confusion matrices of VV - VH and VH - VV S1 SAR dual polarized indices fused with S2 optical imagery. Where BR = Bare rock; BBL = Bramble; FR = Forest; GR = grassland; PA= Producer's accuracy; OA= Overall accuracy and UA = User's accuracy.

	<b>(a) VV - VH</b>					<b>(b) VH - VV</b>				
	<b>BR</b>	<b>BBL</b>	<b>FR</b>	<b>GR</b>	<b>UA (%)</b>	<b>BR</b>	<b>BBL</b>	<b>FR</b>	<b>GR</b>	<b>UA (%)</b>
<b>BR</b>	50	0	5	10	77	43	0	0	10	81
<b>BBL</b>	1	30	5	23	51	1	35	15	23	47
<b>FR</b>	4	5	58	20	67	11	1	45	12	65
<b>GR</b>	1	6	0	85	92	1	6	5	92	88
<b>PA (%)</b>	89	73	85	66		77	83	69	67	
<b>OA (%)</b>	<b>74</b>					<b>72</b>				

The VV - VH and VH - VV spatial distribution map produced improved spatial extents for all land-cover classes considered in this study. From a visual perspective, Bare rock, Bramble and Forest spatial extents were the least over-estimated when compared to other SAR band combinations and ratios considered in this study (Figure 4.3a, Figure 4. 6).

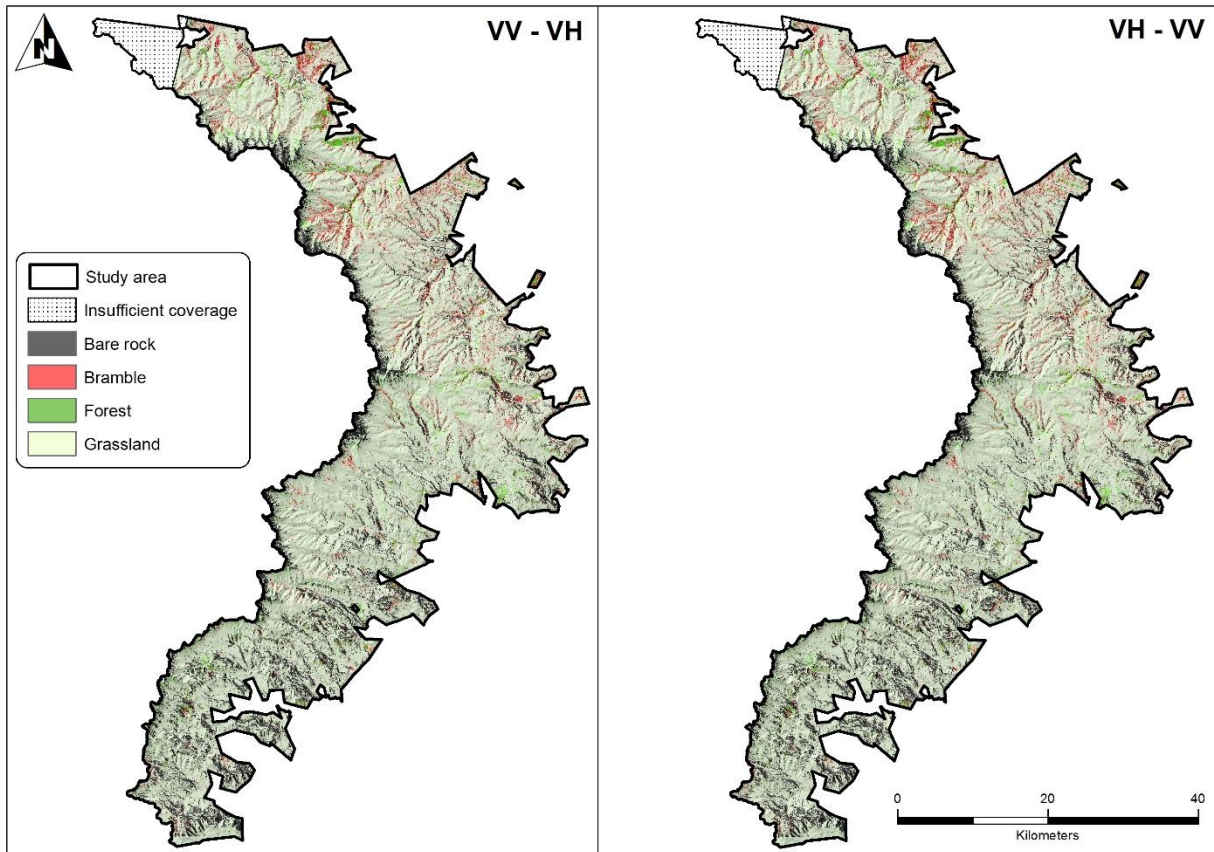


Figure 4.3: Land cover maps produced using VV – VH and VH - VV S1 SAR dual polarized indices fused with S2 optical imagery and SVM classifier.

The VH/VV SAR fused ratio produced an overall user's classification accuracy of 68% (Table 4.2a). The highest user's accuracy was achieved by the grassland land cover class (89%) and the lowest by the Bramble land cover class (43%) (Table 4.2a). The VV/VH SAR ratio resulted in an overall accuracy of 67% (Table 4.2b). User's accuracies ranged from 46% (Forest) to 93% (Grassland) (Table 4.2b). Producer's accuracies ranged from 51% (Grassland) to 100% (Forest).

Table 4.2: Confusion matrices of VH/VV and VV/VH SAR ratios fused with Sentinel-2 optical imagery. Where BR = Bare rock; BBL = Bramble; FR = Forest; GR = grassland; PA= Producers accuracy; OA= Overall accuracy and UA = Users accuracy.

	<b>(a) VH/VV</b>					<b>(b) VV/VH</b>				
	<b>BR</b>	<b>BBL</b>	<b>FR</b>	<b>GR</b>	<b>UA (%)</b>	<b>BR</b>	<b>BBL</b>	<b>FR</b>	<b>GR</b>	<b>UA (%)</b>
<b>BR</b>	51	0	15	18	61	47	0	0	18	72
<b>BBL</b>	11	31	10	21	43	1	32	0	30	51
<b>FR</b>	1	2	46	10	78	6	1	37	36	46
<b>GR</b>	0	9	0	75	89	0	6	0	86	93
<b>PA (%)</b>	81	74	65	60		87	82	100	51	
<b>OA (%)</b>	<b>68</b>					<b>67</b>				

Spatial distribution maps resulting from the VH/VV SAR fused ratio produced improved accuracy of spatial extents of all considered land cover classes (Figure 4.4a and b). There were decreased over estimations of Bare rock and Forest land cover classes as compared to VH x VV and VH + VV SAR fused combinations (Figure 4.5a and b). Bramble spatial distribution across both SAR combinations showed improved accuracy in spatial extents, with decreased over-estimations as compared to the VH x VV and VH + VV SAR fused imagery (Figure 4.6).

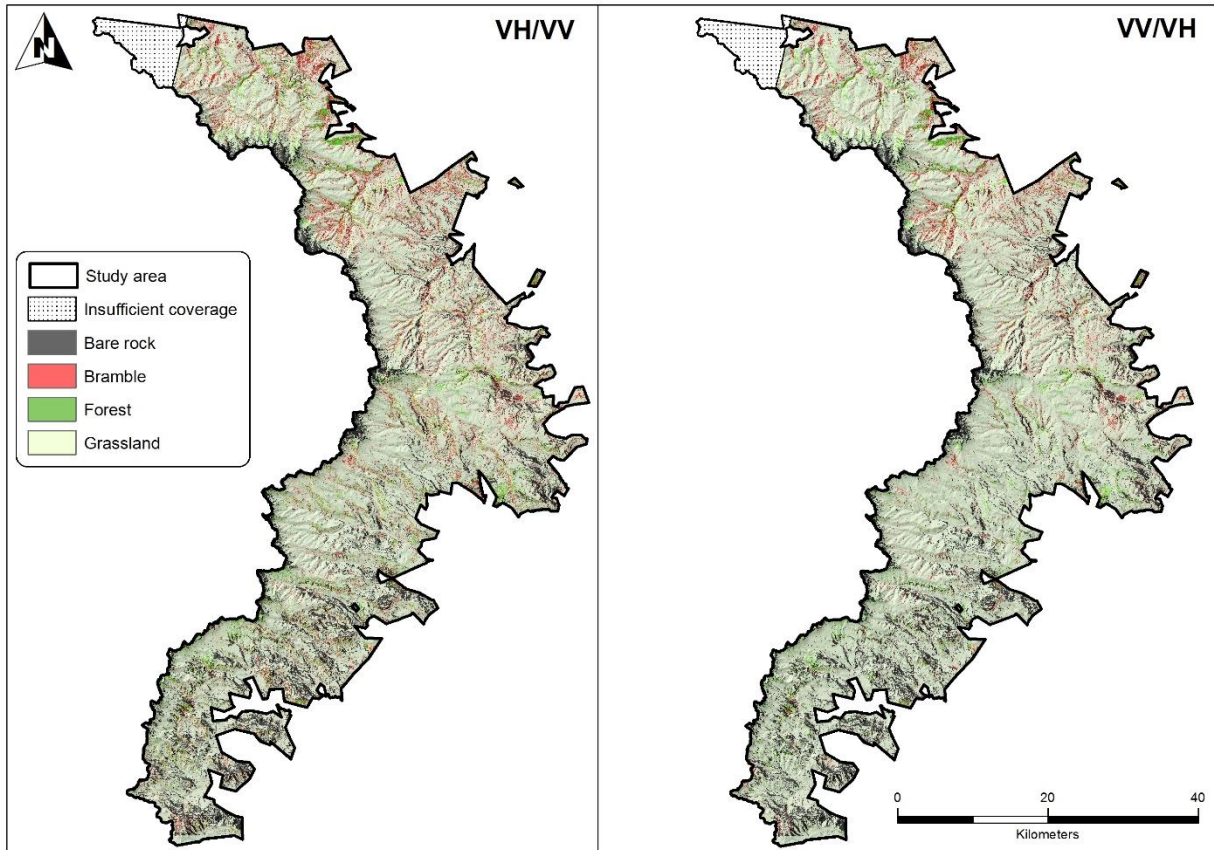


Figure 4.4: Land cover maps produced using VH/VV and VV/VH S1 SAR dual polarized indices fused with S2 optical imagery and SVM classifier.

The VH x VV fused ratio produced an overall classification accuracy of 64% (Table 4.3a), the lowest across all SAR fused imagery. Bramble users and producers accuracies were 56% and 55% respectively and were the lowest across all land cover classes for the VH x VV SAR fused ratio. The VH + VV SAR fused combination produced an improved overall classification (68%) as compared to the VH x VV SAR ratio (Table 4.3b). The bramble land cover class had the lowest users accuracy (40%) for the VH + VV SAR combination (Table 4.3b).

Table 4.3: Confusion matrices of VH x VV and VH + VV SAR combinations fused with Sentinel-2 optical imagery. Where BR = Bare rock; BBL = Bramble; FR = Forest; GR = grassland; PA= Producers accuracy; OA= Overall accuracy and UA = Users accuracy.

	<b>(a) VH x VV</b>					<b>(b) VH + VV</b>				
	<b>BR</b>	<b>BBL</b>	<b>FR</b>	<b>GR</b>	<b>UA (%)</b>	<b>BR</b>	<b>BBL</b>	<b>FR</b>	<b>GR</b>	<b>UA (%)</b>
<b>BR</b>	43	0	9	18	61	42	0	9	16	63
<b>BBL</b>	2	36	0	56	56	2	35	10	40	40
<b>FR</b>	11	4	39	62	62	11	4	39	10	61
<b>GR</b>	0	26	0	74	74	1	15	3	63	77
<b>PA (%)</b>	76	55	81			75	65	64	49	
<b>OA (%)</b>	<b>64</b>					<b>68</b>				

The SVM spatial distribution map produced for the VH x VV fused combination showed a slight over-estimation with regard to the Forest, Bare rock and Bramble classes. Consequently, the spatial distribution of the grassland land cover class showed a minor under-estimation in spatial extent (Figure 4.5a, Figure 4.6).



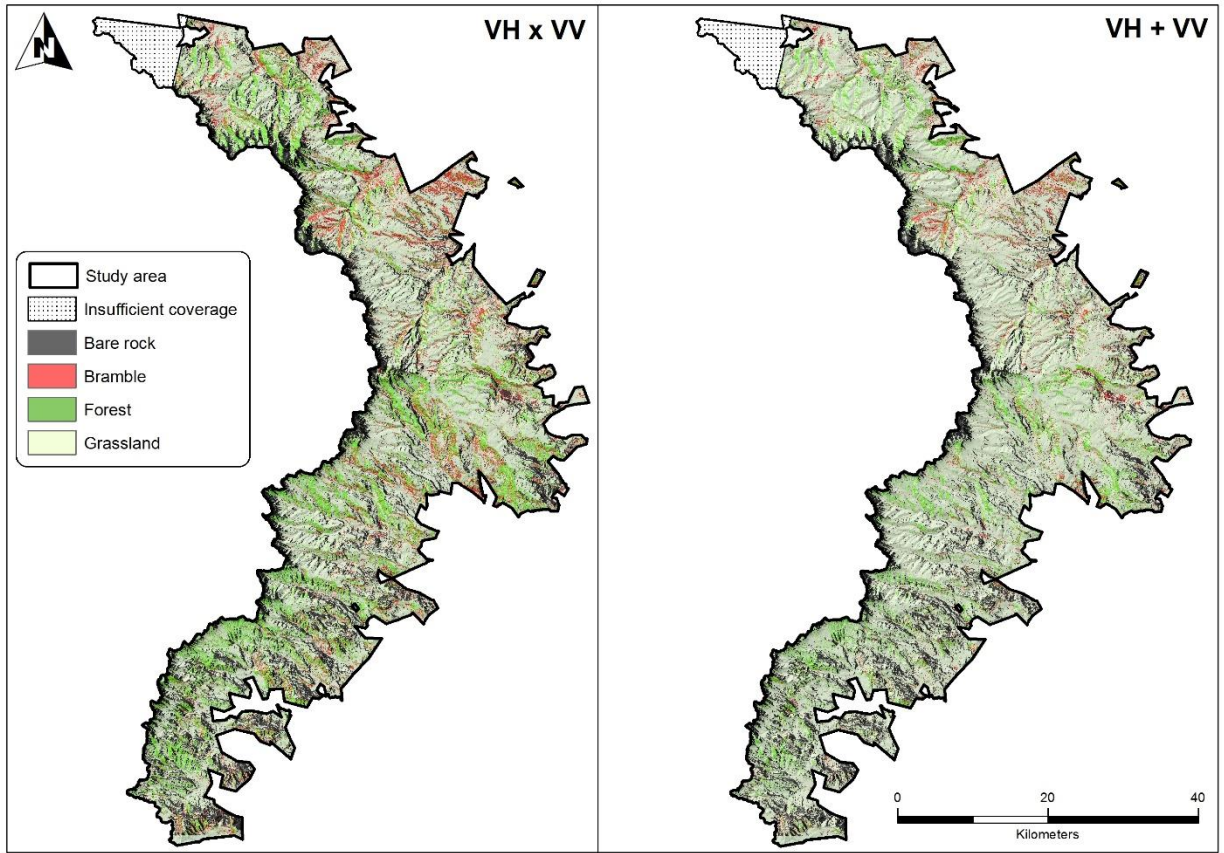


Figure 4.5: Land cover maps produced using VH x VV and VH + VV S1 SAR dual polarized indices fused with S2 optical imagery.

The VH + VV SAR spatial distribution map provided an improved spatial extent of Bramble and Grassland classes, with minimal over-estimation (Figure 4.5b). Bare rock spatial distribution showed a slight improvement as compared to the VH x VV SAR combination, however, over-estimation or bare rock was still visually represented (Figure 4.5a, Figure 4.6).

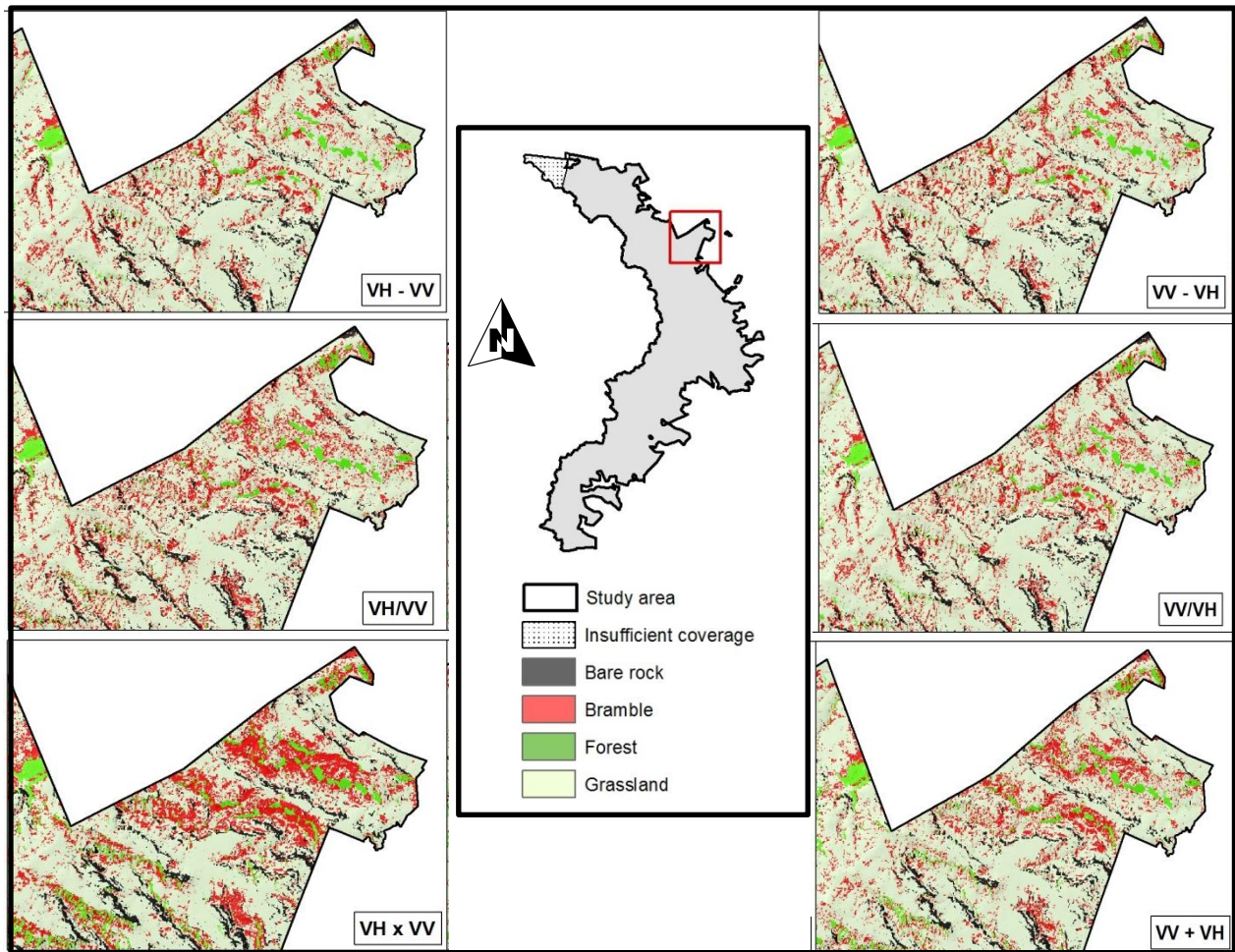


Figure 4 6: Overestimation and underestimation of Bramble classes across VH-VV; VV - VH; VH/VV; VV/VH; VH x VV and VV+VH band combinations and ratios

#### 4.4 Discussion

This study sought to determine the potential synergistic properties of S1 SAR data fused with new age S2 optical imagery for detecting and mapping the American bramble (*Rubus cuneifolius*) invasive plant species. Generally, overall accuracies across all S1 SAR fused polarization indices performed relatively well, with overall accuracies ranging from 64% to 74%. Based on these results, we can affirm that S1 SAR imagery is a valuable supplementary data source to conventional optical imagery. The S1 SAR combination that utilized the difference between VV and VH dual polarized index achieved the highest overall classification accuracy (74%). Depending on the polarization of S1 SAR imagery, target vegetation classification may vary due to specific polarizations being more effective at sensing vegetation parameters. Parameters such as leaf area index, biomass and vegetation water content are the main

determinants of differences in measured SAR backscatter values (Santoro *et al.*, 2011, Naidoo *et al.*, 2013; Schmullius and Evans, 1997). Variations in co- and cross-polarized SAR backscatter measurements are known to occur as a result of sensor incidence angle. According to Baghdadi *et al* (2008), an increase in incidence angle results in an increase in sensitivity to vegetation roughness, which ultimately affects the strength of the received SAR signal. This finding is supported by Betbeder *et al* (2014) who established that SAR imagery, with a moderate incidence angle was successful in discriminating hedgerows and were more susceptible to vegetation roughness. Results from this study are in agreement with Baghdadi *et al* (2008) and Betbeder *et al* (2014), where a large satellite incidence angle range resulted in improved overall accuracies. The incidence angle of S1, which ranges from 29.1 - 40° could have accounted for the VV-VH and VH-VV SAR ratios out-performing all other SAR ratios considered.

The index that measured the difference between VH and VV polarized S1 SAR data achieved the second highest overall classification accuracy (72%). A study by Ghulam *et al* (2014) noted the superior performance of cross-polarized SAR data as compared to co-polarized data. The superior performance was attributed to the sensitivity of cross-polarization to surface vegetation water content. As bramble is known to thrive in moist habitats, water content concentrations within bramble leaves are high. The difference between VH and VV polarized data could have been adequately significant to allow for effective discrimination of Bramble from surrounding native vegetation based on the difference in foliar water content. This finding is in line with a study by Da Costa Freitas *et al* (2009) and Baghdadi *et al* (2009), where the VH SAR polarization showed significant potential for vegetation discrimination as compared to the VV SAR polarization.

The VH + VV SAR combination produced the third lowest overall classification accuracy (68%), compared to the highest (74%) and second highest (72%), proving that the additive effects of cross and co-polarized SAR data for detecting and mapping Bramble within a grassland environment exists. According to Silva *et al* (2009), cross polarized SAR data are more sensitive to vegetation variability as opposed to co-polarized SAR data. Cable *et al* (2014) further notes that ground targets that exhibit similar backscatter intensities are more likely to be separated using co-polarized data. This is attributed to increased phase information commonly associated with co-polarized SAR data. SAR phase information is primarily determined by the distance between the sensor antenna and the ground targets. The addition of the co-polarized VV SAR measurements to the cross-polarized VH measurements could have served to dilute the

sensitivity of the VH SAR backscatter measurements, resulting in the decreased overall classification accuracies achieved when using this index.

The lowest classification accuracy was achieved using the VH x VV fused combination. Baghdadi *et al* (2008) notes that polarization (orientation of emitted and received radar waves) is a key contributing factor to observed SAR backscatter measurements. The VH x VV combination was not suitable for reliable and comprehensive detection of Bramble. McNairn *et al* (2000) notes that vertically emitted SAR waves do not penetrate as deep into vegetation canopy as horizontally emitted waves. Consequently, backscatter measurements from VH and VV SAR imagery could not record sufficient information to accurately discriminate between Bramble and surrounding vegetation. According to McNairn and Brisco (2004) single frequency SAR imagery provides a limited amount of information for precise vegetation separability. Whereas multi-frequency, fully polarimetric data has the potential for improved classification accuracies, until recently, they have not been readily available due to reduced coverages, costs associated with image acquisition, inaccessibility and inferior spatial resolutions. New age sensors produce a higher grade of information and therefore provide an opportunity to improve SAR imagery for vegetation applications (Simental *et al.*, 2005). The recent launch of S1 serves to eliminate issues surrounding cost, coverage and availability of SAR data. The advantage of utilizing varying polarizations of new age S1 SAR data has been evident from the overall accuracies produced when using polarized SAR band ratios and combinations.

#### **4.5 Conclusions**

This study sought to highlight the significance of cost-effective, reliable new age remote sensing techniques, with the goal of contributing to effective management of natural grassland environments. This study contributes to existing literature that aims to improve conventional methods of invasive alien species detection and mapping within a natural grasslands. S2 optical imagery was fused at a feature level with S1 dual polarized SAR imagery, to detect and map American bramble (*Rubus cuneifolius*) from surrounding native vegetation. Although studies that have utilized SAR imagery for vegetation detection and mapping exist (Minchella *et al.*, 2009; Poulain *et al.*, 2009, de Carvalho *et al.*, 2010; Lardeux *et al.*, 2011; Hong *et al.*, 2014), none have tested the variability in potential of SAR polarization modes as done in this study. The fusion of S1 dual polarized SAR indices with S2 optical imagery indicated that specific SAR dual polarized band or index has the potential to detect Bramble from surrounding native grassland vegetation. The SAR dual polarized indices which measured the difference between cross and

co-polarized SAR data (VV – VH and VH – VV) were the most accurate in detecting and mapping Bramble. Hence, this study served to demonstrate the complementarity of polarized S1 SAR imagery to optical imagery. Additionally, this study proves that cost-effective grassland management strategies can be developed at large scale, using the synergistic effects of SAR and optical remote sensing data

## Chapter Five

### **Assessing the synergistic potential of Sentinel-2 spectral reflectance bands and derived vegetation indices for detecting and mapping invasive alien plant species**

**This chapter is based on:** Rajah, P., Odindi, J. and Mutanga, O., and Kiala, S., (*Under review - International Journal of Remote Sensing*): Assessing the synergistic potential of Sentinel-2 spectral reflectance bands and derived vegetation indices for detecting and mapping invasive alien plant species.

#### **Abstract**

Grassland biomes are valuable socio-economic and ecological resources. However, the invasion of grasslands by alien plant species has emerged as one of the biggest threats to their sustainability, management and conservation. Timely, cost-effective and accurate determination of invasive alien plant spatial distribution is paramount for mitigating the adverse effects of alien plants on natural grasslands. While there have been numerous studies on the use of optical bands for invasive alien detection and mapping, there is paucity in literature on the integration of Vegetation Indices (VIs) and optical reflectance bands in understanding the distribution of invasive alien plant species within a landscape. Specifically, there is need to test the value of improved and freely available sensors like Sentinel-2's (S2) in understanding landscape invasion. Hence, this study sought to assess the value of S2's optical bands and VIs for improving the detection and mapping of American Bramble (*Rubus cuneifolius*) within a grassland biome. Variable Importance in the Projection (VIP) was used to identify the most influential reflectance bands and VIs, which were then fused at a feature level. To determine the optimal season for the Bramble mapping, a multi-seasonal analysis was executed using the Support Vector Machine (SVM) learning algorithm. Multi-seasonal analysis indicated that spring was the optimum season for Bramble detection and mapping, with an overall accuracy of 73%. Findings from this study underline the value of complementing VIs and optical bands in determining the distribution of invasive species within grasslands. Furthermore, this study advocates for the adoption and fusion of freely available new age satellite imagery such as Sentinel-2 as a cost effective option in landscape mapping.

**Key words:** Invasive alien plant, Grassland biome, Sentinel-2, Vegetation Indices, Spectral reflectance, Support Vector Machine (SVM).

## 5.1 Introduction

Invasive alien plant species are regarded as the second most severe threat to global biodiversity after anthropogenic habitat destruction (Driver *et al.*, 2012). Globally, vast pristine natural areas have been transformed as a direct result of invasive alien plant invasions, with detrimental impacts to among others human health, ecological resources, agriculture, water and tourism (Pysek *et al.*, 2012). In South Africa, Carbutt and Martindale (2014) note that infestations by invasive species have led to irreversible transformation of between 60-80% of the country's natural grassland. The South African grassland biome is the second largest biome in the country and predominates the country's central high plateau regions of the KwaZulu-Natal and Eastern Cape provinces. Plant invasions in these regions have compromised the biome's ecological integrity and socio-economic potential (Lenda *et al.* 2013).

Traditional methods of identifying invasive alien species involve costly field surveys that are restricted to identification of species within accessible habitats (Edwards *et al.*, 2007). While traditional methods such as the use of aerial photographs are known to be relatively accurate, they require intensive field work and ancillary data analysis, both susceptible to human error. Reliable interpretation of invasive alien plant data collected using conventional field-based surveys is further hampered by the laborious amount of time and effort needed to conduct surveys. Turner *et al* (2003) notes that although traditional methods may work well for smaller areas, they are often unsuitable for use on larger spatial extents, particularly in remote and inaccessible terrain. To overcome the above-named limitations, remote sensing approaches are becoming increasingly popular as an economic and efficient alternative for the detection and mapping of invasive alien species (Huang and Asner, 2009; Müllerová *et al.*, 2013; Bradley, 2014; Rocchini *et al.*, 2015).

Currently, a large number of studies adopting remote sensing approaches for mapping invasive alien plant species use spectral information of high and medium spatial resolution sensors. The use of spectral information assumes that the target invasive species has one or more unique light absorption or reflectance features relative to surrounding native vegetation (Bradley, 2014). Within a landscape, these unique reflectance features are particularly easier to determine when using hyperspectral imagery. The characteristic hundreds of narrow spectral bands of the dataset are capable of distinguishing subtle spectral differences between native and alien vegetation (Bradley, 2014). However, hyperspectral imagery is extremely expensive, requires extensive processing time and has reduced image swath widths (image coverage), hence

unsuitable for mapping large spatial extents. Recently, new generation multispectral imagery from among others Sentinel-2 and WorldView sensors have been successfully tested and used in vegetation mapping (Ng *et al.*, 2017). However, there is a dearth in knowledge on their value in the detection and mapping of invasive alien plant species. The arrival of Sentinel-2 in particular, provides unprecedented opportunity to address the above-mentioned challenges.

To facilitate higher classification accuracy of invasive alien species mapping, there has been an increased use of satellite derived vegetation indices to detect the extent of invaded environments (Levin *et al.*, 2007; Bradley, 2014). According to Basso *et al.* (2004), vegetation indices are more sensitive to vegetation parameters, compared to individual spectral bands, hence more useful when used as surrogates for vegetation and non-vegetation cover. Spectrally derived vegetation indices are particularly valuable as they significantly reduce the effects of soil, topography and satellite view angle (Hunt *et al.*, 2013). Hence, indices have demonstrated ability to accurately quantify vegetation related spatial heterogeneity in complex landscapes (Rochinni *et al.*, 2004; Benayas and Scheiner, 2002). Additionally, indices have been shown to vary across seasons and space, making them useful for detection within-field and intra and inter annual variability (Vina *et al.*, 2011; Gobron *et al.*, 2000).

The efficacy of remote sensing and derived vegetation indices often rely heavily on the characteristics of the sensor utilized. The recent launch of the European Space Agency (ESA) Sentinel-2 (S2) multispectral satellite has availed new opportunities in remote sensing applications. S2 is a 13 band spectral resolution sensor spanning the visible/near-infrared, and short wave infrared spectral range and captures images at 60m, 20m and 10m spatial resolutions (Immitzer *et al.*, 2016). Coupled with a 290km wide swath width and a 5 day temporal resolution, S2 offer new opportunities for both local and regional scale vegetation mapping. The sensor's unique spectral resolution allows for the derivation of numerous vegetation indices that cannot be derived from other freely available multispectral satellites such as Landsat 8 and Moderate Resolution Imaging Spectroradiometer (MODIS). S2 also has three vegetation red edge spectral bands, currently not available in the freely available multispectral sensors (Cho *et al.*, 2012; Hedley *et al.*, 2012). These unique and progressive features, coupled with the sensor's economic viability offer unprecedented opportunities in the discrimination and mapping of invasive alien plant species.

Analysis based on phenological variability is imperative in optimal detection and mapping of vegetation species. According to Verbesselt *et al.* (2009), seasonal changes influence plant



phenology and foliar chemistry, characteristics that can be exploited to determine optimal mapping seasons. Xue and Su (2017) note that remotely sensed information on vegetation vigor and growth can be useful for biodiversity conservation applications such as monitoring bush encroachment and estimating grassland biomass. According to McNairn *et al* (2009), invaders often exploit empty niches within a landscape and have distinct seasonal phenological characteristics from the surrounding native species, characteristics that provide potential for increased discrimination during a particular season. S2's high temporal resolution (5 days), and consequently high data volume is a valuable asset that could be used to exploit these seasonal phenological variabilities. Hence, this study sought to determine the value of fusing the most influential S2 spectral reflectance bands and vegetation indices in mapping the American Bramble within a grassland biome. The study further sought to determine the optimal season for Bramble detection and mapping using the synergistic properties of spectral reflectance and VIs.

## 5.2 Methodology

### 5.2.1 Study area

The Ukhahlamba Drakensberg Park (UDP) (-29.380018°S; 29.539746°E) borders the eastern escarpment of Lesotho and stretches along the western border of the KwaZulu-Natal province (Figure 5.1). The crescent shape of the UDP has an approximate length of 158km and a width of 28km at its widest point (Kruger *et al.*, 2011). The mountainous terrain of the UDP ranges in altitude from 1200m to 3408m above sea level, with mean annual temperatures approximately 16° Celsius. Mean annual precipitation varies from the foothills of the mountain (1000m) to the escarpment (1800m) (Kruger *et al.*, 2011).

#### 5.2.1.1 Target species

The American Bramble (*Rubus cuneifolius*) has been identified as a major threat to native flora and fauna within the South African grassland biome. A sprawling shrub species belonging to the *Rosaceae* family, Bramble is known to thrive in a diverse range of habitats (Bromilow, 2010). Originally from North America, Bramble is believed to be one of the most harmful invasive alien plants in South Africa, specifically across the KwaZulu-Natal province, where the cool and moist climatic conditions favour its growth. Its growth in bush clumps is directly responsible for its adverse effects on biodiversity. According to Henderson *et al* (2001), the impacts of Bramble infestation include a reduction in carrying capacity, alterations in nutrient cycling, increased soil erosion, changes in fire regimes and behavior and the disruption of hydrological process.

Generally, Bramble is considered a severe threat to natural resources and sustainability and its effective management or eradication is of paramount importance.

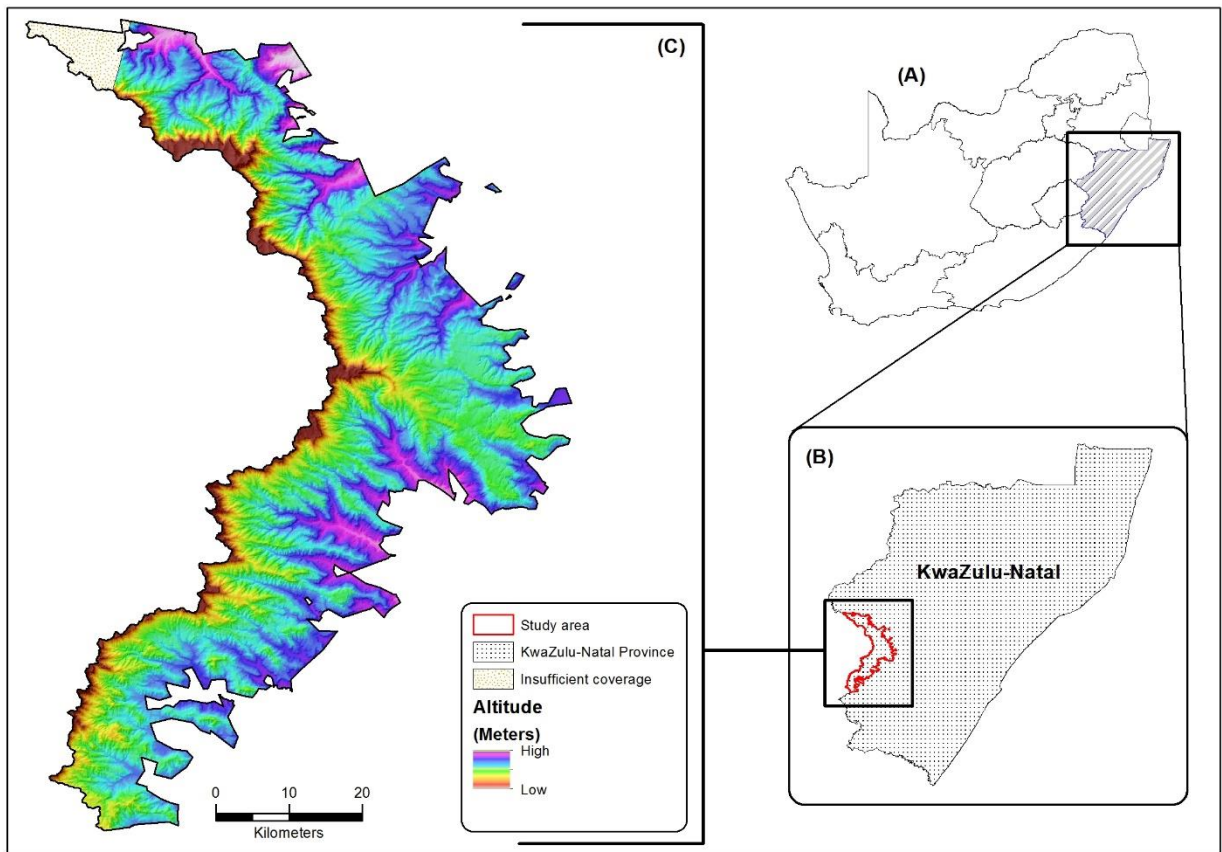


Figure 5.1: The uKhahlamba Drakensberg Park (UDP) (c), located within the KwaZulu-Natal Province (b) of South Africa (a).

#### 5.2.1.2 Field data collection

Four major land cover classes (Bare rock, Bramble, Forest and Grassland) were considered for this study. Ground validation GPS points of the four land cover classes were collected using the purposive sampling technique. Ground validation points were collected during spring and summer of 2016, as these seasons coincide with Bramble flowering (ATLAS, 2014). Hence, data collection during these seasons was preferred as Bramble patches were easily discernable while in field. A GeoXT differentially corrected Trimble GPS was used to record ground validation data. Bramble ground validation points were recorded as close to the centroid of the respective Bramble patch as possible. In order to compensate for sensor spatial resolution, and to ensure collected Bramble ground validation points fell within the sensor pixels and are associated with the unique spectral reflectance, all recorded Bramble patches were spatially

independent and ranged from 15m x 15m to 50m x 50m in size. Owing to the steep and mountainous terrain of the UDP, which restricted access, only Bramble patches accessible by foot were considered for this study. Aerial photographs at a 0.5m spatial resolution captured in 2016 were also used to supplement and verify selected land cover ground truth points.

## 5.2.2 Image acquisition

### 5.2.2.1 Optical imagery

Multi season (spring, summer, autumn and winter) Sentinel-2 (S2) level 1-C raw imagery were acquired from the Sentinel-2 Copernicus open access hub (<https://scihub.copernicus.eu/>). S2 level 1-C raw products (radiance) were converted to level 2-A S2 products (surface reflectance) using the Sen2Cor plugin within the ESA SNAP toolbox 3.0. All S2 level 2-A products were corrected for topographic effects of shadow commonly associated with mountainous regions such as the UDP. Topographic correction was conducted using the System for Automated Geoscientific Analyses SAGA (2.1.2) plugin within a Quantum GIS environment (QGIS), using the SAGA terrain analysis lighting tool on a band by band basis.

### 5.2.2.2 Vegetation indices

Sixty-five vegetation indices selected from the online Index DataBase (IDB) ([www.indexdatabase.de](http://www.indexdatabase.de)) were calculated from level 2A Sentinel-2 multi season optical imagery. Indices were selected on the basis of being specific to Sentinel-2 and are recognized by the IDB as effective and accurate measures of various vegetation parameters, such as vigor, greenness and seasonal influences. The IDB is a tool developed to provide a simple overview of satellite specific vegetation indices that are useable from a specific sensor for a specific application (Henrich *et al.*, 2012). All indices were calculated within a python 2.7.13 environment using listed formulas from the IDB and spectral reflectance Sentinel-2 bands.

## 5.2.3 Variable selection

The Variable Importance in the Projection (VIP) method was implemented within a Python 2.7.13 environment. The VIP method selected the 15 most influential bands across S2 optical bands and derived S2 vegetation indices. Selected VIP bands were used for data fusion and consequently formed the fused images used for image classification. Variable Importance in the Projection can serve to improve classification accuracy by efficiently identifying a subset of all initial variables that if combined, could enhance classification accuracies with parsimonious

representation (Farrés *et al.*, 2015). VIP measures the importance of each variable (S2 optical bands and vegetation indices) with regard to the influence it would have on increasing the classification accuracy. For example, a variable that scores closer to or greater than 1 was considered to be important, hence included in the image classification process, whereas a variable scoring significantly less than 1 was considered less important, hence excluded from the classification process.

#### 5.2.4 Image fusion: Optical bands and Vegetation Indices

Feature level image fusion was adopted to merge the 15 most influential VIP bands. As vegetation indices were calculated from optical bands, selected VIP optical bands and vegetation indices were all calculated at a spatial resolution of 20m. VIP bands were fused using the composite bands tool within an ArcMap 10.4 environment, resulting in four fused images, each representing a single season. The extraction of ground truth points was conducted on an individual basis for VIP optical bands and vegetation indices. The feature level fusion of VIP optical bands and vegetation indices ensured that the corresponding optical spectral reflectance was used for the vegetation index value. Fused optical bands and vegetation indices were then used for image classification.

#### 5.2.5 Image classification

Post feature level fusion image classification was conducted using the Support Vector Machine (SVM) algorithm within a Python environment. The SVM is a supervised statistical learning technique that was developed to deal with binary classifications (Vapnik, 1979). SVM seeks to identify a hyper-plane that can clearly distinguish input dataset into a predefined discrete number of classes that are consistent with training data (Mountrakis *et al.*, 2010). Several evaluations of SVM have shown that the algorithm is capable of classifying/separating several classes with limited support vectors as training data, without ultimately compromising classification accuracies (Foody and Mathur, 2004; Mantero *et al.*, 2005; Bruzzone *et al.*, 2006; Shao *et al.*, 2012; Zheng *et al.*, 2015). Ground truth points were used to extract spectra for the four major land cover classes (Bare rock, Bramble, Forest and Grassland) in the study area. Extracted fused VIP spectral reflectance with vegetation indices measurements were used in the SVM classification process.

## 5.2.6 Spatial distribution map and accuracy assessment

Support Vector Machine classification maps were generated for each seasonal image within a Python environment. Fused (VIP optical and vegetation indices) training data (70%) of all four considered land cover classes were used as the input for the multi-season Bramble spatial distribution maps. The respective test data set (30%) was then used to assess classification accuracies for each season. Confusion matrices were produced from the SVM process in order to quantify the accuracy of seasonal Bramble spatial distribution maps.

## 5.3 Results

### 5.3.1 Optical and Vegetation Indices VIP band selection

A total of the 15 most influential optical bands and vegetation indices were selected per season and considered for further analysis. The S2 SWIR1 (11) and SWIR2 (12) bands were the most influential optical bands as they were selected for spring, summer and winter imagery (Table 5.1). The narrow infrared optical band (8a) was only selected for spring and summer seasonal imagery. From all analyzed vegetation indices, the TM5/TM7, SR520/670, SR800/550 and SRMIR/Red were the only indices selected across all seasonal imagery (Table 5.1). The SR860/550 and RDVI vegetation indices featured across both spring and summer while the Datt2 index featured across both autumn and winter (Table 5.1). Other vegetation indices that featured in multiple seasons include SRNIR/MIR (spring and autumn), SR672/550 (summer and winter), PSSRc2 (summer, autumn and winter), RGR (spring and winter), SIPI3 (spring and winter) and Clrededge (summer and autumn) (Table 5.1).

Table 5.1: Selected VIP optical bands and Vegetation Indices (VIs) across all seasonal imagery (Indices derived from the Index Database - [www.indexdatabase.de](http://www.indexdatabase.de)).

	<b>Season</b>			
	<b>Spring</b>	<b>Summer</b>	<b>Autumn</b>	<b>Winter</b>
<b>Selected optical bands and/or Vegetation Indices (VIs)</b>	8a (Narrow NIR)  11 (SWIR1)	8a (Narrow NIR)  11 (SWIR1)	Rededge1 (Red edge 1)  MSI2 (Moisture Stress Index)	11 (SWIR1)  12 (SWIR2)  TM5/TM7 (Simple Ratio)

	12 (SWIR2)	12 (SWIR2)	TM5/TM7 (Simple Ratio 1650/2218)	1650/2218)
	MSI2 (Moisture Stress Index)	MSI2 (Moisture Stress Index)	SR520/670(Simple Ratio 520/670)	SR520/670 (Simple Ratio 520/670)
	TM5/TM7 (Simple Ratio 1650/2218)	TM5/TM7 (Simple Ratio 1650/2218)	SR774/677 (Simple Ratio 774/677)	SR672/550 (Simple Ratio 672/550 Datt5)
	SR520/670 (Simple Ratio 520/670)	SR520/670 (Simple Ratio 520/670)	PSSRc2 (Simple Ratio 800/470 Pigment specific simple ratio C2)	SR800/470 Pigment specific simple ratio C2)
	SR800/2170, (Simple Ratio 800/2170)	SR672/550 (Simple Ratio 672/550 Datt5)	SR800/550 (Simple Ratio 800/550)	SR800/550 (Simple Ratio 800/550)
	SR800/550 (Simple Ratio 800/550)	PSSRc2 (Simple Ratio 800/470 Pigment specific simple ratio C2)	Datt2 (Simple Ratio 850/710 Datt2)	Datt2 (Simple Ratio 850/710 Datt2)
	SR860/550 (Simple Ratio 860/550)	SR800/550 (Simple Ratio 800/550)	SRMIR/Red (Simple Ratio MIR/Red Eisenhydroxid-Index)	SR860/708 (Simple Ratio 860/708)
	SRMIR/Red (Simple Ratio MIR/Red Eisenhydroxid-Index)	SR833/1649 (Simple Ratio 833/1649 MSHyper)	SRNIR/MIR (Simple Ratio NIR/MIR)	SRNIR/700-715 (Simple Ratio NIR/700-715)
	SRNIR/MIR (Simple Ratio NIR/MIR)	SR860/550 (Simple Ratio 860/550)	SRRed/NIR (Simple Ratio Red/NIR Ratio Vegetation-Index)	RGR (Simple Ratio Red/Green Red-Green Ratio)
	RGR (Simple Ratio Red/Green Red-Green Ratio)	SRMIR/Red (Simple Ratio MIR/Red Eisenhydroxid-Index)	ND790/670 (Normalized Difference 790/670)	RGR (Simple Ratio Red/Green Red-Green Ratio)
	SRSWIRI/NIR (Simple Ratio SWIRI/NIR Ferrous Minerals)	Clrededge (Chlorophyll IndexRedEdge)		SIPI3 (Structure Intensive Pigment Index 3)
	RDVI (Renormalized Difference Vegetation Index)			
	SIPI3 (Structure Intensive Pigment Index 3)			PSSRc2 (Simple Ratio 800/470)

		RDVI (Renormalized Difference Vegetation Index)	Clrededge (Chlorophyll IndexRedEdge)	Pigment specific simple ratio C2
		MGVI (Misra Green Vegetation Index)	mNDVI (Modified NDVI)	SR860/550 (Simple Ratio 860/550)
			mSR (Modified Simple Ratio)	SRMIR/Red (Simple Ratio MIR/Red Eisenhydroxid- Index)

### 5.3.2 Seasonal classification

#### 5.3.2.1 S2 reflectance bands

Seasonal classification using only S2 reflectance bands resulted in overall accuracies ranging from 61-77% (Table 5.2b and d). Summer exhibited the highest overall accuracy while winter produced the lowest. Stand-alone S2 reflectance band results were used as a benchmark to investigate the potential synergistic properties of Sentinel-2 optical bands fused with vegetation indices to increase the accuracy of detection and mapping of Bramble.

#### 5.3.2.2 Fused VIP S2 reflectance bands and Vegetation Indices

Seasonal classification accuracies ranged from 61% to 73%, with spring imagery producing the highest overall accuracy and winter imagery producing the lowest overall accuracy (Table 5.3a and d). Spring results showed high producers and users accuracies for Bramble (73% and 75%) and grassland (78% and 80%) land cover classes (Table 5.3a). The classification map resulting from spring imagery showed a significant overestimation of the grassland land cover class and an underestimation in the bare rock and forest classes (Figure 5.2a). Although Bramble users and producers accuracies were high, a slight overestimation with regard to classification of Bramble patches was evident. Summer results produced the second highest overall classification accuracy (68%) across all seasonal imagery (Table 5.3b). Summer Bramble users (54%) and producers (68%) accuracies decreased as compared to spring results (Table 5.3b). An underestimation in the bare rock and forest land cover classes was observed, while an overestimation in the Bramble and grassland classes were observed when summer classification results were mapped (Figure 5.2b).

Table 5.2: S2 reflectance band Support Vector Machine (SVM) seasonal confusion matrices. Where BR = Bare rock; BBL = Bramble; FR = Forest; GR = grassland; PA= Producers accuracy; OA= Overall accuracy and UA = Users accuracy.

	BR	BBL	FR	GR	UA (%)	BR	BBL	FR	GR	UA (%)
	(a) Spring					(b) Summer				
<b>BR</b>	31	0	0	15	67	32	2	0	12	69
<b>BBL</b>	0	28	0	44	39	0	24	0	29	45
<b>FR</b>	0	0	56	3	94	1	1	54	3	91
<b>GR</b>	1	13	3	70	80	2	3	7	94	88
<b>PA (%)</b>	96	68	94	53		91	80	88	68	
<b>OA (%)</b>	<b>70</b>					<b>77</b>				
	(c) Autumn					(d) Winter				
<b>BR</b>	30	0	0	16	65	34	0	0	12	73
<b>BBL</b>	0	20	1	47	30	0	22	1	69	24
<b>FR</b>	1	0	55	3	93	1	0	53	5	89
<b>GR</b>	1	30	0	60	66	0	15	1	51	76
<b>PA (%)</b>	93	39	98	48		97	59	96	37	
<b>OA (%)</b>	<b>63</b>					<b>61</b>				

Autumn imagery produced an intermediate classification accuracy (60%) across all seasonal imagery (Table 5.3c). Bramble users (43%) and producers (47%) accuracies resulting from autumn imagery were the lowest across all seasons (Table 5.3c). The resulting autumn classification map overestimated Bramble and grassland landcover spatial extent (Figure 5.2c), while underestimating the spatial extent of the bare rock and forest landcover classes (Figure 5.2c). Winter imagery resulted in the lowest overall classification accuracy across all seasons (57%) (Table 5.3d). An overestimation of the grassland and Bramble landcover class was observed in the resulting winter classification map, while an underestimation of the bare rock and forest landcover classes was observed (Figure 5.2d).



Table 5.3: Fused VIP S2 optical bands and Vegetation Indices Support Vector Machine (SVM) seasonal confusion matrices. Where BR = Bare rock; BBL = Bramble; FR = Forest; GR = grassland; PA= Producers accuracy; OA= Overall accuracy and UA = Users accuracy.

	BR	BBL	FR	GR	UA (%)	BR	BBL	FR	GR	UA (%)
	(a) Spring					(b) Summer				
<b>BR</b>	31	0	16	0	65	31	2	5	3	67
<b>BBL</b>	0	42	0	14	75	0	34	1	28	54
<b>FR</b>	17	0	35	0	63	10	0	44	0	79
<b>GR</b>	0	15	0	56	78	0	14	0	44	75
<b>PA (%)</b>	64	73	69	80		75	68	78	59	
<b>OA (%)</b>	<b>73</b>					<b>70</b>				
<b>Autumn</b>	(c) Autumn					(d) Winter				
<b>BR</b>	32	0	4	2	72	30	0	1	5	80
<b>BBL</b>	1	27	5	25	43	3	30	1	19	56
<b>FR</b>	11	0	39	0	75	17	3	29	0	49
<b>GR</b>	0	31	0	48	58	0	16	15	45	56
<b>PA (%)</b>	73	47	69	57		50	61	52	65	
<b>OA (%)</b>	<b>65</b>					<b>61</b>				

Generally, overall classification accuracies decreased with seasonal chronological order, starting with Spring, resulting in varying users and producers accuracies across all seasonal imagery. In assessing the results obtained from fused imagery, although the highest overall accuracy was achieved using only optical bands, fused imagery increased overall classification accuracies during spring and autumn, whilst failing to improve on the benchmark of optical imagery during winter

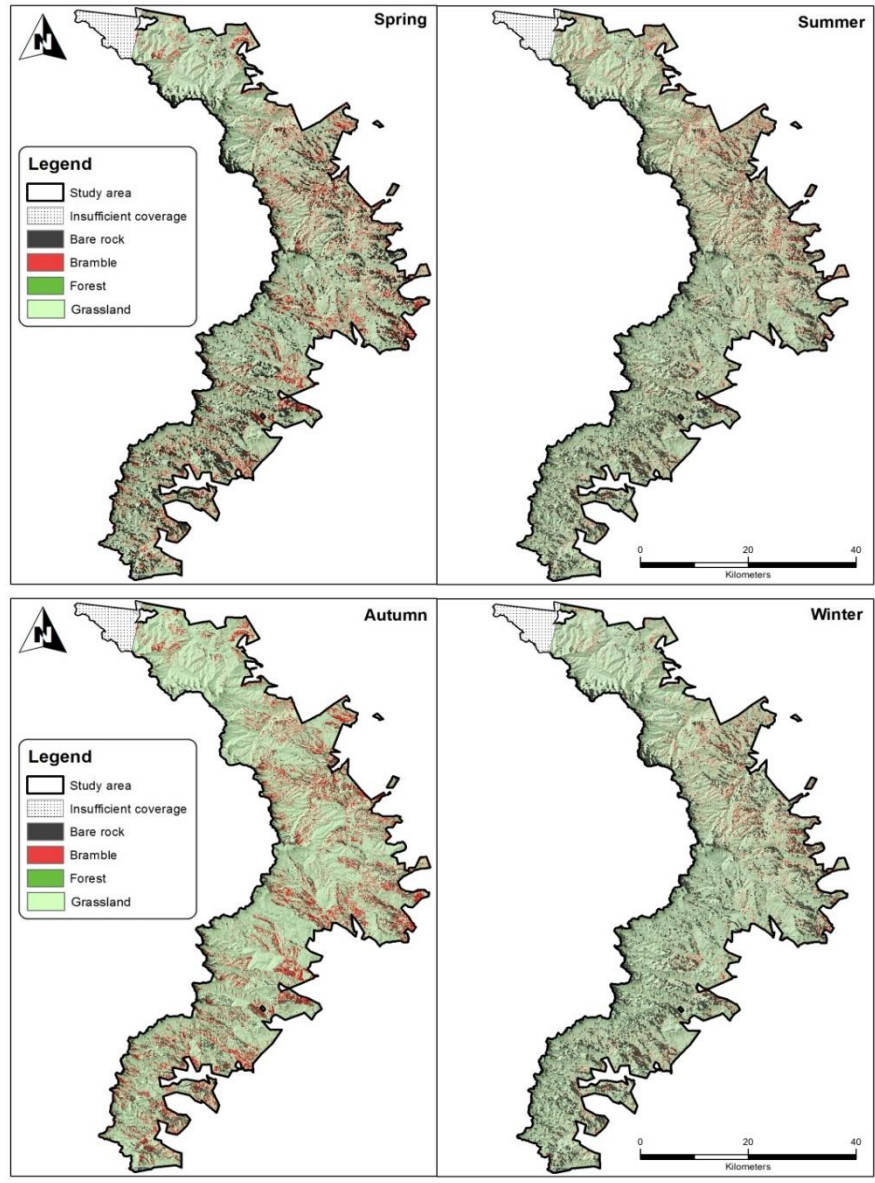


Figure 5.2: Multi-season classification maps produced using VIP selected optical bands and vegetation indices. Where (a) = Spring; (b) = Summer; (c) = Autumn and (d) = Winter.

**5.4 Discussion**

This study sought to determine if the synergistic properties of new generation optical imagery and derived vegetation indices have the potential to increase the discrimination and mapping of American Bramble (*Rubus cuneifolius*) from surrounding native vegetation. In addition, this study sought to determine the optimum season for the detection and mapping of Bramble. Generally, overall accuracies across the wet season (spring and summer) were greater, with spring achieving the highest accuracy (73%) across all seasons. Dry season (autumn and

winter) detection and mapping of Bramble was poor, with winter resulting in the lowest classification accuracy (61%) across all seasons. Wet season overall accuracies suggest that the combination of new age optical imagery bands and vegetation indices derived from these bands have sufficient potential for mapping and detecting Bramble. Sentinel-2 (S2) has an unprecedented three SWIR optical bands; two among the three were considered to be important variables (VIP) for spring, summer and winter seasonal imagery. Indices using the Shortwave Infrared (SWIR) optical band are known to be robust and provide an additional axis for potential vegetation discrimination (Kandwal *et al.*, 2009). These unique characteristics of SWIR optical bands coupled with the increased S2 spectral resolution within the SWIR region, known to be sensitive to foliar water content (Kim *et al.*, 2012), could have contributed to the elevated accuracies seen for spring and summer seasonal imagery.

Simple ratio vegetation indices were repeatedly selected as a result of the VIP process and subsequently utilized in multi-season classification analysis. According to Xue and Su (2017), the simple ratio combination of visible and Near Infrared (NIR) bands significantly improves the ability to distinguish between varying vegetation phenological parameters. This could explain the increased overall classification accuracies experienced during spring and summer as opposed to autumn and winter. Bramble is known to start flowering from early to mid-spring, resulting in white inflorescence (Denny, 1990), an important phenological feature that could have been responsible for the superior performance of vegetation indices during spring. This finding is in agreement with Laba *et al* (2005) and Evangelista *et al* (2009) who similarly compared time series imagery and derivative spectral analyses to map particular invasive alien species, where similar seasonal classification trends were observed in the respective case studies.

Gilmore *et al* (2008) notes that vegetation spectral properties and consequently species separability is dependent on several variables that include leaf pigmentation, water content and leaf structure and size. The red-edge region of the electromagnetic spectrum is known to accurately detect subtle differences between the above-mentioned variables (Cho *et al.*, 2012). Although Sentinel-2 possesses an unprecedented three red-edge bands, none of them were deemed to have a substantial effect as a stand-alone variable on overall classification accuracy. In the instance, the Red edge 1 band was selected as a standalone variable for autumn imagery, which produced the second lowest (65%) overall classification accuracy. However, numerous vegetation indices that incorporated Red edge bands were commonly selected as VIP bands across all seasons. This finding is in agreement with Delegido *et al* (2013), who

developed a unique red-edge normalized vegetation index and successfully validated it against field data, noting it as an integral variable in determining vegetation physiological parameters.

The reduced classification accuracies in the autumn and winter imagery could be closely linked to similarities between the phenological life cycle of Bramble and surrounding native grass and shrub species. Bramble is known to flower during spring and senesce just before autumn and winter (Denny, 1990), thus in synchrony with the inter-annual growth patterns of dominant native grass and shrub species found within the UDP. Successful detection based on phenological characteristics depends on seasonal variability or inter seasonal growth pattern of the target species from surrounding native vegetation (Bradley, 2014). Hence, as Bramble follows the same inter-seasonal growth pattern of surrounding native vegetation, there is an increased probability of misclassification between the target species and surrounding native vegetation (Liu *et al.*, 2013; Taylor *et al.*, 2013; Evangelista *et al.*, 2009). This became evident when attempting to detect and map Bramble using autumn and winter Sentinel-2 imagery.

In comparison to benchmark results achieved by Rajah *et al* (2018), who solely utilized S2 spectral reflectance bands to detect and map Bramble, the synergistic nature of spectral reflectance bands and vegetation indices only increased overall classification accuracies during specific seasons (spring and autumn). Using fused S2 optical imagery and vegetation indices, the optimum season for the detection and mapping of Bramble was determined to be spring. Even though results from this study differ from those of the benchmark, the synergistic nature of fused imagery has reasonable potential to advocate further research within the field of data fusion for invasive alien plant detection and mapping.

## **5.5 Conclusion**

The primary aim of this study was to determine the potential of combined Sentinel-2 spectral bands and vegetation indices in increasing the discrimination and mapping accuracy of American Bramble (*Rubus cuneifolius*). An additional aim was to determine the optimal season for the most effective and accurate Bramble detection and mapping. Results obtained from this study allude to the practical and operational potential within the synergistic properties of combining Sentinel-2 spectral bands and vegetation indices. Furthermore, the optimum season for Bramble detection and mapping was spring, with the highest overall accuracy (73%) across all seasons. In addition to these practical advantages, free availability, wide swath width and short re-visit time of Sentinel-2 are particularly attractive traits that offer unprecedented opportunity for invasive alien mapping at a regional scale.

## Chapter Six

### The utility of Sentinel-2 Vegetation Indices (VIs) and Sentinel-1 Synthetic Aperture Radar (SAR) for invasive alien species detection and mapping

**This chapter is based on:** Rajah, P., Odindi, J. and Mutanga, O., (*Under review: Awaiting Subject editor's decision – Nature Conservation*): The utility of Sentinel-2 Vegetation Indices (VIs) and Sentinel-1 Synthetic Aperture Radar (SAR) for invasive alien species detection and mapping.

#### Abstract

The threat of invasive alien plant species is increasingly becoming a serious global concern. Alien plant invasions adversely affect both ecological services and socio-economic systems. Hence, accurate detection and mapping of invasive alien species is valuable in mitigating adverse ecological and socio-economic effects. Recent advances in active and passive remote sensing technology have created new and cost-effective opportunities for the adoption of remote sensing for invasive species mapping. In this study, new generation Sentinel-2 (S2) optical imagery was compared to: (1) S2 derived Vegetation Indices (VIs) and (2) fused S2 VIs and Sentinel-1 (S1) Synthetic Aperture Radar (SAR) imagery for detecting and mapping the American Bramble (*Rubus cuneifolius*). Fusion of S2 VIs and S1 SAR imagery was conducted at a feature level and multi-class Support Vector Machine (SVM) image classification algorithm used to determine the dominant land use land cover classes. Results indicated that S2 derived VIs were the most accurate (80%) in detecting and mapping Bramble, while fused S2 VIs and S1 SAR were the least accurate (54%). Findings from this study suggest that the application of S2 VIs is more suitable for Bramble detection and mapping than the fused S2 VIs and S1 SAR. The superior performance of S2 VIs highlights the value of the new age S2 VIs for invasive alien species detection and mapping. Furthermore, this study recommends the use of freely available new age satellite imagery for cost effective and timeous mapping of Bramble from surrounding native vegetation and other land use land cover types.

**Key words:** Alien species invasions, Sentinel-1, Synthetic Aperture Radar (SAR), Sentinel-2, Vegetation Indices (VIs), American Bramble, Fusion, Support Vector Machine (SVM).

## 6.1 Introduction

Global biodiversity is increasingly becoming susceptible to pressure from invasive species (Butchart *et al.*, 2010). Specifically, the rapid spread of invasive alien plants in several regions of the world has adversely impacted ecosystem health, native species diversity and local and national economies (Pysek *et al.*, 2012; Schirmel *et al.*, 2016; Convention on Biological Diversity 2009). Brooks *et al.* (2006) highlights the imperative need for the protection of native biodiversity, a need further emphasized by the United Nations (UN), declaring the period between 2010 and 2020 as the decade of biodiversity. The perversity of effects associated with plant species invasion has increased impetus on development of efficient and cost effective approaches for the control and management of invasive alien plants.

In South Africa, approximately two million hectares of land has been invaded by invasive alien plant species (Van Wilgen *et al.* 2012). The south western, southern and eastern coastal and interior regions have been identified as highly vulnerable to invasion (Kotze *et al.*, 2010; Van Wilgen *et al.*, 2012; Clusella-Trullas and Garcia, 2017). In KwaZulu-Natal (KZN) province for instance, Erasmus (1984) notes that the cool and moist conditions favour a range of invasive alien plant species. The American Bramble (*Rubus cuneifolius*) has particularly thrived in the province's western mountain ranges (Henderson, 2011). Originating from North America, Bramble belongs to the *Rosaceae* family and has adverse direct and indirect impacts on biodiversity, which include changes in nutrient cycling, increase in soil erosion, reduction in rangeland carrying capacity and viability, natural plant succession, fire patterns and behavior and hydrological processes (Henderson, 2001).

To develop optimal mitigation of spread and eradication approaches, determination of spatial distribution and extent of Bramble infestation is paramount. Traditionally, surveys have been adopted for mapping and monitoring of invasive alien plant species (Tan *et al.*, 2012; Shah and Reshi, 2014). However, reliance on field based surveys is often restrictive, as they are commonly time consuming, labor and resource intensive and unsuitable in inaccessible sites. Hence, the adoption of remotely sensed imagery for invasive alien species detection and mapping has recently gained popularity. Huang and Asner (2009) attribute this increase to improved sensor technology, facilitating detailed and large scale landscape mapping and monitoring. To date, majority of invasive alien plant species detection and mapping applications have relied on the use of spatial and spectral characteristics (Feilhauer *et al.*, 2017; Mirik *et al.*, 2013; Müllerová *et al.*, 2013). However, the advent of new sensors with radar scanning

capabilities provides new opportunities for invasive plant species detection and mapping (Bradley, 2014). One such example is the European Space Agency's (ESA) sentinel constellation, which consists of the Sentinel-1 (S1) and Sentinel-2 (S2) earth observation instruments. Both sensors disseminate freely available multispectral optical (S2) and multi-polarized SAR (S1) imagery. Unique S1 and S2 sensor characteristics, such as large swath widths, medium to fine scale spatial resolutions, short re-visit times and unique spectral bands (Frampton *et al.*, 2013; Sentinel-1 User handbook, 2013) provide numerous opportunities to evaluate the potential of the sensors to improve the reliability of remote sensing approaches for invasive alien plant species mapping.

Conventional remote sensing of invasive alien species utilizes spectral wavelengths of absorbed and reflected light by distinguishing certain pigments in leaves and inflorescence (Huang and Asner, 2009; Mirik *et al.*, 2013; Weisberg *et al.*, 2017; Müllerová *et al.*, 2013; Bradley, 2014). Hence, the potential to adopt S2 to detect and map invasive alien species exists (Rajah *et al.*, 2018). Specifically, the sensor's unparalleled spectral resolution can be used to derive numerous band ratios and indices useful for vegetation mapping. For example, spectral vegetation indices (VIs) derived from remotely sensed data have become valuable in mapping and monitoring vegetation species (Sun *et al.*, 2007). VIs have several advantages over stand-alone spectral bands that include; reduced effect of atmospheric conditions, canopy geometry and shading, decreased effect of soil background on canopy reflectance and enhanced variability of spectral reflectance of target vegetation (Liu *et al.*, 2004; Vina *et al.*, 2011). On the other hand, the unique characteristics of S1 SAR imagery could provide additional variables that could improve invasive alien species detection and mapping. SAR data can operate at wavelengths irrespective of cloud conditions or lack of illumination and is capable of acquiring data during day and night (Sentinel-1 User handbook, 2013). SAR offers detailed information on the often difficult to detect characteristics of vegetation such as shape, moisture and roughness (Chen *et al.*, 2010). However, despite this potential, previous adoption of SAR imagery for invasive alien plant species mapping has been limited by high acquisition cost, limited area coverages and complex data pre-processing (McNairn *et al.*, 2009). Hence, the provision of freely available SAR imagery from the S1 sensor provides new prospects for advancing the mapping and detection of invasive alien plant species.

Asner *et al.* (2008) and Zhang (2010) note that the fusion of imagery from various sensors, while applying appropriate methodologies may be valuable for invasive alien species detection and

mapping. Furthermore, conventional optical imagery and SAR are commonly believed to be complimentary (Zhu *et al.*, 2012). Considering the above-mentioned advantages, as well as S2s unprecedented potential to derive unique VIs, the fusion of these datasets provides a unique opportunity to investigate the value of new generation sensors such as S1 and S2 in mapping alien species. Accordingly, this study sought to determine the performance of conventional stand-alone S2 optical imagery, stand-alone S2 derived VIs and fused S2 VIs with S1 Synthetic Aperture Radar (SAR) imagery in detecting and mapping the American Bramble.

## 6.2 Methodology

### 6.2.1 Study site

This study was conducted at the uKhahlamba-Drakensberg Park (UDP), a UNESCO World heritage site that borders the western escarpment of the KwaZulu-Natal province of South Africa (Figure 6.1). The UDP is predominantly a natural grassland, with patches of thicket and natural shrub. Seasonal gradients range from cold and dry winters with regular occurrences of frost and snow, to wet and humid summers, with rainfall ranging from 990-1130mm (Dollar and Goudy, 1999).

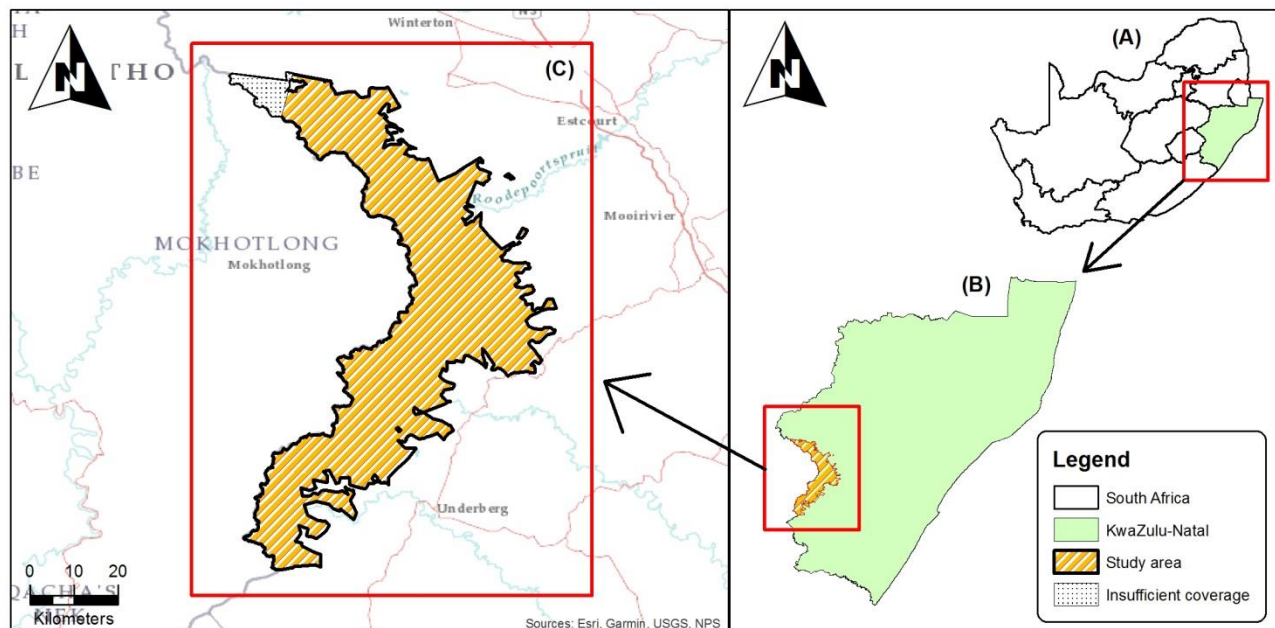


Figure 6.1: The uKhahlamba Drakensberg Park (UDP) (C) located within the KwaZulu-Natal Province (B) of South Africa (A).



#### 6.2.1.1 Field data collection

Field data collection was conducted during spring and summer of 2016. Purposive sampling technique was utilized to record ground truth points of Bramble patches. These seasons were chosen for field data collection as Bramble patches are most phenologically discernable from native vegetation. Ground control points were recorded as close to the centroid of Bramble patches as possible. Collected Bramble patches ranged from 15m x 15m to 50m x 50m. Ground truth point data collected from Bramble patches were spatially independent from each other to compensate for the spatial resolution of satellite imagery utilized. This ensured that each Bramble patch fell within a single image pixel and could be associated with the unique spectral reflectance of a specific pixel. Due to the area's steep and mountainous terrain, hence restricted accessibility, only Bramble patches that could be accessed by foot were considered for this study. In addition, aerial photographs at a 0.5m spatial resolution captured in 2016 were used to supplement and verify selected land cover ground truth points.

#### 6.2.2 Image acquisition

##### 6.2.2.1 Optical Imagery

The ESA SNAP toolbox 3.0 was used to convert summer Sentinel-2 level-1C raw products to surface reflectance values in the Sen2Cor plugin. Images were corrected for topographic effects of shadow associated with mountainous areas using the System for Automated Geoscientific Analyses SAGA (2.1.2) terrain analysis lighting tool within the Quantum GIS (QGIS) environment on a band by band basis. QGIS is a GIS freeware and is comparable to ESRI ArcMap commercial GIS software. SAGA is a plugin that works in conjunction with QGIS. The correction of topographic effects is a tool within the SAGA plugin that best adjusts optical imagery for topographic effects of shadow.

##### 6.2.2.2 Sentinel-1 Synthetic Aperture Radar (SAR) Imagery

Summer Synthetic Aperture Radar (SAR) images were downloaded from the Sentinel-1 data hub. Sentinel-1 level-1 Ground Range Detected (GRD) products were multi-looked and projected to ground range using an earth ellipsoid model. SAR Vertical-Horizontal (VH) polarized imagery was acquired using the Interferometric Wide Swath (IW) mode, with a spatial resolution of 20 meters and a 250km<sup>2</sup> swath width. Pre-processing of SAR imagery was conducted using the ESA SNAP toolbox following the methodology outlined in Bevington (2016). The Bevington (2016) SAR image processing chain consists of 5 steps: (1) Application

of orbit file to SAR image; (2) Radiometric calibration; (3) Terrain correction; (4) Application of speckle filter; (5) Convert SAR DN to Gamma backscatter values. Polarisation of SAR imagery recorded in Vertical Horizontal (VH) acquisition mode was fused with S2 derived VIs. SAR backscatter measurements are believed to be a function of polarization and target object characteristics such as geometry, roughness and dielectric properties (Vyjayanthia and Nizalapur, 2010).

#### 6.2.2.3 Sentinel-2 derived Vegetation Indices (VIs)

Sixty-five Vegetation Indices (VIs) selected from the online Index DataBase (IDB) ([www.indexdatabase.de](http://www.indexdatabase.de)) were calculated from summer Sentinel-2 surface reflectance optical imagery. The IDB is a tool developed to provide a simple overview of satellite specific vegetation indices that are useable from a specific sensor for a specific application (Henrich *et al.*, 2012). All VIs were calculated within a python 2.7.13 environment using listed formulas from the IDB and spectral reflectance Sentinel-2 bands. The 10 most influential VIs were selected for stand-alone classification results and subsequent image fusion with SAR imagery in order to produce a fused VIs and SAR classification result. Top 10 VI selections were done using the Variable Importance in the Projection (VIP) method. Variable Importance in the Projection aims to improve classification accuracy by recognizing a subset of all initial variables (VIs) that if combined, could increase classification accuracies with parsimonious representation (Farrés *et al.*, 2015). VIP measured the importance of each VI with regard to the impact it had on increasing overall classification accuracy.

#### 6.2.3 Image fusion

Feature level image fusion was adopted to merge the ten most influential VIP VIs and Sentinel-1 SAR imagery. All VIs were derived from S2 optical bands at a spatial resolution of 20m. The extraction of ground truth points was done on an individual basis for VIs and SAR imagery. The feature level fusion of VIs and SAR ensured that the corresponding SAR value was used for the same VI value. Image fusion at a feature level as outlined above, further contributes information to features (ground truth points), and ultimately provides additional information for image analysis (Pandit, 2015). The extracted VI and SAR feature values were combined to form an optimum feature set. This fused optimum feature set was used to conduct the classification process.

#### 6.2.4 Image classification

Image classification was conducted post feature level image fusion as outlined in Pandit (2015). The Support Vector Machine (SVM) algorithm was used within a Python environment. The SVM algorithm is a supervised statistical learning technique initially developed to handle binary classification (Vapnik 1979). SVM aims to identify a hyper-plane that is able to distinguish the input dataset into a predefined discrete number of classes consistent with training data (Mountrakis *et al.*, 2010). Several evaluations of SVM have shown that the algorithm is capable of classifying/separating several classes with limited support vectors as training data, without ultimately compromising classification accuracies (Foody and Mathur, 2004; Mantero *et al.*, 2005; Bruzzone *et al.*, 2006; Shao *et al.*, 2012; Zheng *et al.*, 2015). Spectra were extracted using ground truth points for four major land cover classes (Bare rock, Bramble, Forest and Grassland) within the study area. The fused VIP vegetation indices and SAR image measurements were used in the SVM classification process.

#### 6.2.5 Determination of spatial distribution and validation

Support Vector Machine classification maps were generated for S2 optical imagery; Vegetation Indices and for the fused VIs and SAR imagery within a Python environment. Training data (70%) of all four considered land cover classes were used as the input for Bramble spatial distribution maps. The respective test data set (30%) was then used to assess classification accuracies across all imagery. A confusion matrix generated from the SVM process was used to quantify the accuracy of resultant Bramble spatial distribution maps.

### 6.3 Results

#### 6.3.1 Vegetation Indices (VIs)

Discrimination and mapping of Bramble using stand-alone vegetation indices produced the highest overall accuracy (80%) when compared to the benchmark of using only S2 optical image bands (Table 6.1). A users' accuracy of 70% for Bramble surpassed those achieved by S2 optical imagery as well as fused vegetation indices and SAR imagery (Table 6.1).

Table 6.1: Support Vector Machine (SVM) confusion matrix using Vegetation Indices for Bramble mapping and discrimination. Where BR = Bare rock; BBL = Bramble; FR = Forest; and GR = Grassland, UA = Users accuracy; PA = Producers accuracy and OA = Overall accuracy.

<b>Vegetation Indices (VIs)</b>	<b>BR</b>	<b>BBL</b>	<b>FR</b>	<b>GR</b>	<b>UA (%)</b>
<b>BR</b>	52	11	0	0	83
<b>BBL</b>	0	53	18	5	70
<b>FR</b>	1	0	51	0	98
<b>GR</b>	11	7	0	55	75
<b>PA (%)</b>	81	75	74	92	
<b>OA (%)</b>	80				

The classification map resulting from fused vegetation indices and SAR imagery showed the most accurate discrimination and spatial distribution of all considered land cover classes. The Grassland and Bare rock classes were well represented and accurately discriminated (Figure 6.2a and 6.3b). In addition, the spatial discrimination and distribution of Bramble was well represented as compared to the S2 optical band benchmark and the fused VIs and SAR imagery (Figure 6.2a and 6.3b). The Forest class was the only class that was underestimated using VIs and the SVM algorithm.

### 6.3.2 Sentinel-2 optical bands

The overall accuracy using S2 optical bands for Bramble discrimination and mapping was 77% (Table 6.2). Bramble produced the lowest users' accuracy (45%) across all considered classes, while Grassland produced the lowest producers' accuracy (68%) (Table 6.2). Results produced using only S2 optical bands were used as a benchmark for classification using VIs and VIs fused with SAR imagery.

Table 6.2: Support Vector Machine (SVM) confusion matrix using Sentinel-2 optical bands for Bramble mapping and discrimination. Where BR = Bae rock; BBL = Bramble; FR = Forest; and GR = Grassland, UA = Users accuracy; PA = Producers accuracy and OA = Overall accuracy.

<b>. S2 (Optical bands)</b>	<b>BR</b>	<b>BBL</b>	<b>FR</b>	<b>GR</b>	<b>UA (%)</b>
<b>BR</b>	32	2	0	12	69
<b>BBL</b>	0	24	0	29	45
<b>FR</b>	1	1	54	3	91
<b>GR</b>	2	3	7	94	88
<b>PA (%)</b>	91	80	88	68	
<b>OA (%)</b>	<b>77</b>				

A large over-estimation of Bramble discrimination and spatial distribution using S2 optical bands was evident (Figure 6.2b and 6.3a). An underestimation in Grassland discrimination and spatial distribution was observed, as the SVM algorithm could not effectively distinguish between Bramble and Grassland (Table 6.2, Figure 6.2b). An underestimation in the spatial distribution of the Bare rock class was also evident, as there was consistent misclassification of Bare rock from Grassland and Bramble (Figure 6.2b and 6.3a).

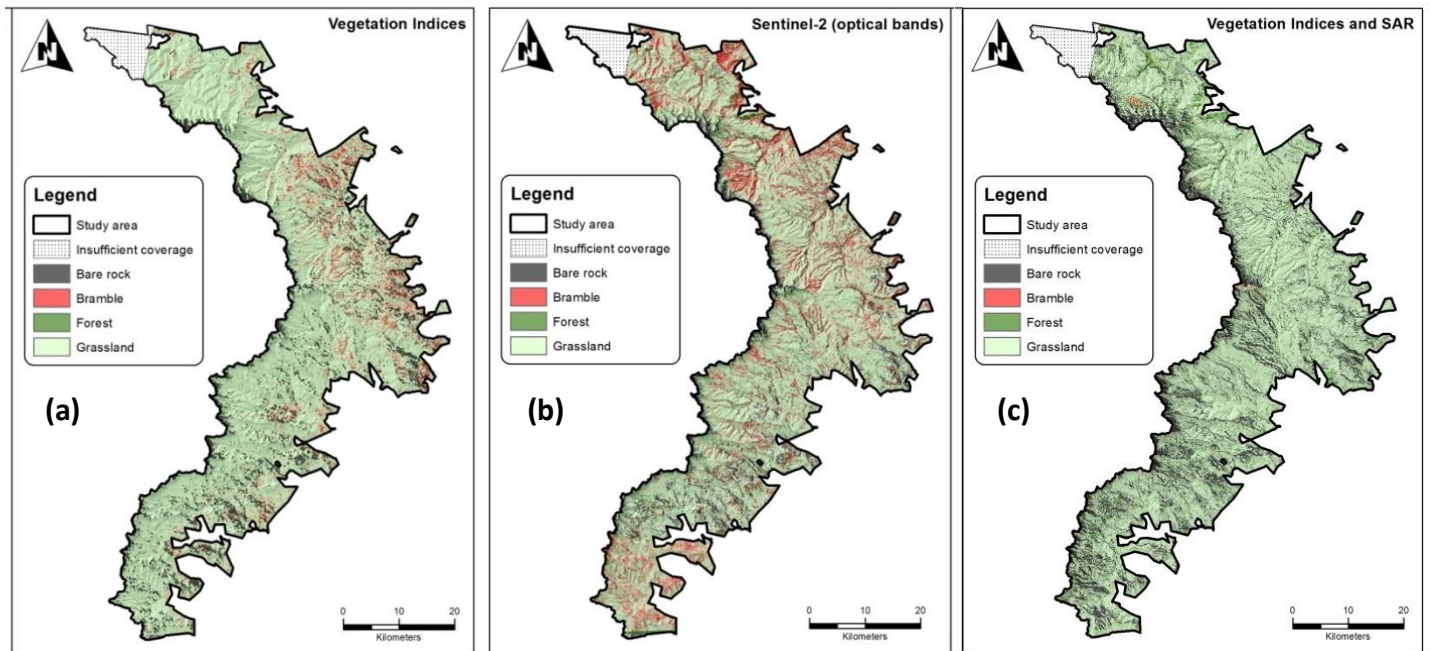


Figure 6.2: Support Vector Machine (SVM) classification maps produced utilizing (a) Vegetation Indices; (b) S2 optical bands and (c) Fused VIs and SAR.

### 6.3.3 Vegetation Indices (VIs) and S1 SAR imagery

The ten most influential S2 VIs were selected for feature level image fusion with S1 SAR imagery. Influence of VIs was identified by the importance each VI had on increasing overall classification accuracy. The ten bands that generated ten highest classification accuracies were selected. Five of the selected VIs incorporated the Near Infrared (NIR) optical band, while three selected VIs were derived using Shortwave Infrared 1 (SWIR1) and Shortwave Infrared 2 (SWIR2) optical bands (Table 6.3). The SR520/670 and SR672/550 VIs were the only two VIP VIs derived using bands within the visible portion of the electromagnetic spectrum (Table 6.3).

Table 6.3: Selected S2 derived VIP vegetation indices subsequently utilized for SAR fusion.

VIP Vegetation Indices (VIs)	VI formula (S2 optical bands)
Datt2 (Simple Ratio 850/710)	Near Infrared (NIR)/Red Edge 1
PSSRc2 (Simple Ratio 800/470 Pigment specific simple ratio C2)	Near Infrared (NIR)/Blue
RDVI (Renormalized Difference Vegetation Index)	$\text{Near Infrared} - \text{Red} / (\text{Near Infrared} + \text{Red})^{0.5}$
SR520/670 (Simple Ratio 520/670)	Blue/Red
SR672/550 (Simple Ratio 672/550)	Red/Green
SR800/550 (Simple Ratio 800/550)	Near Infrared/Green
SR833/1649 (Simple Ratio 833/1649 MSIhyper)	Near Infrared /Shortwave Infrared1
SR860/550 (Simple Ratio 860/550)	Narrow-Near Infrared/Green
SRMIR/Red (Simple Ratio MIR/Red Eisenhydroxid-Index)	Shortwave Infrared2/Red Edge 1
TM5/TM7 (Simple Ratio 1650/2218)	Shortwave Infrared1/ Shortwave Infrared2

The fusion of VIs and S1 SAR imagery produced the lowest overall accuracy (54%) when compared to the benchmark of S2 optical band results (Table 6.4). Bramble users' and producers' accuracies were 28% and 21% respectively (Table 6.4), the lowest in all classes. The Forest (77% and 98%) and Bare rock (77% and 100%) classes were the highest users and producers accuracies, respectively.

Table 6.4: Support Vector Machine (SVM) confusion matrix using fused Vegetation Indices and SAR imagery for Bramble mapping and discrimination. Where BR = Bae rock; BBL = Bramble; FR = Forest; and GR = Grassland, UA = Users accuracy; PA = Producers accuracy and OA = Overall accuracy.

<b>(c) VIs and SAR</b>	<b>BR</b>	<b>BBL</b>	<b>FR</b>	<b>GR</b>	<b>UA (%)</b>
<b>BR</b>	43	2	0	11	77
<b>BBL</b>	0	15	0	38	28
<b>FR</b>	1	0	45	17	71
<b>GR</b>	0	53	0	39	42
<b>PA (%)</b>	98	21	100	37	
<b>OA (%)</b>	<b>54</b>				

The SVM classification map produced using fused vegetation indices and SAR resulted in an underestimation of the Bramble class, while an overestimation of the Grassland class was observed (Figure 6.2c). Although the Forest class received high users and producers accuracies, the overall distribution and discrimination was over estimated as compared to the benchmark (Figure 6.2c and 6.3c).



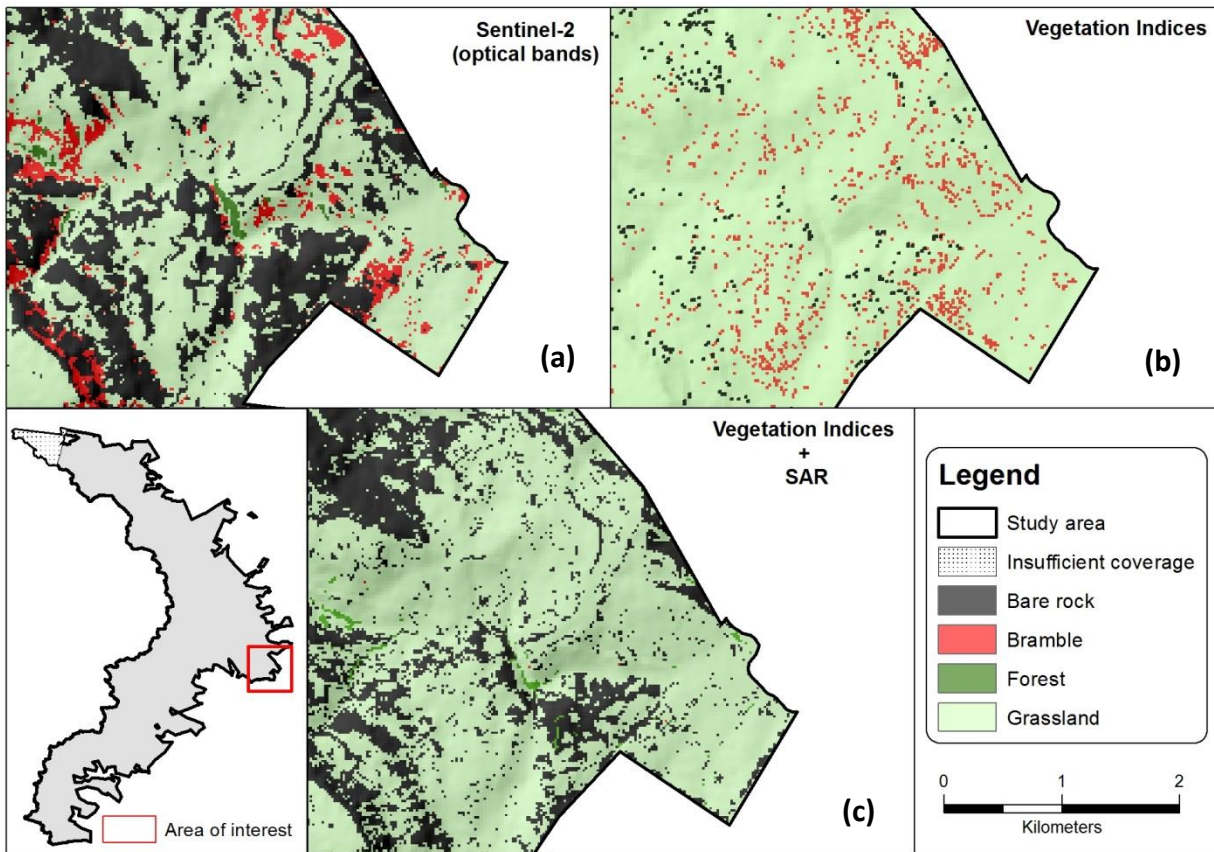


Figure 6.3: Over-estimation and under-estimation of land-cover classes within an area of interest where (a) = S2 optical bands; (b) = Vegetation indices (VIs) and (c) = VIs and SAR imagery.

## 6.4 Discussion

This study sought to determine the potential of derived Vegetation Indices (VIs) and fused VIs and Synthetic Aperture Radar (SAR) imagery to improve invasive alien species detection and mapping. The overall classification accuracy of optical imagery was used as the benchmark for comparison of the results achieved using S2 VIs and fused VIs and SAR. Opposing the expected outcome, fused VIs and SAR imagery produced the lowest classification accuracy (54%) compared to conventional S2 optical imagery (77%). Moreover, S2 derived VIs produced the highest classification accuracy (80%) when compared to conventional S2 optical imagery and fused VIs and SAR.

Poor performance of fused VIs and SAR imagery was unanticipated and opposes research done by Sano *et al* (2005), who noted that the combination of VIs and SAR for discrimination within a savannah environment was complementary and improved overall discriminant analysis.

Sano *et al* (2005) also noted that VIs and SAR were able to easily separate Grassland from woodlands, a result that further opposes those achieved in this study. However, Sano *et al* (2005) also reported increased confusion between Grassland and shrub species when utilizing fused VIs and SAR. This provides some indication that previous research has also encountered unanticipated results when combining VIs and SAR for discrimination purposes. Poor overall classification accuracies of fused VIs and SAR imagery can further be attributed to vegetation structure and roughness, as this plays a major role in measured SAR backscatter values. Similar difficulties were documented by Millard and Richardson (2018), who note that even though it is well established that vegetation roughness influences SAR backscatter, there still remains difficulty in characterizing these variables spatially and temporally within natural environments. Although results from fused VIs and SAR were unexpected, similar poor performance using the same combination of variables is not unrealistic. For example, Rakwatin *et al* (2005) and Toma *et al* (2004) also experienced poor performance when fusing VIs and SAR.

Patel *et al* (2006) and Srivastava *et al* (2009) note that the magnitude of SAR backscatter is dependent on SAR band frequency, for instance, SAR backscatter signatures at high frequency (eg. X-band SAR) are known to be sensitive to subtle variations in vegetation phenology. This is attributed to deep canopy penetration of X-band SAR. Sentinel-1 C-band SAR is considered low frequency (decreased canopy penetration) SAR imagery, and could have experienced difficulty discerning between Bramble characteristics and surrounding native vegetation, providing further explanation for decreased accuracies resulting from fused VIs and S1 SAR imagery (Khosravi *et al.*, 2017; Duguay *et al.*, 2015; Naidoo *et al.*, 2015; Hajj *et al.*, 2014; van Beijma *et al.*, 2014; Turkar *et al.*, 2012). The influence of sensor incident angle on SAR backscatter is known to be interpreted using the same mechanism, particularly for lower frequencies of SAR. Inoue *et al* (2003) notes that correlations to plant physiological characteristics, such as Leaf Area Index (LAI), canopy height and stem density decrease with an increasing incident angle. This is mainly attributed to the penetration of SAR microwaves responsible for backscatter measurements, as smaller incident angles are able to penetrate deeper into canopy cover hence extract more physiological information (McNairn *et al.*, 2009). The relatively large incident angle of S1 (46°) (Sentinel-1 User handbook, 2013) could have hindered its ability to distinguish vegetation physiological information, which could serve to justify decreased classification accuracies achieved using fused VIs and SAR imagery (de Almeida Furtado *et al.*, 2016; Naidoo *et al.*, 2015; Frampton *et al.*, 2013; Vyjayanthia and Nizalapur, 2010). The influence of soil moisture

and roughness on leaf and stalk SAR backscatter measurements is considered a weakness of SAR imagery across specific classification applications (Moran *et al.*, 2002). SAR imagery could have served to increase confusion between Bramble and surrounding native vegetation when fused with S2 VIs.

The use of S2 VIs outperformed the benchmark accuracy achieved by conventional S2 optical imagery. Similar results were achieved by Kandwal *et al* (2009), where selected VIs performed well in discriminating *Lantana camara* (*Verbenaceae*), an invasive alien plant with similar growth pattern and phenology to Bramble. Majority of VIs selected as VIP indices were dominated by VIs incorporating the Near Infrared (NIR), Shortwave Infrared (SWIR) and red edge S2 bands. A study conducted by Zhao *et al* (2007) produced similar results, where VIs derived from SWIR, red-edge and NIR bands were reported to be closely correlated to canopy LAI and canopy chlorophyll density. Eight of the ten VIP VIs selected for Bramble discrimination and mapping were derived from at least one of these three spectral bands. The strong relationship between NIR, SWIR and red edge bands to variable vegetation parameters could have resulted in the increased accuracy of Bramble discrimination and mapping. Moreover, reflectance within the visible region of the spectrum is largely determined by vegetation pigments, and are commonly used to quantify vegetation physiological properties (Li *et al.*, 2013; Zhao *et al.*, 2007). The collective capability of combined VIs to discriminate various vegetation parameters could further explain the increased overall classification accuracy achieved using stand-alone vegetation indices.

According to Motohka *et al* (2010), the potential of green-red VIs for phenological vegetation discrimination exists. VIs derived from ratios of red and green optical bands are known to be sensitive to variations in canopy colour, where changes in visible characteristics of vegetation canopy are often timeously detected (Motohka *et al.*, 2010). The SR672/550 VI, an index derived solely from S2 red and green optical bands suggest an agreement with Motohka *et al* (2010). The SR672/550 VI could have assisted in the discrimination of Bramble as it produces noticeable white inflorescence during summer, a significant phenological trait that could have been exploited. Although the combined potential of VIs and SAR imagery produced the lowest overall classification accuracy, the potential of new age spectrally derived VIs was evident when compared to the benchmark set by conventional S2 optical imagery. While the fusion of S2 VIs and SAR showed limited utility with regard to accurately mapping Bramble, the complementarity of these data sets has previously been documented. Continued research into the application of new age sensors to improve alien invasive detection and mapping should concentrate on

innovative methods of integrating products derived from active and passive remote sensing technology.

## **6.5 Conclusion**

This study utilized freely available new age Sentinel-1 radar and Sentinel-2 optical imagery, with the aim of evaluating spectrally derived VIs and fusing Synthetic Aperture Radar (SAR) imagery for improving American Bramble (*Rubus cuneifolius*) detection and mapping. This study contributes to the evaluation of economically viable, efficient and large scale invasive alien species detection and mapping. Conventional S2 optical imagery was used as a benchmark for comparison to results achieved using S2 VIs and fused VIs and S1 SAR imagery. The use of S2 VIs increased overall classification accuracies as compared to traditional optical imagery results, while the fusion of S2 VIs and S1 SAR decreased the overall accuracies significantly. Hence this study demonstrated that new age S2 VIs have the potential to increase the detection and mapping of Bramble from surrounding native vegetation. Results further indicate that the fusion of VIs and SAR imagery for Bramble detection and mapping failed to increase overall classification accuracies, hence have limited utility when applied to Bramble detection and mapping. Since new age sensors such as S1 and S2 possess unprecedented sensor characteristics that can be used to improve landscape delineation, the utility of S1 and S2 Bramble mapping. It is this type of innovative and continued research that will ultimately guide effective, economical and accurate invasive alien plant eradication and management strategies.

## Chapter Seven

### **The synergistic potential of dual-polarized Synthetic Aperture Radar (SAR) and multispectral optical imagery for invasive alien species detection and mapping**

**This chapter is based on:** Rajah, P., Odindi, J. and Mutanga, O., (*In preparation*): The synergistic potential of dual-polarized Synthetic Aperture Radar (SAR) and multispectral optical imagery for invasive alien species detection and mapping.

#### **Abstract**

Invasive alien species are a major threat to global biodiversity, and ultimately result in adverse environmental and socio-economic implications such as reduced ecosystem services, reduced landscape productivity and costly eradication initiatives. The ability to monitor the extent and spread of alien species invasions provides valuable insight for the mitigation of these adverse implications. The new generation Earth Observation (EO) Sentinel sensor provides unprecedented freely-available imagery suitable for both local and regional invasive species monitoring. Specifically, its radar (S1) and optical (S2) sensors offer unique tandem datasets valuable for landscape analysis. Hence, this study sought to fuse S1 dual-polarized Synthetic Aperture Radar (SAR) imagery with S2 optical imagery to determine their synergistic potential for invasive alien species detection and mapping. S1 and S2 imagery were fused at feature level and the Support Vector Machine (SVM) algorithm used for multi-class image classification. Results indicated that the fusion of S1<sub>vv-vh</sub> dual-polarized imagery with S2 optical imagery produced the highest classification accuracy (85%), while stand-alone S2 optical bands produced the lowest classification accuracy (79%). Findings from this study underline the significant synergistic potential and complementarity of new age S2 optical imagery and dual-polarized S1 SAR imagery for invasive alien species detection and mapping. Due to large swath, higher pixel resolution, free availability and possible tandem complementarity between optical and SAR sensors, this study recommends Sentinel EO imagery as an economically viable option for invasive alien species detection and mapping.

**Key words:** Invasive alien species, Dual-polarized, Synthetic Aperture Radar (SAR), Sentinel-1, Sentinel-2, Image fusion, synergistic, Support Vector Machine (SVM)

## 7.1 Introduction

The European Union (EU) Global Monitoring for Environment and Security (GMES) programme launched the Sentinel satellite constellation that consists of two new age remote sensing satellites; Sentinel-1 (Synthetic Aperture Radar - SAR) and Sentinel-2 (multispectral) optical sensors. Both sensors provide freely available 250km<sup>2</sup> multi-polarized SAR imagery and 290km<sup>2</sup> multispectral optical imagery respectively. Goa *et al* (2017) notes that the tandem operation and the respective unique characteristics of these two satellites have established a new paradigm for remote sensing applications. According to Schmidt *et al* (2017), the timeous launch of the GMES satellite constellation could serve to increase the applicability of remote sensing-based approaches for practical landscape mapping and monitoring

Recently, invasive alien species detection and mapping using remote sensing approaches has received increased attention (Haug, 2009). Alien invasive species can be detrimental to ecosystem services and functioning, integrated water resource management, fire regimes, the movement of wild animals and domestic livestock, rangeland biodiversity, human health and local and regional biodiversity (Avery *et al.*, 2017; Ghulam *et al.*, 2011; Dorigo *et al.*, 2012; Bromilow, 2010). Hence, reliable, timeous and cost effective monitoring of alien species invasions is paramount in mitigating their effects. Haug (2009) notes that the recent increase in the adoption of remote sensing to invasive alien species detection and mapping is largely attributed to improvement in sensor characteristics and missions (Haug, 2009).

The Sentinel mission with S1 and S2 sensors offers improved SAR and optical imagery respectively. The potential for complementarity between SAR (S1) and optical imagery (S2) has been noted in literature (Joshi *et al.*, 2016; Baghdadi *et al.*, 2016; Ghulam *et al.*, 2014). According to Mohan *et al* (2011), SAR has demonstrated potential in characterizing vegetation due to its sensitivity to variations in vegetation structure and biomass. The value of SAR complementarity to optical imagery lies in its ability to measure vegetation physical structure, a trait that is only partially described by optical imagery (Schmidt *et al.*, 2017; Laurin *et al.*, 2013). SAR signals utilize transverse electromagnetic waves, hence varying polarization characteristics. Polarization refers to the orientation of the electric field vector of the transmitted and received SAR electromagnetic waves. SAR imagery can be broadly categorized into four polarization modes; single-polarization, dual-polarization, compact polarization and fully polarized imagery (Song *et al.*, 2018). According to Kourgli *et al* (2010), certain polarizations are more sensitive to different target specific characteristics and properties like roughness and

structure. Although the adoption of single polarized SAR imagery for invasive species mapping has been well documented (Naidoo *et al.*, 2015; Ghulam *et al.*, 2014; Hong *et al.*, 2014; Bourgeau-Chavez *et al.*, 2013; Ghulam *et al.*, 2011), the use of dual-polarized SAR imagery for invasive alien species mapping and detection remains largely unexplored.

The integration (fusion) of S1 and S2 imagery provide unique opportunities for invasive plant detection and mapping. The purpose of image fusion is to integrate complementary data to obtain additional or enhanced feature or surface characteristics, often difficult to derive from single sensor datasets (Zeng *et al.*, 2006; Jiang *et al.*, 2013). Hence, the synergy of conventional spectral reflectance and unique dual-polarized SAR characteristics such as the ability to infer canopy characteristics (Ghulam *et al.*, 2014), increased signal sensitivity, and the ability to quantify vegetation structure (Naidoo *et al.*, 2015) offer great potential for invasive species detection and mapping.

Remote sensing image fusion techniques are classified into three categories; pixel, feature and decision level fusion (Solberg, 2006; Sahu and Parsai, 2012; Pandit and Bhiwani, 2015). Feature level image fusion is the intermediate category of fusion and will be further explained. Typically, feature level image fusion ensures correlative feature information, eliminates redundant features and form new compound features, hence increasing reliability of feature information (Simone *et al.*, 2002; Jiang, 2013). Advantages such as optimality for real-time processing, information compression and increased feature information are some of the major benefits associated with use of feature level fusion (Jiang, 2013; Zhang, 2010).

To date, the majority of invasive species detection and mapping studies have solely relied on optical sensors and spectral reflectance (Evangelista *et al.* 2009; Kimothi and Dasari, 2010; He *et al.*, 2011; Gil, *et al.*, 2013; Hauglin and Ørka, 2016). Although conventional multispectral imagery has generated reasonable success (Bradley, 2014), the application of new-age remotely sensed imagery has great potential for increased accuracy. SAR sensors such as S1 are capable of providing diverse polarization and frequency acquisitions. These offer more comprehensive information regarding target variables, consequently offering potential for increased mapping accuracies (Shang *et al.*, 2009). Furthermore, new age satellite imagery circumnavigates challenges involving spatial and spectral resolution, cost, data size and data processing time, which often render conventional detection and mapping approaches impractical, laborious and costly, particularly at large spatial extents. The ability of S1 to acquire dual-polarized SAR imagery in tandem with S2's unique spectral and spatial resolution provides

a novel opportunity to investigate the use of dual-polarized SAR imagery for invasive alien species detection and mapping. Accordingly, this study sought to determine the potential of Sentinel-1 dual-polarized SAR imagery fused with Sentinel-2 optical imagery for invasive alien species detection and mapping.

## 7.2 Methodology

### 7.2.1 Study area

This study was conducted at the uKhahlamba Drakensberg Park (UDP) UNESCO World Heritage site situated along the western escarpment of the KwaZulu-Natal province, South Africa (Figure 7.1). The UDP is dominated by natural grassland with patches of native scrubs, bushland and natural forest environments. Seasonal characteristics of the UDP range from cold dry winters with occasional frost and regular snowing to humid wet summers with rainfall ranging between 990 and 1130mm (Dollar and Goudy, 1999).

### 7.2.2 Target species

Native flora and fauna within South African grasslands are significantly threatened by the recent emergence of the American bramble (*Rubus cuneifolius*). Bromilow (2010) describes Bramble as a sprawling shrub species belonging to the *Rosaceae* family. Originating from North America, Bramble has successfully invaded vast natural grassland landscape within the KwaZulu-Natal (KZN) province of South Africa. The province's favourable cool and moist climate allows it to thrive.



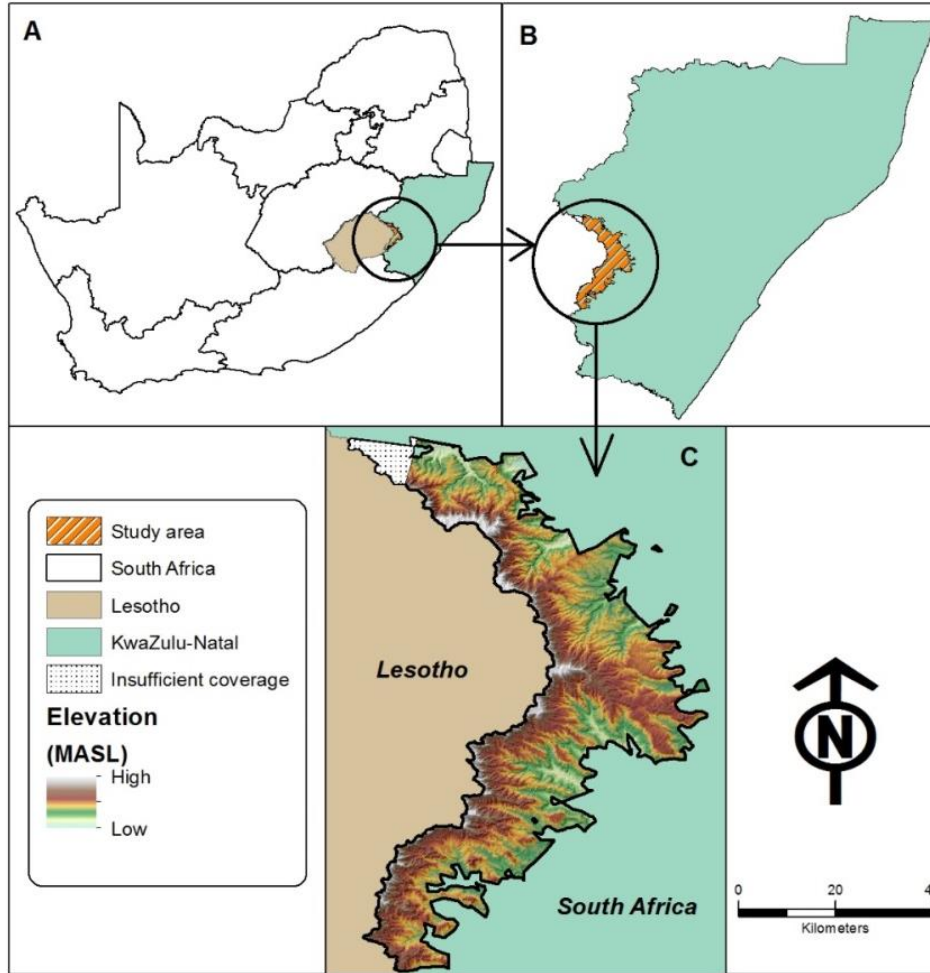


Figure 7.1: The uKhahlamba Drakensberg Park boundary (C), located within the KwaZulu-Natal province (B) of South Africa (A).

Some of the consequences attributed to these Bramble's invasion include increased soil erosion, altered nutrient cycling, reductions in grazing land's carrying capacity, changes in fire regimes and a general disruption of hydrological processes (Henderson *et al.*, 2001). Within the study area, Bramble is considered a severe threat to natural resources and sustainability, hence, its effective management or eradication is of paramount importance.

### 7.2.3 Field data collection

Ground truth data was collected using purposive sampling technique that involved the collection of ground truth validation points of four major land-cover classes within the UDP. Ground truth point data was collected for grassland, bare rock, bramble and forest. All ground truthing data

was collected during the spring and summer seasons as target species (Bramble) patches are easily discernible from surrounding vegetation. A GeoXT-Trimble differentially corrected GPS was used to record Bramble patches and surrounding vegetation classes. All land-cover ground truth points were captured (GPS-co-ords) as close to the centroid of the respective land-cover as possible. To ensure all land-cover ground truth data were associated with their respective pixel values, all field collected land-cover classes were spatially independent from each other. Target species (Bramble) patches collected ranged from 15m x 15m to 50m x 50m in size. Bramble ground truth points were only collected if located more than one-pixel away from the next Bramble patch, hence ensuring spatial independence. Due to the area's steep mountainous terrain with restricted accessibility, only Bramble patches accessible on foot were considered for the study. Aerial photographs of 0.5m spatial resolution captured in 2016 were also used to supplement and verify selected land-cover ground truth points. A total of 1000 ground truth points were collected and used in the study.

#### 7.2.4 Dual polarized Sentinel-1 Synthetic Aperture Radar (SAR) imagery

Summer Sentinel-1 dual polarized Synthetic Aperture Radar (SAR) imagery was downloaded from the Copernicus open access data hub (<https://scihub.copernicus.eu/dhus/>). Sentinel-1 level-1 Ground Range Detected (GRD) products were utilized for this study. All dual polarized level-1 GRD products were multi-looked and projected to ground range using an earth ellipsoid model. S1 dual polarized imagery was recorded using the Interferometric Wide Swath (IW) mode, with a 20 m spatial resolution and a 250km<sup>2</sup> swath width. The Bevington (2016) step-by-step SAR imagery pre-processing methodology was followed. The SAR image processing chain consists of five steps: (1) Application of orbit file to SAR image; (2) Radiometric calibration; (3) Terrain correction; (4) Application of speckle filter and (5) Conversion of SAR DN to Gamma backscatter values (Bevington 2016). The Sentinel-1 mission has a predefined observation plan in order to prevent potential conflicts of interest among users regarding SAR operation modes or polarisation schemas over particular geographical areas. Hence, the general principle for S1 dual-polarisation SAR imagery is as follows: HH-HV/HH polarization for the monitoring of polar environments or sea-ice zones and VV-VH/VV polarization for all other observation zones. The two available dual polarized data sets over the UDP were used for image fusion i.e. VV-VH and VV-VV dual-polarized combinations.

### 7.2.5 Sentinel-2 optical imagery

Summer Sentinel-2 optical imagery was downloaded from the Copernicus open access data hub (<https://scihub.copernicus.eu/dhus/>). The Sentinel-2 open access data hub provides access to freely available level-1C raw Sentinel-2 optical data products. Level-1C Sentinel-2 optical data products are disseminated in radians. The ESA SNAP toolbox 3.0 was used to convert summer level-1C raw products from radian pixel values to surface reflectance values using the Sen2Cor plugin. Sen2Cor applies Sentinel-2 Atmospheric Correction (S2AC) and performs atmospheric correction based on the LIBRADTRAN radiative transfer model (Richter *et al.*, 2011; Mayer and Kyling, 2000). Due to the mountainous terrain associated with the UDP, Sentinel-2 images were corrected for topographic effects of shadowing. Topographic correction was performed using the System for Automated Geoscientific Analyses SAGA (2.1.2) terrain analysis lightening tool within the freeware Quantum GIS (QGIS) environment. The terrain analysis lightening tool topographically corrected all images using the Minnaert Correction method, a method which considers satellite azimuth and height.

Sentinel-2s Vegetation Red Edge 1; Vegetation Red Edge 2; Vegetation Red Edge 3; Near Infrared; Narrow-Near Infrared; Shortwave Infrared 1 and Shortwave Infrared 2 bands were the optical bands considered for feature level image fusion. The use of these bands in vegetation classification is well documented (Frampton *et al.*, 2013; Hill, 2013), and the unprecedented spectral resolution of these S2 bands provide a unique opportunity to assess their combined potential for invasive species detection and mapping.

### 7.2.6 Feature level image fusion

Feature level image fusion was employed to fuse S2 optical and S1 dual-polarized SAR imagery. Dual-polarized SAR images were resampled to a 20 meter spatial resolution so as to ensure all fused imagery possessed a standard spatial resolution (Sentinel-2). The extraction of features (ground truth points) was done separately for optical imagery (spectral) and dual-polarized SAR imagery (backscatter), where subsequent backscatter measurements were allocated to the corresponding extracted S2 spectral reflectance measurement. The extracted spectral reflectance and SAR backscatter feature values were combined to form a fused optimum feature set. The fused optimum feature set was subsequently used for the classification.

### 7.2.7 Image classification

The optimum feature set (fused optical and SAR) was classified using SVM algorithm. SVM is a supervised statistical learning technique first developed by Vapnik (1979) to deal with binary classifications. The algorithm aims to find a hyper-plane that divides the dataset into a discrete predefined number of classes consistent with training data (Mountrakis *et al.*, 2010). Studies have demonstrated that SVM is proficient in classifying several classes using limited support vectors as training samples, without compromising overall accuracies (Foody and Mathur, 2004; Mantero *et al.*, 2005; Bruzzone *et al.*, 2006; Shao *et al.*, 2012; Zheng *et al.*, 2015). The four most dominant land cover classes within the UDP were considered for image classification (Bare rock, Bramble, Forest and Grassland).

### 7.2.8 Spatial distribution maps and validation

Python 2.7.13 was used to generate SVM classification maps of the four major land cover classes considered in this study. Fused (optical and dual-polarized SAR) training pixel spectra/backscatter (70%) of all four classes served as the input for multi-season Bramble spatial distribution maps. Multi-season classification accuracy was assessed using the respective fused test pixel spectra/ backscatter (30%). Confusion matrices were produced for all fused optical and SAR imagery classification results. Confusion matrices were used to validate classification accuracies across all fused results.

## 7.3 Results

The highest overall classification accuracy of 85% was achieved by fusing S2 optical band with S1<sub>w-vh</sub> dual polarized SAR imagery (Table 7.1a). User's and producers accuracies for Bramble ranged between 80 and 89% respectively, while the forest land-cover class achieved the highest users and producers accuracies (Table 7.1a). Bare rock land-cover class and the grassland land-cover class had the lowest users and producer's accuracy, respectively (Table 7.1a).

The spatial distribution of all land-cover classes mapped using multiclass SVM resulted in minimal overestimation and underestimation of individual classes. Minimal confusion between the grassland class and all other land-cover classes resulted in a slight underestimation of grassland cover as compared to the Bare rock, Forest and Bramble classes (Figure 7.2a).

Table 7.1: Confusion matrices of fused S2 optical bands and (a) S1<sub>vv-vh</sub> ; (b) S1<sub>vv-vv</sub> SAR imagery compared to S2 optical band Confusion matrix. Where BR = Bare rock; BBL = Bramble; FR = Forest; GR = grassland; PA= Producers accuracy; OA= Overall accuracy and UA = Users accuracy.

<b>(a) S2 bands + S1<sub>vv-vh</sub></b>	<b>BR</b>	<b>BBL</b>	<b>FR</b>	<b>GR</b>	<b>UA (%)</b>
<b>BR</b>	45	0	1	11	<b>79</b>
<b>BBL</b>	2	73	0	16	<b>80</b>
<b>FR</b>	0	4	51	1	<b>91</b>
<b>GR</b>	2	5	2	77	<b>90</b>
<b>PA (%)</b>	<b>92</b>	<b>89</b>	<b>94</b>	<b>73</b>	
<b>OA (%)</b>	<b>85</b>				
<b>(b) S2 bands + S1<sub>vv-vv</sub></b>					
<b>BR</b>	42	0	6	0	<b>88</b>
<b>BBL</b>	2	69	0	24	<b>73</b>
<b>FR</b>	3	3	48	2	<b>86</b>
<b>GR</b>	1	8	4	78	<b>86</b>
<b>PA (%)</b>	<b>88</b>	<b>86</b>	<b>83</b>	<b>75</b>	
<b>OA (%)</b>	<b>82</b>				
<b>(c) S2 optical bands</b>					
<b>BR</b>	45	0	1	11	<b>79</b>
<b>BBL</b>	2	65	1	16	<b>77</b>
<b>FR</b>	12	4	31	1	<b>65</b>
<b>GR</b>	2	10	2	87	<b>86</b>
<b>PA (%)</b>	<b>74</b>	<b>82</b>	<b>89</b>	<b>76</b>	
<b>OA (%)</b>	<b>79</b>				

Fusion of S2 optical bands and S1<sub>vv-vv</sub> dual polarized imagery resulted in the second highest overall classification accuracy (82%) (Table 7.1b). Bramble users (73%) and producers (86%) accuracies were inferior compared to results achieved by fusing S2 optical bands and S1<sub>vv-vh</sub> imagery (Table 7.1a). The Bare rock land-cover class produced the highest user's (88%) and producer's (88%) accuracies respectively, while Grassland (75%) achieved the lowest producers accuracy across all land-cover classes (Table 7.1b).

The spatial detection and distribution of Bramble from surrounding classes produced marginal underestimation across specific land-cover classes (Figure 7.2b). Grassland, Forest and Bramble land-cover distributions were overestimated as compared to  $S1_{vv-vh}$  spatial distributions, with consistent confusion across all three classes (Table 7.1b). The Bare rock class was the most accurately represented land-cover class, with minimal overestimation as compared to results produced using stand-alone S2 optical bands (Figure 7.2b and 7.2c).

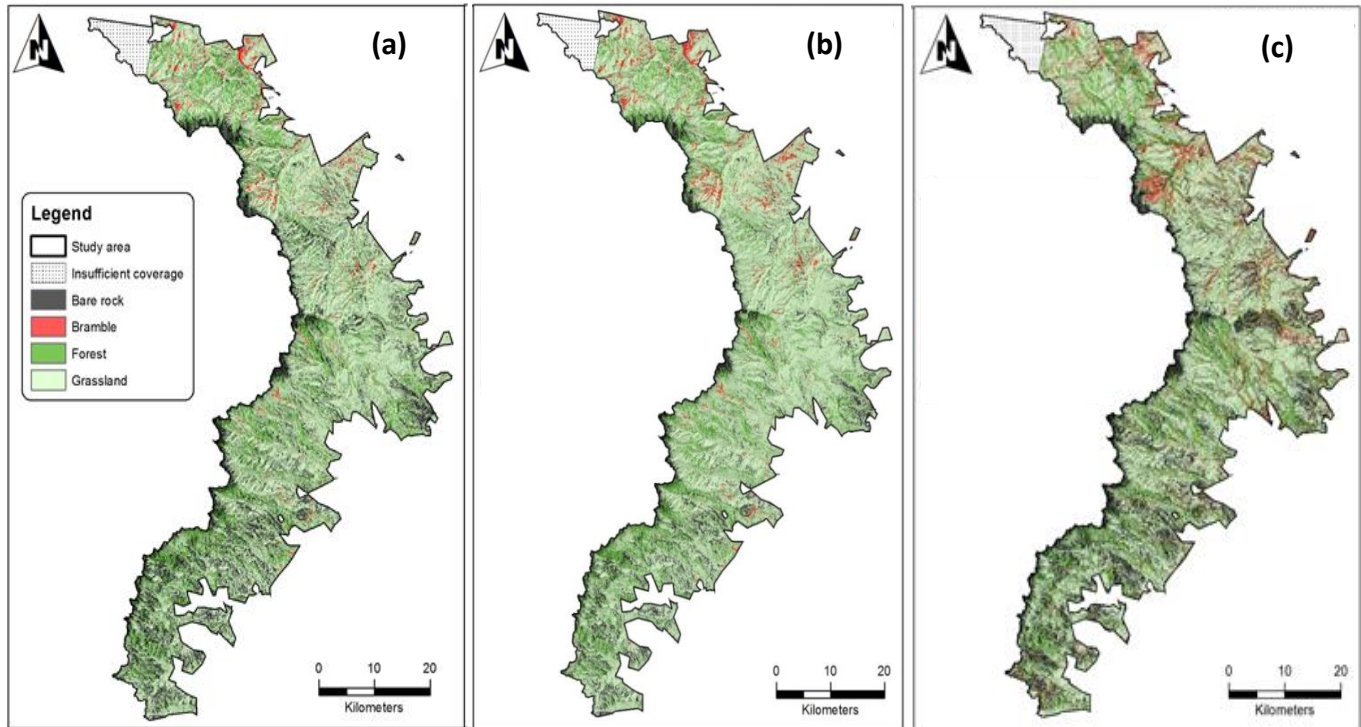


Figure 7.2: Spatial distribution maps of fused S2 optical bands and (a)  $S1_{vv-vh}$ ; (b)  $S1_{vv-vv}$  dual-polarized SAR imagery compared to (c) S2 optical band spatial distribution map.

The use of selected stand-alone S2 optical bands for Bramble discrimination and mapping generated the lowest overall classification (79%) (Table 7.1c). Bramble user's (77%) and producers (82%) accuracies decreased as compared to results achieved using S2 selected optical bands fused with  $S1_{vv-vh}$  SAR imagery (Table 7.3).

The Forest land-cover class produced the lowest user's accuracy (65%) while the Bare rock class achieved the lowest producers accuracy (74%) (Table 7.1c). There was evident overestimation of certain land-cover classes as compared to results achieved using S2 optical bands and  $S1_{vv-vh}$  imagery (Figure 7.3). The spatial distribution of Bramble was considerably overestimated and was regularly misclassified as Grassland and Forest (Table 7.1c). The

Forest land-cover class was also frequently misclassified as Bare rock and Bramble, resulting in an overestimation of Forest spatial distribution (Figure 7.3).

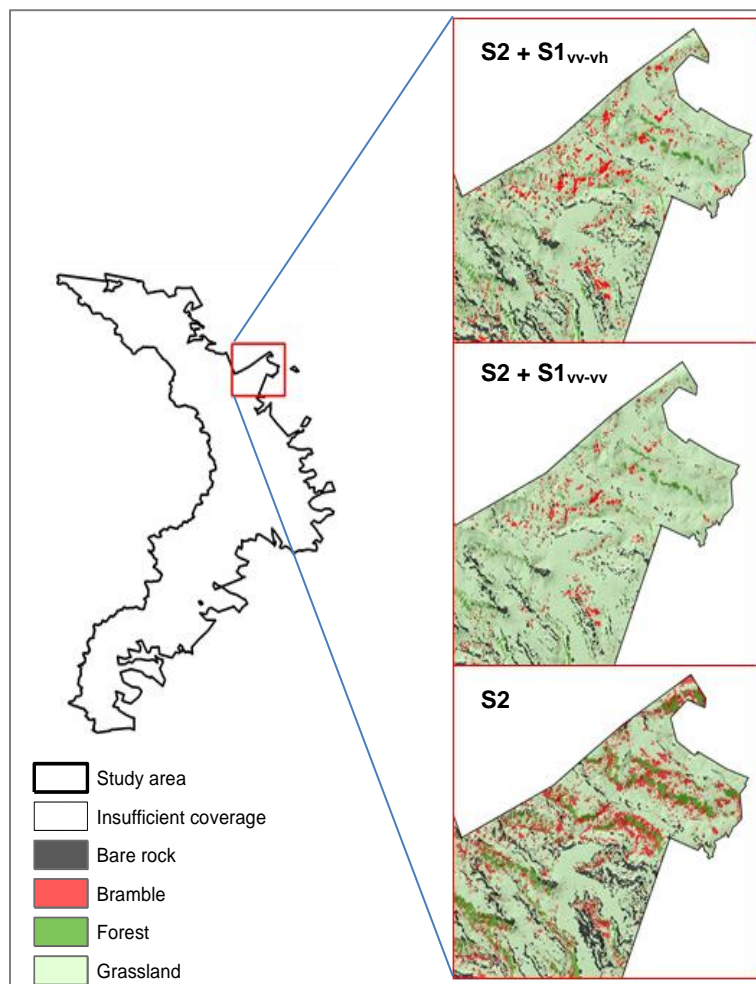


Figure 7.3: An example of mapped classification accuracies across S2+S1<sub>vv-vh</sub> ; S2+S1<sub>vv-vv</sub> and S2 optical bands

#### 7.4. Discussion

This study sought to determine the potential of fusing dual-polarized Sentinel-1 SAR imagery with Sentinel-2 optical imagery for the discrimination and mapping of the American bramble (*Rubus cuneifolius*). Generally, overall classification accuracies achieved using fused imagery outperformed accuracies achieved using stand-alone Sentinel-2 imagery. The fusion of S2 and S1<sub>vv-vh</sub> SAR imagery produced the highest classification accuracy (85%) while stand-alone S2 imagery produced the lowest (79%). S1 information coupled with the unprecedented spectral resolution of S2 optical bands that span the vegetation Red Edge, Near Infrared, Narrow-Near Infrared and Shortwave-Infrared regions, indicate the complementarity of S1 and S2 imagery.



Based on these findings, the value of dual-polarized SAR imagery for invasive alien species detection and mapping is evident.

C-band SAR sensors (Sentinel-1) are known to be sensitive to leaves and small branches (Huang *et al.*, 2010). Specifically, the short Sentinel-1 C-band SAR wavelength is known to be effectively sensitive to the upper part of vegetation canopies, a trait believed to be valuable for retrieving and recording varying biophysical vegetation parameters (Schmidt *et al.*, 2017). Castro-Gomez (2017) suggests that VV-VH dual-polarized SAR data strongly account for vegetation's vertical orientation. The thorny, stalky nature of Bramble stem phenology is markedly different from the phenology of surrounding grassland dominated landscape within the UDP, hence  $S1_{VV-VH}$  sensitivity could have effectively discriminated Bramble from surrounding land-cover classes. These results are consistent with Coleman and Buckley (2010) who noted an effective discrimination of invasive alien species and brush within a grassland environment. Furthermore, the value of  $S1_{VV-VH}$  dual polarized SAR has been previously established for use in agricultural classification applications (Voormansik *et al.*, 2016; De Wit and Clevers, 2004; McNairn *et al.*, 2009).

The value of single-polarized SAR data as a complimentary dataset for various environmental applications has been well documented (Shi *et al.* 2012; Ghulam *et al.*, 2014; Hong *et al.*, 2014; Martinez and Toan, 2007). Ferro-Famil *et al.* (2001) and Rajah *et al.* (2018) noted that dual-polarized SAR data was more effective in discriminating landscapes than single-polarized SAR. From a vegetation classification perspective, results from this study affirm those achieved by Abdikan *et al.* (2016), where overall accuracies obtained with the combination of optical imagery and dual polarized SAR showed improvement when compared to accuracies achieved using single-polarized SAR data.

Generally invasive alien species detection and mapping is often characterized by high spectral confusions, causing difficulty when using optical imagery alone. However, SAR is known to be sensitive to a range of geometric properties that include plant height and shape, leaf size and canopy structure (Zhang *et al.*, 2018). SAR data is sensitive to these properties and thus can be used to improve the overall classification accuracy.

The dominant scattering of microwave (e.g., C-band SAR in this study) in the SAR backscattering mechanisms greatly depends on vegetation height and biomass, which have been reported to vary significantly between Bramble and the surrounding natural grassland



(Masson *et al.*, 2015; Reynolds and Symes, 2013). For example, the natural thickety nature of Bramble has higher biomass and often towers above natural grassland species, traits that can be reflected in the backscattering coefficient of dual-polarized C-band SAR data (Zhang *et al.*, 2018). Although improvements in accuracy attributable to this unique backscattering mechanism may be small ( $\approx 3\%$  in this study), it may be essential for more efficient and cost-effective large-scale Bramble monitoring. A similar positive valuation of dual-polarized SAR was established by Ziolkowski *et al.* (2013), who used dual-polarimetric SAR to model vegetation biophysical parameters. Similar to this study, Ziolkowski *et al.* (2013) also noted that varying products of dual-polarized SAR data exhibit variability in accuracy achieved based on the type, seasonal stage, and water content of target vegetation. The above-mentioned variability in classification accuracies further substantiates findings from this study between  $S1_{VV-VH}$  and  $S1_{VV-VV}$ .

Results from this study highlight the potential of S1 C-band dual polarized SAR to improve Bramble detection and mapping. Similar improvements were observed by Lardeux *et al.* (2011), who reported that despite C-band SARs reduced canopy penetration capability, major contributions to vegetation classification accuracies were recorded when using dual-polarized C-band SAR. Within a comparable context to this research, Laurin *et al.* (2013), who evaluated synergies between optical and SAR imagery achieved the best vegetation classification accuracy by integrating freely available dual-polarized SAR and Landsat 8 imagery. Findings from this study emphasize and underline the contribution of dual-polarized SAR imagery towards improving the detection and mapping of invasive alien species. The freely available nature of both S1 and S2, coupled with the diversity in sensor payloads, provide a cost-effective and efficient alternative to conventional stand-alone remote sensing methodologies. Considering the benefits derived from increasing accuracies, it should be considered beneficial to integrate dual-polarized SAR data to compensate conventional optical data for improving invasive alien species detection and mapping.

## **7.5. Conclusion**

This study sought to fuse conventional multispectral optical imagery with new age Synthetic Aperture Radar (SAR) imagery to determine the synergistic potential for invasive alien species mapping. Comparative analysis of stand-alone optical imagery fused with variations of dual polarized SAR data indicated that image fusion at a feature level has the potential to accurately detect and map the American Bramble within a native grassland environment. The sensitivity of SAR backscatter measurements to shape, size, texture, surface roughness and complex

permittivity of vegetation effectively complemented conventional optical imagery in delineating Bramble infested landscapes. The fused S2 optical and S1<sub>vv-vh</sub> dual polarized SAR synergy outperformed the stand alone S2 imagery as well as fused S2 optical and S1<sub>vv-vv</sub> imagery. These findings provide further evidence of the complementarity of dual-polarized SAR and S2 optical imagery. Hence, the fusion of freely available dual polarized S1 radar imagery and S2 optical imagery can be considered a viable and cost-effective opportunity for specific invasive alien species detection and mapping applications.

## **Chapter Eight**

**Detecting and mapping invasive alien plants using freely available active and passive remotely sensed imagery: A synthesis**

## 8.1 Introduction

Invasive Alien Plants (IAPs) have recently received significant attention due to among others their rapid spread, severe threat to native biodiversity and adverse implication on ecosystem condition and associated services (Simberloff, 2010; Wilson *et al.*, 2013). Hence, numerous countries have ratified the Convention on Biodiversity, which requires countries to 'prevent the introduction of, control or eradicate alien species which threaten ecosystems, habitats or native species' (Terblanche *et al.*, 2016: Pg. 1). In South Africa, the national government has recently disseminated regulations under the National Environmental Management: Biodiversity Act (NEMBA) that makes provision for the development of national-level invasive species management programmes for priority invasive alien species (DEAT, 2009). Whereas a list of these priority species has not yet been defined, the urgent need to develop cost-effective and timeous methodologies for the detection and mapping of established invasive species is critical in fulfilling these regulations.

Spatially explicit data defines invaded areas as well as the extent and density of invasion, thus facilitating appropriate management actions (Le Bourgeois *et al.*, 2016). In this context, the utility of freely available, new generation remote sensing technology offer a practical solution for the detection and mapping of invasive alien species. However, challenges in the use of conventional remotely sensed imagery for invasive alien species detection and mapping has been extensively documented (Feilhauer *et al.*, 2017; Rocchini *et al.*, 2015; Bradley, 2014; Shezi and Poona, 2010). The advent and launch of new generation, freely available sensors such as Sentinel-1 (S1) and Sentinel-2 (S2) with both optical and radar capabilities offer new opportunities to determine the value of combining optical and Synthetic Aperture Radar (SAR) properties for invasive alien species detection and mapping. The stand-alone and synergistic potential of S1 and S2 has shown great promise in vegetation mapping (Munyati, 2017; Stratoulas *et al.*, 2015; D'Odorico *et al.*, 2013; Gascon *et al.*, 2009). In addition, the high operational ability, acquired data and potential products of the Sentinel missions also present significant scientific opportunity. Enhanced characteristics of Sentinel missions such as long-term continuity of measurements (>20 years-time series building on previous observationally compatible missions), global and generally frequent coverage, careful calibration of the satellite sensors, data delivery and archiving that meet the rigorous performance requirements of operational and practical applications, and a broad variety of sensing methods (optical and

microwave, active and passive, etc.) (Berger *et al.*, 2012), offer new opportunities in landscape mapping.

Hence, this study sought to: (1) Evaluate the potential of new generation Sentinel-2 imagery for the detection and mapping of American bramble (*Rubus cuneifolius*), (2) investigate the potential of fused Sentinel-1 and Sentinel-2 imagery for the detection and mapping of American bramble (*Rubus cuneifolius*), (3) investigate the capability of fused Sentinel-2 optical imagery Sentinel-1 SAR band combinations and ratios for American Bramble (*Rubus cuneifolius*) detection and mapping, (4) Assess the combined potential of Sentinel-2 spectral reflectance bands and derived vegetation indices for detecting and mapping American bramble (*Rubus cuneifolius*), (5) Evaluate the utility of Sentinel-2 Vegetation Indices (VIs) and Sentinel-1 Synthetic Aperture Radar (SAR) for American bramble (*Rubus cuneifolius*) detection and mapping and (6) Assess the synergistic potential of dual-polarized Synthetic Aperture Radar (SAR) fused with Sentinel-2 imagery for improving American bramble (*Rubus cuneifolius*) detection and mapping. The findings of each objective in this thesis are described below.

## 8.2 Evaluating the potential of freely available multispectral remotely sensed imagery for mapping invasive alien plant species

The potential of new generation freely available multispectral remotely sensed imagery to detect and map Bramble within the UDP was assessed in chapter two. A comparison of multi-season Landsat 8 and new generation Sentinel-2 (S2) imagery resulted in S2 outperforming Landsat 8 across all seasons (spring, summer, autumn and winter). Hence the application of multi-class Support Vector Machine (SVM) better discriminated between Bramble and surrounding native vegetation using selected S2 VIP bands.

The optimum season for Bramble detection and mapping using S2 imagery was summer, which generated an overall accuracy of 77%, with individual landcover class accuracies ranging from 45% and 91% (Table 8.1). Bare rock and Forest were the most correctly classified land-cover classes, while Grassland was predominantly confused for other classes (Figure 8.1). Hence the detection and mapping of Bramble within the UDP was regarded as suitable, but the need for further investigation into the improvement of detection of Bramble was considered.

Table 8.1: Seasonal overall classification accuracies resulting from Landsat 8 and Sentinel-2 imagery

Overall Accuracies				
	Spring	Summer	Autumn	Winter
<b>Landsat-8</b>	55%	57%	50%	55%
<b>Sentinel-2</b>	70%	77%	63%	61%

In summary, the key finding in this chapter was the superior performance of S2 as compared to Landsat8 in Bramble detection and mapping. Furthermore, summer was identified as the optimal season for Bramble detection and mapping.

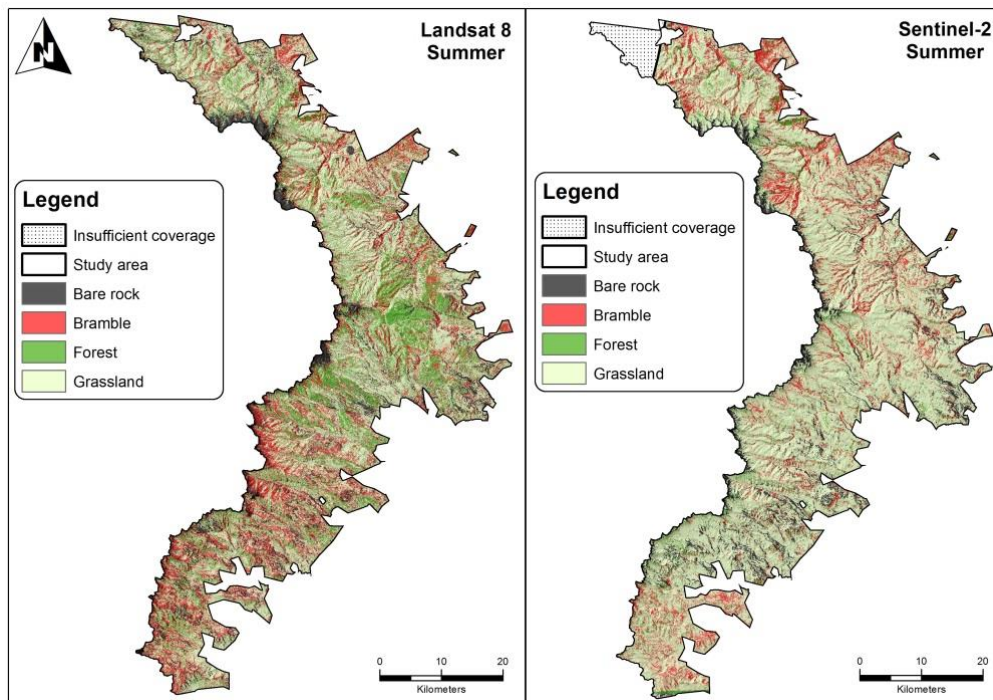


Figure 8 1: Comparison of Landsat 8 and Sentinel-2 spatial distribution of all landcover classes considered in this study.

The proposed methodology provides an efficient and cost-effective alternative to using labour intensive in-field methods to obtain spatial information related to invasive alien plant species. The application of S2 imagery is potentially valuable to conservation managers, ecologists and regional planners in supporting their decisions and operational tasks such as promoting and developing effective eradication strategies in relation to particular invasive species (Atkinson *et al.*, 2014; Little *et al.*, 1997).

### 8.3 Feature level image fusion of optical imagery and Synthetic Aperture Radar (SAR) for invasive alien plant species detection and mapping

In chapter three, Synthetic Aperture Radar (SAR) imagery was introduced and the potential to compliment the data with conventional optical imagery was assessed. Results indicated that the fusion of L8 and SAR increased Bramble detection and mapping accuracies across all seasons. Winter L8 fused with VH produced the highest overall classification accuracy (71%) while S2 Winter and summer fused with VH produced the highest overall classification accuracies (76%) (Table 8.2). The study demonstrated the value of fusing SAR with new generation multi-spectral optical imagery in mapping Bramble. Results showed an improved overall classification accuracies using imagery captured in Autumn and Winter seasons.

Table 8.2: Seasonal overall accuracies of fused Landsat 8 and Sentinel-1 SAR and Sentinel-2 and Sentinel-1 SAR

Fused combination	Spring		Summer		Autumn		Winter	
	VH	VV	VH	VV	VH	VV	VH	VV
<b>Landsat-8</b>	64%	64%	65%	68%	71%	66%	72%	64%
<b>Sentinel-2</b>	67%	72%	76%	68%	71%	70%	76%	71%

These results provide evidence of the complementarity between SAR and conventional optical imagery. The increase in overall classification accuracy seen in this research is comparable to that of previous vegetation discrimination studies using SAR and optical image fusion (Walsh, 2018; Pandit and Bhiwani, 2015; Hong *et al.*, 2014; Vaglio *et al.*, 2013; Vyjayanthia and Nizalapur, 2010; Zhang, 2010). Although findings from this chapter are progressive, the potential to utilize variations in SAR image acquisition still exists, and could be exploited to

further improve Bramble detection and mapping. Nevertheless, the proposed concept of the synergy between freely available new generation optical imagery and SAR has potential to provide an efficient and economical alternative to conventional invasive species mapping methodologies.

#### 8.4 The fusion of multispectral optical imagery and SAR polarization combinations/ratios for invasive alien plant detection and mapping

Chapter four builds on results achieved from the previous chapter. In this chapter, Synthetic Aperture Radar (SAR) polarization combinations and ratios were developed and fused with Sentinel-2 (S2) imagery. The VH/VV, VH – VV, VH + VV, VH x VV, VV/VH and VV – VH SAR polarization band combinations and ratios were developed for feature level image fusion with S2 optical imagery. The overall accuracy of fused S2 and SAR polarization combinations and ratios ranged between from 64% to 74% for VH x VV and VV - VH, respectively (Table 8.3).

Table 8.3: Overall accuracies of fused Sentinel-2 imagery and Sentinel-1 SAR polarization combinations and ratios

<b>S1 SAR polarization combination/ratio + S2 optical imagery</b>	<b>Overall accuracy achieved</b>
VV - VH	74%
VH - VV	72%
VH/VV	68%
VV/VH	67%
VH x VV	64%
VH + VV	68%

This study demonstrated the potential of varying SAR polarization combinations and ratios for invasive alien species detection and mapping. Confusion matrices illustrated that the difference between VV and VH S1 SAR polarizations was optimal for Bramble detection and mapping. Figure 8.2 illustrates the visual differences across classification accuracies resulting from the fusion of S2 optical imagery and the various S1 SAR polarization combinations and ratios. Findings reported in this chapter illustrate the dynamic and variable nature of SAR imagery



acquired at different polarizations. These findings are consistent with Hong *et al* (2014); Inoue *et al* (2014); Lardeux *et al* (2011); Srivastava *et al* (2009); Vyjayanthia and Nizalapur (2010) and Schmullius and Evans (1997) who noted SAR capability as well as variability in results using differing SAR polarizations.

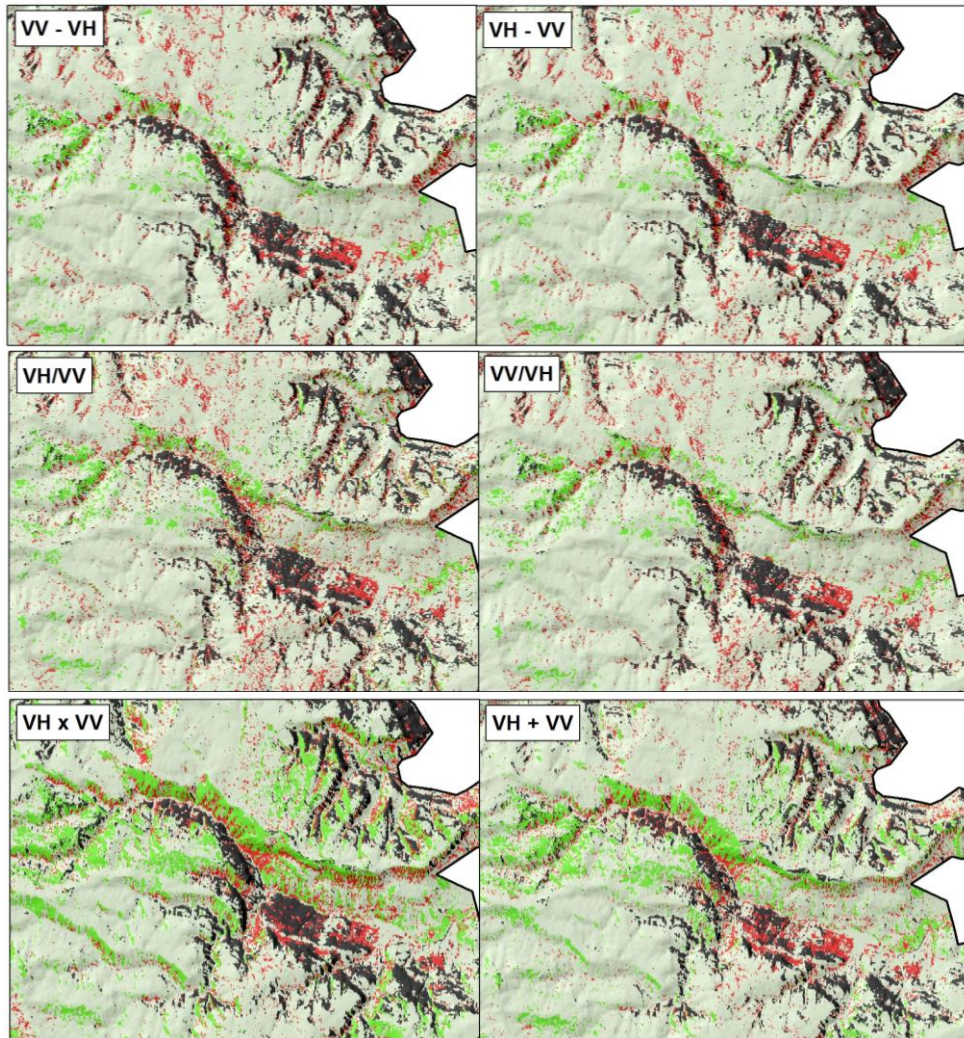


Figure 8.2: Overestimation and underestimation of Bramble classes across VH-VV; VV - VH; VH/VV; VV/VH; VH x VV and VV+VH band combinations and ratios

8.5 Assessing the combined potential of Sentinel-2 spectral reflectance bands, derived Vegetation Indices (VIs) and Synthetic Aperture Radar (SAR) for detecting and mapping invasive alien species

Chapter five sought to integrate S2 spectral reflectance bands with S2 derived Vegetation Indices (VIs) in order to improve overall seasonal detection and mapping accuracy of Bramble.

A total of 65 VIs were derived from S2 optical bands. The Variable Importance in the Projection (VIP) was used to select the 15 most influential VIs and S2 reflectance bands for feature level image fusion. Benchmark classification accuracies were derived and mapped using only S2 reflectance bands in all seasons.

The Support Vector Machine (SVM) classification algorithm was used to classify multi-season fused VIs and S2 spectral reflectance bands. Results indicated that spring imagery produced the highest classification accuracy (73%) in all seasons, while winter produced the lowest (61%). Fused VIs and S2 reflectance bands improved overall accuracies across spring and autumn (65%), while winter (61%) overall accuracy remained unchanged as compared to when using only S2 reflectance bands. Summer was the only season where fused VIs and S2 reflectance produced a lower overall accuracy (70%) as compared to S2 reflectance bands (77%) (Table 8.4).

Table 8.4: Seasonal overall accuracies of stand-alone Sentinel-2 imagery compared to fused Sentinel-2 and Vegetation Indices (VIs)

	<b>Spring</b>	<b>Summer</b>	<b>Autumn</b>	<b>Winter</b>
<b>S2</b>	70%	77%	63%	61%
<b>S2 + VIs</b>	73%	70%	65%	61%

Based on the outcome in chapter 5, chapter six investigated the synergistic potential of fused S2 VIs and S1 SAR for invasive species detection and mapping. Stand-alone S2 optical imagery was used as the overall accuracy benchmark for comparison to stand alone S2 VIs and fused S2 optical imagery and S2 VIs. Feature level image fusion was conducted in order to fuse VIP S2 VIs and S1 SAR imagery. The SVM learning algorithm was used for classifications.

Table 8.5: Overall accuracies produced using stand-alone Sentinel-2 optical bands, VIP Vegetation Indices (Vis) and fused Sentinel-2 and Vegetation Indices

	<b>VIP VIs</b>	<b>S2</b>	<b>S2 derived VIs</b>
<b>Overall accuracy</b>	54%	77%	80%

Stand-alone S2 derived VIs produced the highest classification accuracy (80%) across all three comparisons, while S2 optical imagery fused with S1 SAR produced the lowest overall classification accuracy (54%) (Table 8.5)

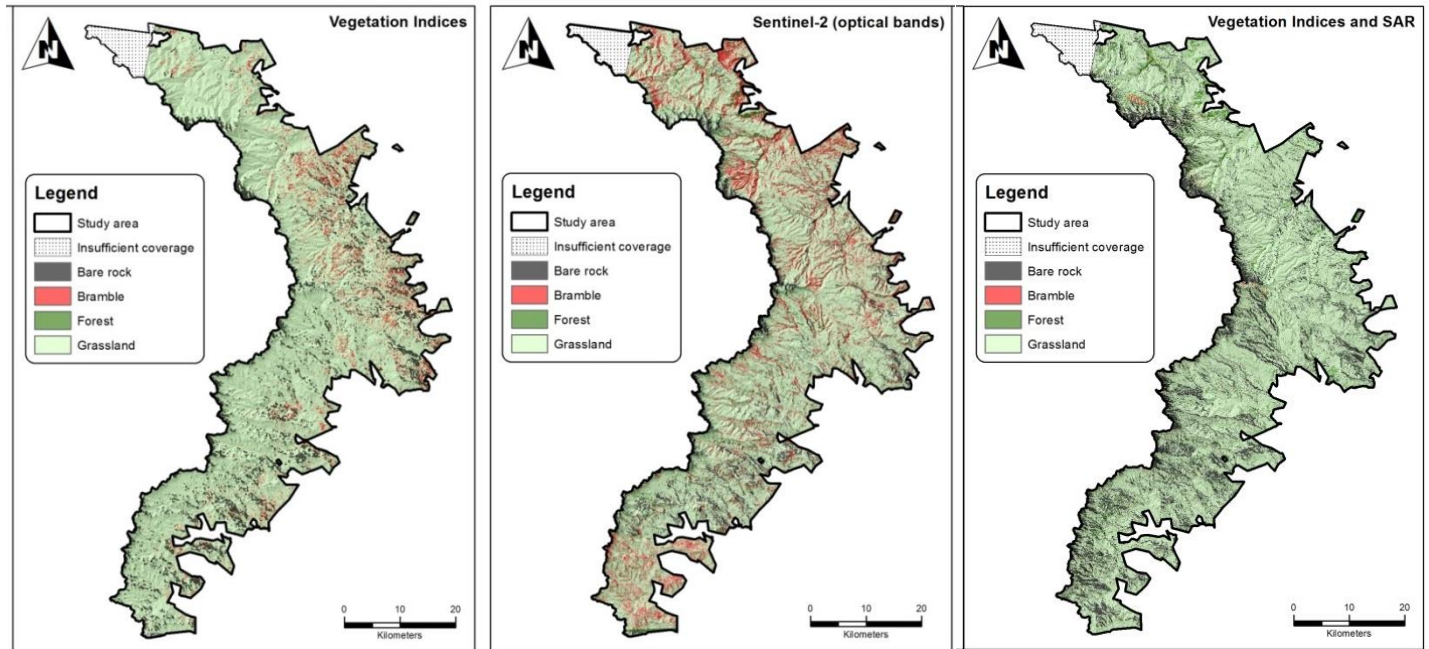


Figure 8.3: Support Vector Machine (SVM) classification maps produced utilizing (a) Vegetation Indices; (b) S2 optical bands and (c) Fused VIs and SAR.

### 8.6 The synergistic potential of dual-polarized Synthetic Aperture Radar (SAR) fused with multispectral optical imagery for invasive alien species detection and mapping

In the final chapter there is chapter 6 and 7, the study evaluated the synergistic potential of dual-polarized S1 SAR and S2 optical imagery. Selected VIP S2 optical bands were fused with two variations of dual-polarized SAR imagery ( $S2 + S1_{VV-VH}$  and  $S2 + S1_{VV-VV}$ ). Results showed that there was a 3-6% improvement in overall classification accuracies with fusion of dual polarized S1 SAR and VIP S2 bands. Feature level image fusion of  $S2 + S1_{VV-VH}$  produced the highest overall accuracy (85%) across all comparisons, while  $S2 + S1_{VV-VV}$  fused imagery produced an overall accuracy of 82% (Table 8.6). Benchmark stand-alone VIP S2 optical bands resulted in an overall classification accuracy of 79% (Table 8.6).

Table 8.6: Overall accuracies produced using Sentinel-2 optical imagery fused with dual-polarized Sentinel-1 SAR imagery

<b>S2 and S1 fusion combination</b>	<b>Overall accuracy</b>
S2 + S1 <sub>VV-VH</sub>	85%
S2 + S1 <sub>VV-VV</sub>	82%
Stand-alone S2 bands	79%

The fusion of dual-polarized S1 SAR (VV-VH and VV-VV) with S2 optical imagery produced the highest overall classification in results reported in all chapters. Hence, the study has demonstrated that fusing dual-polarized SAR imagery with new-age S2 optical imagery improves Bramble detection and mapping. Consequently, this chapter outlines the potential synergistic value of dual-polarized S1 SAR imagery. In addition, the wide swath width and high temporal resolution of S1 and S2 satellites facilitates regional mapping using the presented methodology. The use of dual-polarized SAR in conjunction with new-age remotely sensed imagery offers a cost-effective alternative to the often tedious and costly traditional ground-based mapping approaches.



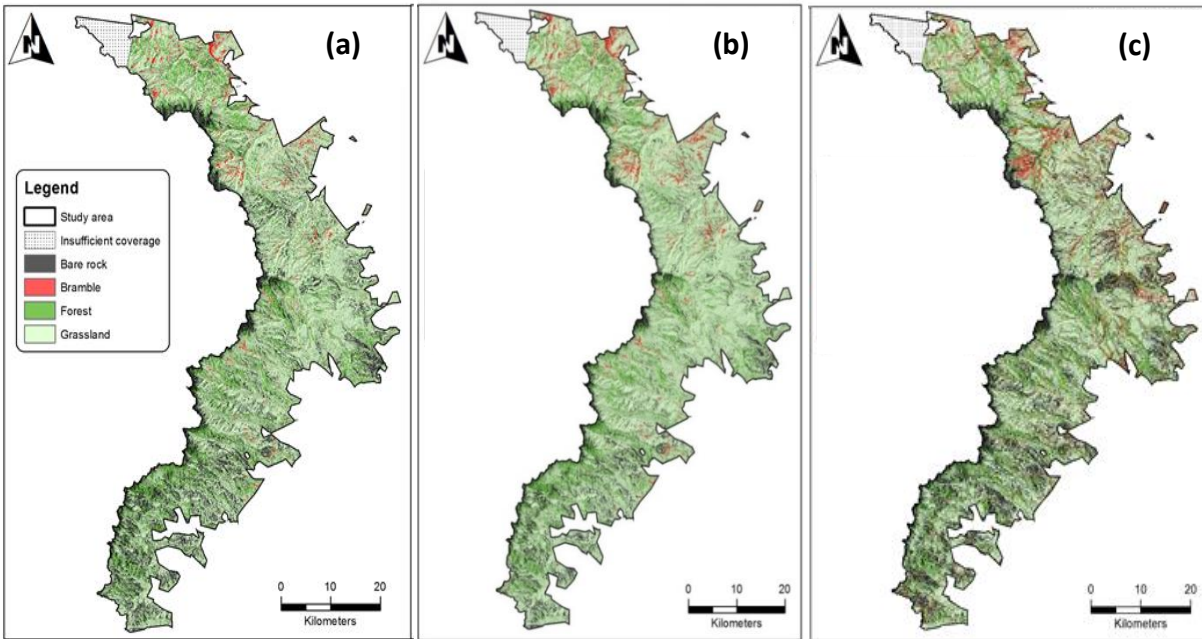


Figure 8.4: Spatial distribution maps of fused S2 optical bands and (a)  $S1_{vv-vh}$ ; (b)  $S1_{vv-vv}$  dual-polarized SAR imagery compared to (c) S2 optical band spatial distribution map.

## 8.8 Conclusions

This thesis aimed to investigate the potential of freely available new-age remote sensing technology to detect and map American Bramble (*Rubus cuneifolius*) within the uKuhlamba Drakensberg Park (UDP) UNESCO world heritage site. Findings in this study have demonstrated the capability of fusing active and passive remotely sensed imagery and data to detect and map Bramble within the UDP. The study concludes that;

1. Sentinel-2 multispectral imagery outperforms Landsat 8 in the detection and mapping of Bramble and surrounding native vegetation.
2. Feature level fusion of Sentinel-2/Landsat 8 optical imagery and Sentinel-1 Synthetic Aperture Radar (SAR) can be used to improve the detection and mapping of Bramble
3. The fusion of Sentinel-1 Synthetic Aperture Radar (SAR) polarization band combinations and ratios with Sentinel-2 optical imagery can be used to improve detection and mapping of Bramble.
4. The synergistic potential of Sentinel-2 derived Vegetation Indices and stand-alone Sentinel-2 optical bands showed limited potential in Bramble detection and mapping. However,

classification results showed improvement, in comparison to the use of S2 optical imagery alone.

5. The integration of S2 VIs and Sentinel-1 (S1) SAR did not increase the overall classification accuracies.

6. Dual-polarized Synthetic Aperture Radar (SAR) fused with Sentinel-2 optical imagery showed increased potential in detecting and mapping of Bramble. All variations of dual-polarized SAR increased overall Bramble detection and mapping accuracies. This synergistic combination of active and passive remote sensing imagery produced the most effective results.

## **8.9 The future**

The future of Bramble detection and mapping lies in understanding the spatial distribution of the plant invader in relation to the surrounding environment. This could be achieved by incorporating additional ancillary data representing environmental, topographical and edaphic variables in detection and mapping Bramble invasion. While such variables would improve the spatial recognition of Bramble and facilitate appropriate management and eradication strategies, the mapping and determination of areas at risk of invasion or habitat suitability should also be investigated.

Future research should also focus on variations within Synthetic Aperture Radar (SAR), both with single and dual-polarization acquisition modes. Findings from this study confirm the complementarity of SAR to conventional optical remotely sensed imagery. However, the need for further application and continued testing with several more easily detectable invasive alien species is essential to understand the caveats and advantages associated with the fusion of SAR and new-age optical imagery. The technical aspects associated with SAR image pre-processing is an additional focal point that should be investigated, as variables such as SAR speckle filter techniques could serve to produce increased classification accuracies. The use of freely available active (S1) and passive (S2) remotely sensed imagery has the potential to provide cost-effective, large scale invasive alien species detection and mapping. Future opportunities should seek to optimize this technical process by developing near real-time data acquisition and image processing workflows

Finally, while this thesis focused on detecting and mapping Bramble infestation within the UDP, future research may consider up-scaling the proposed methods to a larger landscape. In this context, the development of practically applied detection and mapping techniques would be

valuable to environmental managers, but most importantly, in developing individual national-level invasive species management programmes.

## References

- Adelabu, S., Mutanga, O., and Adam, E., 2014: Evaluating the impact of red-edge band from RapidEye image for classifying insect defoliation levels. *ISPRS Journal of Photogrammetry and Remote Sensing*, 95, 34-41.
- Andrew, M.E., and Ustin, S.L., 2008: The role of environmental context in mapping invasive plants with hyperspectral image data. *Remote Sensing of the Environment*, 112, 4301-4317.
- Asner, G.P., Knapp DE, Kennedy-Bowdoin T, Jones MO, Martin RE, Boardman J, and Hughes, RF, 2008: Invasive species detection in Hawaiian rainforests using airborne imaging spectroscopy and LiDAR. *Remote Sensing of Environment* 112, 1942-1955.
- Atkinson, J.T., Ismail, R., and Robertson, M., 2014: Mapping Bugweed (*Solanum mauritianum*) Infestations in *Pinus patula* Plantations Using Hyperspectral Imagery and Support Vector Machines. *IEEE Journal of Selected Topics in Applied Earth Observation and Remote Sensing*, 7, 17-28.
- ATLAS, S.A.P.I., 2014: SAPIA News.
- Avery, R., Greenman, D., Landesman, K., Vaa, J., and Whaley, T., 2017: Mapping invasive species to efficiently monitor Southwestern National Park areas, *Connections Across People, Place, and Time*, Proceedings of the 2017 George Wright Society Conference on Parks, Protected Areas, and Cultural Sites. Hancock, Michigan.
- Baghdadi, N.N., El Hajj, M., Zribi, M., and Fayad, I., 2016: Coupling SAR C-band and optical data for soil moisture and leaf area index retrieval over irrigated grasslands. *IEEE Journal of Selected Topics in Applied Earth Observations and Remote Sensing*, 9, 1229-1243.
- Baghdadi, N., M., El Hajj., M., Zribi, M., and Fayad, I., 2015: Coupling SAR C-band and optical data for soil moisture and leaf area index retrieval over irrigated grasslands, *IEEE Journal of Selected Topics in Applied Earth Observations and Remote Sensing*, IEEE, 1-15.
- Baghdadi, N., Boyer, N., Todoroff, P., El Hajj, M.E., and Begue, A., 2009: Potential of SAR sensors TerraSAR-X, ASAR/ENVISAT and PALSAR/ALOS for monitoring sugarcane crops on Réunion Island, *Remote Sensing Environment*, 113, 1724-1738.



Baghdadi, N., Loumagne, C., Ansart, P., and Anguela, T.P., 2008: Analysis of TerraSAR-X data and their sensitivity to soil surface parameters over bare agricultural fields. *Remote Sensing of Environment* 112, 4370-4379.

Basso, B., Cammarano, D., and De Vita, P., 2004: Remotely sensed vegetation indices: Theory and applications for crop management. *Rivista Italiana di Agrometeorologia*, 1, 36-53.

Benayas, J.M.R., and Scheiner, S.M., 2002: Plant diversity, biogeography and environment in Iberia: Patterns and possible causal factors, *Journal of Vegetation Science*, 13, 245–258.

Berger, M., Moreno, J., Johannessen, J., Levelt, P., and Hanssen, R., 2012: ESA's Sentinel Missions In Support of Earth System Science. *Remote Sensing of Environment*, 120, 84–90.

Betbeder, J., Nabucet, J., Pottier, E., Baudry, J., Corgne, S., and Hubert-Moy, L., 2014: Detection and characterization of hedgerows using TerraSAR-X Imagery, *Remote Sensing*, 6, 3752-3769.

Bevington., A., 2016: Polarimetric Synthetic Aperture Radar (InSAR) analysis of Prince George UNBC Remote Sensing Lab.

Bourgeau-Chavez, L.L., Kowalski, K.P., Mazur, M.L.C., Scarbrough, K.A., Powell, R.B., Brooks, C.N., Huberty, B., Jenkins, L.K., Banda, E.C., Galbraith, D.M., and Laubach, Z.M., 2013: Mapping invasive *Phragmites australis* in the coastal Great Lakes with ALOS PALSAR satellite imagery for decision support, *Journal of Great Lakes Research*, 65-77.

Bradley, B.A., 2014: Remote detection of invasive plants: A review of spectral, textural and phenological approaches, *Biological Invasions*, 16, 1411–1425.

Bradley, B.A. and Mustard, J.F., 2006: Characterizing the landscape dynamics of an invasive plant and risk of invasion using remote sensing, *Ecological Applications*, 16 ,1132-1147.

Bromilow, C., 2010: *Problem Plants and Alien Weeds of South Africa*, Briza Publications.

Brooks, T.M., Mittermeier, R.A., da Fonseca, G.A.B., Gerlach, J., and Hoffmann, M., 2006: Global biodiversity conservation priorities, *Science* 313, 58–61. DOI: 10.1126/science.1127609.

Bruzzone, L., and Chi, M., 2006: A novel transductive SVM for semisupervised classification of remote-sensing images. *IEEE Transactions on Geoscience and Remote Sensing* 44, 3363–3373.

Butchart, S.H., Walpole, M., Collen, B., Van Strien, A., Scharlemann, J.P., Almond, R.E., Baillie, J.E., Bomhard, B., Brown, C., Bruno, J., and Carpenter, K.E., 2010: Global biodiversity: indicators of recent declines. *Science*: 1187512.

Cable, J.W., Kovacs, J.M., Shang, J., and Jiao, X., 2014: Multi-temporal polarimetric RADARSAT-2 for land-cover monitoring in Northeastern Ontario, Canada. *Remote Sensing*, 6, 2372-2392.

Carbutt, C., and Martindale, G., 2014: Temperate indigenous grassland gains in South Africa: Lessons being learned in a developing country, *Parks* 20, 104–125.

Carlier, L., Rotar, I., Vlahova, M. and Vidican, R., 2009: Importance and functions of grasslands, *Notulae Botanicae Horti Agrobotanici Cluj-Napoca* 37, 25–30.

Castro-Gomez, M.G., 2017: Joint use of Sentinel-1 and Sentinel-2 for land cover classification: A machine learning approach. Lund University GEM thesis series.

Chaneton, E.J., Mazía, N., Batista, W.B., Rolhauser, A.G. and Ghersa, C.M., 2012: Woody plant invasions in Pampa grasslands: a biogeographical and community assembly perspective. In: *Ecotones between forest and grassland*, 115-144, Springer, New York.

Chen, S., Zhang, R., Su, H., Tian, J. and Xia, J., 2010: SAR and multispectral image fusion using generalized IHS transform based on a trous wavelet and EMD decompositions. *Sensors Journal, IEEE*, 10, 737-745.

Cho, M.A., Mathieu, R., Asner, G.P., Naidoo, L., van Aardt, J., Ramoelo, A., Debba, P., Wessels, K., Main, R., Smit, I.P.J., and Erasmus, B., 2012: Mapping tree species composition in South African savannas using an integrated airborne spectral and LiDAR system, *Remote Sensing of Environment*, 125, 214-226.

Cho, M.A. and Skidmore, A.K., 2006: A new technique for extracting the red edge position from hyperspectral data: The linear extrapolation method, *Remote Sensing of environment*, 181-193.

Clusella-Trullas, S., and Garcia, R.A., 2017: Impacts of invasive plants on animal diversity in South Africa: A synthesis, *Bothalia-African Biodiversity and Conservation*, 47, 1-12.

Coleman, A.J., and Buckley, J.R., 2010: Finding weeds from space: Experiences with synthetic aperture radar polarimetry of prairie rangelands. *Proceedings The Prairie Summit*, 85.

Convention on Biological Diversity., 2009: Strategic Plan for Biodiversity 2011-2020 and the Aichi Targets, Convention on Biological Diversity, United Nations, Montreal, Quebec, Canada.

D'Antonio, C.M., and Vitousek, P.M., 1992: Biological invasions by exotic grasses, the grass/fire cycle, and global change, *Annual review of ecology and systematics*, 23, 63-87.

de Almeida Furtado, L.F., Silva, T.S.F., and de Moraes Novo, E.M.L., 2016: Dual-season and full-polarimetric C band SAR assessment for vegetation mapping in the Amazon várzea wetlands, *Remote Sensing of Environment*, 174, 212-222.

da Costa Freitas C, de Souza Soler L, Sant'Anna SJS, Dutra LV, dos Santos JR, Mura JC and Correia AH 2008: Land use and land cover mapping in the Brazilian Amazon using polarimetric airborne P-band SAR data. *IEEE Transactions on Geoscience and Remote Sensing*, 46, 2956-2970.

Davies, K.W., and Johnson, D.D., 2011: Are we “missing the boat” on preventing the spread of invasive plants in rangelands?, *Invasive Plant Science and Management*, 4, 166-171.

de Carvalho, L.M.T., Rahman, M.M., Hayb, G.J., and Yackel, J., 2010: Optical and SAR imagery for mapping vegetation gradients in Brazilian savannas: synergy between pixel-based and object-based approaches. In: *International Conference on Geographic Object-based Image Analysis*, 1-7.

De Lange, and W.J, Van Wilgen, B.W., 2012: An economic assessment of the contribution of biological control to the management of invasive alien plants and to the protection of ecosystem services in South African, *Biological Invasions*, 12, 4113-4124.

Delegido, J., Verrelst, J., Meza, C.M., Rivera, J.P., Alonso, L., and Moreno, J., 2013: A red-edge spectral index for remote sensing estimation of green LAI over agroecosystems. *European Journal of Agronomy*, 46, 42-52.

Denny, R., 1990: Control of American Bramble, Cedara Weeds Laboratory, Plant Protection Research Institute.

De Wit, A.J.W. and Clevers, J.G.P.W., 2004: Efficiency and accuracy of per-field classification for operational crop mapping. *International journal of remote sensing*, 25, 4091-4112.

Dilts, T.E., 2015: Landsat toolbox for ArcGIS 10.1. University of Nevada Reno. Available at: <http://www.arcgis.com/home/item.html?id=a6060120a79f45ae990bb85f4d12edee>

D'Odorico, P., Gonsamo, A., Damm, A. and Schaepman, M.E., 2013: Experimental evaluation of Sentinel-2 spectral response functions for NDVI time-series continuity. *IEEE Transactions on Geoscience and Remote Sensing*, 51, 1336-1348.

Dollar, E., and Goudy, A., 1999: Environmental Change: In: Fox, R., and Rowntree, K. (eds), *The Geography of South Africa in a Changing World*. Oxford University Press, Oxford.

Dornelas, M., 2010: Disturbance and change in biodiversity, *Philosophical Transactions of the Royal Society, Biological Sciences*, 365, 3719-3727.

Dong, X.L., and Srivastava, D., 2013: Big data integration. In *Data Engineering (ICDE): IEEE 29th International Conference*, 1245-1248.

Dorigo, W., Lucieer, A., Podobnikar, T., and Čarni, A., 2012: Mapping invasive *Fallopia japonica* by combined spectral, spatial, and temporal analysis of digital orthophotos, *International Journal of Applied Earth Observation and Geoinformation*, 19, 185-195.

Driver, A., Sink, K.J., Nel, J.N., Holness, S., Van Niekerk, L., Daniels, F., Jonas, Z., Majiedt, P.A., Harris, L., and Maze, K., 2012: *National Biodiversity Assessment 2011: An assessment of South Africa's biodiversity and ecosystems. Synthesis Report*, Pretoria: South African National Biodiversity Institute and Department of Environmental Affairs

Duguay Y, Bernier M, Lévesque E and Tremblay B., 2015: Potential of C and X band SAR for shrub growth monitoring in sub-arctic environments. *Remote Sensing*, 7, 9410-9430.

Dusseux, P., Corpetti, T., Hubert-Moy, L. and Corgne, S., 2014: Combined use of multi-temporal optical and radar satellite images for grassland monitoring, *Remote Sensing*, 6, 6163-6182.

Edwards, T.C., Cutler, D.R., Beard, K.H., Gibson, J., 2007: Predicting invasive plant species occurrences in 493 national parks: a process for prioritizing prevention. Final Project Report No. 2007-1, USGS Utah 494 Cooperative Fish and Wildlife Research Unit, Utah State University, Logan, UT 84322-5290 USA.

Erasmus, D.J., 1984: *Bramble, Weeds, Farming in South Africa*.

Evangelista, P.H., Stohlgren, T.J., Morissette, J.T., and Kumar, S., 2009: Mapping invasive tamarisk (*Tamarix*): a comparison of single-scene and time-series analyses of remotely sensed data. *Remote Sensing*, 1, 519-533.

Everson, C.S., and Everson, T., 2016: The long-term effects of fire regime on primary production of montane grasslands in South Africa, *Journal of Range Forage Science*, 33–41.

Fairbanks, D.H.K., Thompson, M.W., Vink, D.E., Newby, T.S., Van den Berg, H.M. and Everard, D.D.2., 2000: The South African land-cover characteristics database: A synopsis of the landscape. *South African Journal of Science*, 96.

Fard, T.A., Hasanlou, M. and Arefi, H., 2014: Classifier fusion of high-resolution optical and synthetic aperture radar (SAR) satellite imagery for classification in urban area. *The International Archives of Photogrammetry, Remote Sensing and Spatial Information Sciences*, 40,25.

Farrés, M., Platikanov, S., Tsakovski, S., and Tauler, R., 2015: Comparison of the variable importance in projection (VIP) and of the selectivity ratio (SR) methods for variable selection and interpretation, *Journal of Chemometrics*, 29, 528-536.

Ferro-Famil, L., Pottier, E., and Lee, J.S., 2001: Unsupervised classification of multifrequency and fully polarimetric SAR images based on the H/A/Alpha-Wishart classifier. *IEEE Transactions on Geoscience and Remote Sensing*, 39, 2332-2342.

Feilhauer, H., Somers, B., and van der Linden, S., 2017: Optical trait indicators for remote sensing of plant species composition: Predictive power and seasonal variability. *Ecological indicators* 73: 825-833.

Fontanelli, G., Paloscia, S., Zribi, M., and Chahbi, A., 2013: Sensitivity analysis of X-band SAR to wheat and barley leaf area index in the Merguellil Basin, *Remote Sensing Letters*, 1107-1116.

Foody, G.M., and Mathur, A., 2004: Toward intelligent training of supervised image classifications: directing training data acquisition for SVM classification, *Remote Sensing of Environment*, 93, 107–117.

Fourie, L., Rouget, M. and Lötter, M., 2015: Landscape connectivity of the grassland biome in Mpumalanga, South Africa. *Austral Ecology*, 40, 67-76.

Foxcroft, L.C., Richardson, D.M., Rejmánek, M. and Pyšek, P., 2010: Alien plant invasions in tropical and sub-tropical savannas: Patterns, processes and prospects, *Biological Invasions*, 12, 3913-3933.

Frampton, W.J., Dash, J., Watmough, G.R. and Milton, E.J., 2013: Evaluating the capabilities of Sentinel-2 for quantitative estimation of biophysical variables in vegetation. *ISPRS Journal of Photogrammetry and Remote Sensing*, 82, 83-92.

Gao, Q., Zribi, M., Escorihuela, M.J. and Baghdadi, N., 2017: Synergetic use of Sentinel-1 and Sentinel-2 data for soil moisture mapping at 100 m resolution. *Sensors*, 17,1966.

Gascon, F., Martimort, P. and Spoto, F., 2009: September. Sentinel-2 optical high-resolution mission for GMES land operational services. In *Sensors, Systems, and Next-Generation Satellites*, International Society for Optics and Photonics. 747404.

Gharbia, R., Azar, A.T., Baz, A.E., and Hassanien, A.E., 2014: Image fusion techniques in remote sensing, arXiv preprint arXiv, 1403.5473.

Ghasemi, N., Sahebi, M.R. and Mohammadzadeh, A., 2011: A review on biomass estimation methods using synthetic aperture radar data. *International Journal of Geomatics and Geosciences*, 1.

Ghulam, A., Porton, I. and Freeman, K., 2014: Detecting subcanopy invasive plant species in tropical rainforest by integrating optical and microwave (InSAR/PolInSAR) remote sensing data, and a decision tree algorithm. *ISPRS Journal of Photogrammetry and Remote Sensing*, 88,174-192.

Ghulam, A., Freeman, K., Bollen, A., Ripperdan, R., and Porton, I., 2011: Mapping invasive plant species in tropical rainforest using polarimetric Radarsat-2 and Palsar data, *Conference Paper*, 3514-3517.

Gil, A., Lobo, A., Abadi, M., Silva, L. and Calado, H., 2013: Mapping invasive woody plants in Azores Protected Areas by using very high-resolution multispectral imagery, *European Journal of Remote Sensing*, 46, 289-304.

Gilmore, M.S., Wilson, E.H., Barrett, N., Civco, D.L., Prisloe, S., Hurd, J.D., and Chadwick, G., 2008: Integrating multi-temporal and structural information to map wetland vegetation in a lower Connecticut River tidal marsh, *Remote Sensing of Environment*, 112, 4048-4060.

Gobron, N., Pinty, B., Verstraete, M., and Widlowski, J. L., 2000: Advanced vegetation indices optimized for up-coming sensors: Design, performance, and applications. *IEEE Transactions on Geoscience and Remote Sensing*, 38, 2489–2505.

Hajj, M.E., Baghdadi, N., Belaud, G., Zribi, M., Cheviron, B., Courault, D., Hagolle, O., and Charron F., 2014: Irrigated grassland monitoring using a time series of terraSAR-X and COSMO-skyMed X-Band SAR Data. *Remote Sensing* 6, 0002-10032.

Hauglin, M., and Ørka, H.O., 2016: Discriminating between Native Norway Spruce and Invasive Sitka Spruce - A Comparison of Multitemporal Landsat 8 Imagery, Aerial Images and Airborne Laser Scanner Data, *Remote Sensing*, 8, 363.

He, K.S., Rocchini, D., Neteler, M. and Nagendra, H., 2011: Benefits of hyperspectral remote sensing for tracking plant invasions. *Diversity and Distributions*, 17, 381-392.

Hedley, J., Roelfsema, C., Koetz, B., and Phinn, S., 2012: Capability of the Sentinel 2 mission for tropical coral reef mapping and coral bleaching detection, *Remote Sensing of Environment*, 120, 145-155.

Henderson, L., 2011: SAPIA News, Southern African Plant Invaders Atlas, Agricultural Research Council - Plant Protection Research Institute, 19, Pretoria.

Henderson, L., 2001: Alien Weeds and Invasive Plants: A Complete Guide to Declared Weeds and Invaders in South Africa. Plant Protection Research Institute, Agricultural Research Council, Pretoria.

Henrich, V., Jung, A., Götze, C., Sandow, C., Thürkow, D., Gläßer, C., 2012: Development of an online indices database: Motivation, concept and implementation. 6th EARSeL Imaging Spectroscopy SIG Workshop Innovative Tool for Scientific and Commercial Environment Applications Tel Aviv, Israel, March 16-18.

Henrich, V., Krauss, G., Götze, C., and Sandow, C., 2012: IDB - [www.indexdatabase.de](http://www.indexdatabase.de), Entwicklung einer Datenbank für Fernerkundungsindizes. AK Fernerkundung, Bochum, 4.-5.

Hill, M.J., 2013: Vegetation index suites as indicators of vegetation state in grassland and savanna: An analysis with simulated Sentinel-2 data for a North American transect. *Remote Sensing of Environment*, 137, 94-111.

Hojas-Gascón, L., Belward, A., Eva, H., Ceccherini, G., Hagolle, O., Garcia, J., and Cerutti, P., 2015: Potential improvement for forest cover and forest degradation mapping with the

forthcoming Sentinel-2 program. The International Archives of Photogrammetry, Remote Sensing and Spatial Information Sciences, 40, 417-423.

Hong, G., Zhang, A., Zhou, F. and Brisco, B., 2014: Integration of optical and synthetic aperture radar (SAR) images to differentiate grassland and alfalfa in Prairie area. International Journal of Applied Earth Observation and Geoinformation, 28, 12-19.

Huang, W., Sun, G., Ni, W., Zhang, Z., and Dubayah, R., 2015: Sensitivity of multi-source SAR backscatter to changes in forest aboveground biomass, Remote Sensing, 7, 9587-9609.

Huang, S., Potter, C., Crabtree, R.L., Hager, S. and Gross, P., 2010: Fusing optical and radar data to estimate sagebrush, herbaceous, and bare ground cover in Yellowstone. Remote Sensing of Environment, 114, 251-264.

Huang, C.Y., and Asner, G.P., 2009: Applications of remote sensing to alien invasive plant studies. Sensors, 9, 4869-4889.

Hulme, P.E., 2009: Trade, transport and trouble: managing invasive species pathways in an era of globalization. Journal of applied ecology, 46, 10-18.

Hunt, E.R., Doraiswamy, P.C., McMurtrey, J.E., Daughtry, C.S., Perry, E.M., and Akhmedov, B., 2013: A visible band index for remote sensing leaf chlorophyll content at the canopy scale. International Journal of Applied Earth Observation and Geoinformation, 21, 103-112.

Immitzer, M., Vuolo, F., and Atzberger, C., 2016: First Experience with Sentinel-2 Data for Crop and Tree Species Classifications in Central Europe, Remote sensing, 8, 166.

Inoue, Y., Sakaiya, E., and Wang, C., 2014: Capability of C-band backscattering coefficients from high-resolution satellite SAR sensors to assess biophysical variables in paddy rice, Remote Sensing of the Environment, 140, 257–266.

Inoue, Y., Kurosu, T., Maeno, H., Uratsuka, S., Kozu, T., Dabrowska-Zielinska K., and Qi J., 2003: Season-long daily measurements of multifrequency (Ka, Ku, X, C, and L) and full-polarization backscatter signatures over paddy rice field and their relationship with biological variables. Remote Sensing of Environment 81: 194-204.

Jiang, D., Zhuang, D. and Huang, Y., 2013: Investigation of image fusion for remote sensing application. In New Advances in Image Fusion. InTech.



Joshi, N., Baumann, M., Ehammer, A., Fensholt, R., Grogan, K., Hostert, P., Jepsen, M.R., Kuemmerle, T., Meyfroidt, P., Mitchard, E.T., and Reiche, J., 2016: A review of the application of optical and radar remote sensing data fusion to land use mapping and monitoring, *Remote Sensing*, 8, 70.

Kandwal, R., Jeganathan, C., Tolpekin, V., and Kushwaha, S.P.S., 2009: Discriminating the species "Lantana" using vegetation indices, *Journal of Indian Society of Remote Sensing*, 37, 275-290.

Karimi, Y., Prasher, S.O., Patel, R.M., and Kim, S.H., 2006: Application of support vector machines technology for weed and nitrogen stress detection in corn. *Computer and electronics in agriculture*, 51, 99-109.

Kavzoglu, T., and Colkesen, I., 2009: A kernel functions analysis for support vector machines for land cover classification, *International Journal of Applied Earth Observation and Geoinformation*, 11, 352-359.

Khosravi, I., Safari, A., and Homayouni, S., 2017: Separability analysis of multifrequency SAR polarimetric features for land cover classification. *Remote Sensing Letters*, 8, 1152-1161.

Kim, Y., Jackson, T., Bindlish, R., Lee, H., and Hong, S., 2012: Radar vegetation index for estimating the vegetation water content of rice and soybean. *IEEE Geoscience and Remote Sensing Letters*, 9, 564-568.

Kimothi, M.M., and Dasari, A., 2010: Methodology to map the spread of an invasive plant (*Lantana camara* L.) in forest ecosystems using Indian remote sensing satellite data, *International Journal of Remote Sensing*, 31, 3273-3289.

Kourgli, A., Quarzeddine, M., Oukil, Y., and BelhadjAissa, A., 2010: Landcover identification using polarimetric SAR images. *IAPRS XXXVIII (7A)* July 5-7.

Kotzé, J.D.F., Beukes, H., van der Beg, E., and Newby T., 2010: National Invasive Alien Plant Survey – Dataset, Agricultural Research Council: Institute for Soil, Climate and Water, Pretoria.

Kruger, S.C., Rusworth, I.A., and Oliver, K., 2011: The verification of wilderness area boundaries as part of a buffer zone demarcation process: A case study from the uKhahlamba Drakensberg Park World Heritage Site, *USDA Forest Service Proceedings RMRS-P-64*.

Laba, M., Tsai, F., Ogurcak, D., Smith, S., and Richmond, M.E., 2005: Field determination of optimal dates for the discrimination of invasive wetland plant species using derivative spectral analysis, *Photogrammetric Engineering and Remote Sensing*, 71, 603-611.

Lardeux, C., Frison, P.L., Tison, C., Souyris, J.C., Stoll, B., Fruneau, B. and Rudant, J.P., 2011: Classification of tropical vegetation using multifrequency partial SAR polarimetry. *IEEE Geoscience and Remote Sensing Letters*, 8, 133-137.

Laurin, G.V., Liesenberg, V., Chen, Q., Guerriero, L., Del Frate, F., Bartolini, A., Coomes, D., Wilebore, B., Lindsell, J. and Valentini, R., 2013: Optical and SAR sensor synergies for forest and land cover mapping in a tropical site in West Africa. *International Journal of Applied Earth Observation and Geoinformation*, 21, 7-16.

Le Bourgeois, T., Thompson, D.I., Guezou, A., Foxcroft, L.C., Grard, P., Taylor, R.W., Marshall, T. and Carrara, A., 2016: Using information technology, communication and citizen science in alien invasive plant management in Kruger National Park, South Africa. *Botanists*, 103.

Le Hegarat-Masclé, S., Quesney, A., and Vidal-Madjar, D., 2000: Land cover discrimination from multitemporal ERS images and multispectral Landsat images: A study case in an agricultural area in France, *International Journal of Remote Sensing*, 21, 435-456.

Lenda, M., Witek, M., Skórka, P., Moroń, D., and Woyciechowski, M., 2013: Invasive alien plants affect grassland ant communities, colony size and foraging behavior, *Biological Invasions*, 15, 2403-2414.

Levin, N., Shmida, A., Levanoni, O., Tamari, H., and Kark, S., 2007: Predicting mountain plant richness and rarity from space using satellite-derived vegetation indices. *Diversity and Distributions*, 13, 692-703.

Li, K., Shao, Y., Zhang, F., 2011: Rice information extraction using multi-polarization airborne synthetic aperture radar data. *Journal of Zhejiang University (Agriculture and Life Sciences)* 2011, 181–186.

Li, P., Jiang, L., and Feng, Z., 2013: Cross-comparison of vegetation indices derived from Landsat-7 enhanced thematic mapper plus (ETM+) and Landsat-8 operational land imager (OLI) sensors. *Remote Sensing* 6, 310-329.

Liu, Y., Zha, Y., Gao, J., Ni, S., 2004: Assessment of grassland degradation near Lake Qinghai, West China, using Landsat TM and in situ reflectance spectra data. *International Journal of Remote Sensing* 25: 4177-4189.

Little, K., Kritzing, J., Maxfield, M., 1997: Some principles of vegetation management explained. The Institute for Commercial Forestry Research. University of KwaZulu-Natal, Pietermaritzburg.

Macelloni, G., Paloscia, S., Pampaloni, P., Marliani, F., and Gai, M., 2001: The relationship between the backscattering coefficient and the biomass of narrow and broad leaf crops, *IEEE Transactions on Geoscience and Remote Sensing*, 873-884.

Malanson, G.P., Walsh, S.J., 2013: A geographical approach to optimization of response to invasive species. In Walsh SJ and Mena C, eds. *Science and Conservation in the Galapagos Islands: Frameworks and Perspectives*. Springer, New York, 199-215.

Mansour, K., Mutanga, O., Everson, T., and Adam, E., 2012: Discriminating indicator grass species for rangeland degradation assessment using hyperspectral data resampled to AISA Eagle resolution, *ISPRS Journal of Photogrammetry and Remote Sensing*. 70, 56–65.

Mantero, P., Moser, G., and Serpico, S.B., 2005: Partially supervised classification of remote sensing images through SVM-based probability density estimation, *IEEE Transactions on Geoscience and Remote Sensing*, 43, 559–570.

Martinez, J.M., and Le Toan, T., 2007: Mapping of flood dynamics and spatial distribution of vegetation in the Amazon floodplain using multitemporal SAR data. *Remote sensing of Environment*, 108, 209-223.

Masocha, M., and Skidmore, A. K., 2011: Integrating conventional classifiers with a GIS expert system to increase the accuracy of invasive species mapping. *International Journal of Applied Earth Observation and Geoinformation* 13, 487–494.

Masson, S., Mesléard, F. and Dutoit, T., 2015: Using shrub clearing, draining, and herbivory to control bramble invasion in Mediterranean Dry Grasslands. *Environmental management*, 56, 933-945.

Mathieu, R., L. Naidoo, M.A. Cho, B. Leblon, R. Main, K. Wessels, G.P. Asner, J. Buckley, J. Van Aardt, J., Erasmus, B.F., and Smit, I.P., 2013: Toward structural assessment of semi-arid

African savannahs and woodlands: the potential of multitemporal polarimetric RADARSAT-2 fine beam images, *Remote Sensing of Environment*, 215-231.

Maron, J.L., Auge, H., Pearson, D.E., Korell, L., Hensen, I., Suding, K.N. and Stein, C., 2014: Staged invasions across disparate grasslands: effects of seed provenance, consumers and disturbance on productivity and species richness, *Ecology letters*, 17, 499-507.

Mayer, B., and Kylling, A., 2000: The libRadtran software package for radiative transfer calculations-description and examples of use, *Atmospheric Chemistry and Physics*, 1855-1877.

McLean, P., Gallien, L., Wilson, J.R., Gaertner, M. and Richardson, D.M., 2017: Small urban centres as launching sites for plant invasions in natural areas: insights from South Africa. *Biological Invasions*, 19,3541-3555.

McNairn, H., Champagne, C., Shang, J., Holmstrom, D., and Reichert, G., 2009: Integration of optical and Synthetic Aperture Radar (SAR) imagery for delivering operational annual crop inventories, *ISPRS Journal of Photogrammetry and Remote Sensing*, 64, 434-449.

McNairn, H., Van der Sanden, J.J., Brown, R.J. and Ellis, J., 2000: The potential of RADARSAT-2 for crop mapping and assessing crop condition. In *Proceedings of the Second International Conference on Geospatial Information in Agriculture and Forestry*, 2, 81-88.

McNairn, H. and Brisco, B., 2004: The application of C-band polarimetric SAR for agriculture: a review. *Canadian Journal of Remote Sensing*, 30, 525-542.

Melgani, F., and Bruzzone, L., 2004: Classification of hyperspectral remote sensing images with support vector machines, *IEEE Transactions on Geoscience and Remote Sensing*, 42, 1778-1790.

Millard, K., and Richardson, M., 2018: Quantifying the relative contributions of vegetation and soil moisture conditions to polarimetric C-Band SAR response in a temperate peatland. *Remote Sensing of Environment* 206: 123-138.

Minchella, A., Del Frate, F., Capogna, F., Anselmi, S. and Manes, F., 2009: Use of multitemporal SAR data for monitoring vegetation recovery of Mediterranean burned areas. *Remote Sensing of Environment*, 113, 588-597.

Mirik, M., Ansley, R.J., Steddom, K., Jones, D.C., Rush, C.M., Michels, G.J. and Elliott, N.C., 2013: Remote Distinction of A Noxious Weed (Musk Thistle: *CarduusNutans*) Using Airborne

Hyperspectral Imagery and the Support Vector Machine Classifier, *Remote Sensing*, 5, 612-630.

Mitchell, H.B., 2010: *Image Fusion: Theories, Techniques and Applications*, Springer-Verlag Berlin Heidelberg.

Mohan, S., Das, A., Haldar, D. and Maity, S., 2011: Monitoring and retrieval of vegetation parameter using multi-frequency polarimetric SAR data. In *Synthetic Aperture Radar (AP SAR)*, 2011 3rd International Asia-Pacific Conference on IEEE, 1-4.

Moran, M.S., Hymer, D.C., Qi, J., and Kerr, Y., 2002: Comparison of ERS-2 SAR and Landsat TM imagery for monitoring agricultural crop and soil conditions. *Remote Sensing of the Environment* 79: 243–252.

Motohka, T., Nasahara, K.N., Oguma, H., and Tsuchida, S., 2010: Applicability of green-red vegetation index for remote sensing of vegetation phenology. *Remote Sensing* 2: 2369-2387.

Mountrakis, G., Im, J., and Ogole, C., 2011: Support vector machines in remote sensing: A review. *ISPRS Journal of Photogrammetry and Remote Sensing*, 66 , 247-259.

Müllerová, J., Pergl, J., and Pyšek, P., 2013: Remote sensing as a tool for monitoring plant invasions: Testing the effects of data resolution and image classification approach on the detection of a model plant species *Heracleum mantegazzianum* (giant hogweed). *International Journal of Applied Earth Observation and Geoinformation*, 25, 55-65.

Munyati, C., 2017: The potential for integrating Sentinel 2 MSI with SPOT 5 HRG and Landsat 8 OLI imagery for monitoring semi-arid savannah woody cover. *International journal of remote sensing*, 38, 4888-4913.

Nagendra, H., Lucas, R., Honrado, J.P., Jongman, R.H., Tarantino, C., Adamo, M. and Mairota, P., 2013: Remote sensing for conservation monitoring: Assessing protected areas, habitat extent, habitat condition, species diversity, and threats. *Ecological Indicators*, 33, 45-59.

Naidoo, L., Mathieu, R., Main, R., Kleynhans, W., Wessels, K., Asner, G., and Leblon, B., 2015: Savannah woody structure modelling and mapping using multi-frequency (X-, C-and L-band) Synthetic Aperture Radar data. *ISPRS Journal of Photogrammetry and Remote Sensing* 105: 234-250.

Naidoo, L., Mathieu, R., and Cho, M., 2013: Toward structural assessment of semi-arid African savannahs and woodlands: The potential of multitemporal polarimetric RADARSAT-2 fine beam images, *Remote Sensing of the Environment*, 215-231.

Nel, J., Egoh, B., Jonas, Z., Rouget, M., 2005: National Grasslands Biodiversity Program: Grassland Biodiversity Profile and Spatial Biodiversity Priority Assessment CSIR Report Number: ENV-S-C 2005e102.

Nel, J.L., Richardson, D.M., Rouget, M., Mgidi, T.N., Mdzeke, N., Le Maitre, D.C., Van Wilgen, B.W., Schonegevel, L., Henderson, L., and Naser, S., 2004: Proposed classification of invasive alien plant species in South Africa: towards prioritizing species and areas for management action.

Ng, W.T., Rima, P., Einzmann, K., Immitzer, M., Atzberger, C. and Eckert, S., 2017: Assessing the Potential of Sentinel-2 and Pléiades Data for the Detection of *Prosopis* and *Vachellia* spp. in Kenya. *Remote sensing*, 9,74.

Niphadkar, M., Nagendra, H., Tarantino, C., Adamo, M. and Blonda, P., 2017: Comparing pixel and object-based approaches to map an understory invasive shrub in tropical mixed forests, *Frontiers In: Plant Science*, 8, 892.

Odindi, J., Mutanga, O., Rouget, M., and Hlanguza, N., 2016: Mapping alien and indigenous vegetation in the KwaZulu-Natal Sandstone Sourveld using remotely sensed data. *Bothalia-African Biodiversity and Conservation*, 46, 1-9.

Oldeland, J., Dorigo, W., Wesuls, D., and Jürgens, N., 2010: Mapping bush encroaching species by seasonal differences in hyperspectral imagery, *Remote Sensing*, 2, 1416-1438

Pandit, V.R. and Bhiwani, R.J., 2015: Image fusion in remote sensing applications: A review, *International Journal of Computer Applications*, 120.

Palubinskas, G., 2012: How to fuse optical and radar imagery?, In: *Geoscience and Remote Sensing Symposium (IGARSS)*, IEEE International, 2171-2174.

Patel, P., Srivastava, H.S., Panigrahy, S., and Parihar, J.S., 2006: Comparative evaluation of the sensitivity of multi-polarized multi-frequency SAR backscatter to plant density. *International Journal of Remote Sensing* 27, 293-305.

Peerbhay, K., Mutanga, O., and Ismail, R., 2016: The identification and remote detection of alien invasive plants in commercial forests: An Overview, *South African Journal of Geomatics*, 5

Poulain, V., Inglada, J., Spigai, M., Tourneret, J.Y. and Marthon, P., 2009: Fusion of high resolution optical and SAR images with vector data bases for change detection. In *Geoscience and Remote Sensing Symposium, 2009 IEEE International, IGARSS*.

Proença, V., Martin, L.J., Pereira, H.M., Fernandez, M., McRae, L., Belnap, J., Böhm, M., Brummitt, N., García-Moreno, J., Gregory, R.D. and Honrado, J.P., 2017: Global biodiversity monitoring: from data sources to essential biodiversity variables. *Biological Conservation*, 213, 256-263.

Pysek, P., Jarosik, V., Hulme, P., Pergl, J., Hejda, M., Schaffner, U., and Vila M., 2012: A global assessment of invasive plant impacts on resident species, communities and ecosystems: the interaction of impact measures, invading species' traits and environment, *Global Change Biology*, 1725-737.

QGIS Development Team, 2016: QGIS Geographic Information System. Open Source Geospatial Foundation. URL <http://qgis.osgeo.org>.

Rajah, P., Odindi, J., and Mutanga, O., 2018: Evaluating the potential of freely available multispectral remotely sensed imagery in mapping American bramble (*Rubus cuneifolius*), *South African Geographical Journal*,

Rajah, P., Odindi, J. and Mutanga, O., 2018: Feature level image fusion of optical imagery and Synthetic Aperture Radar (SAR) for invasive alien plant species detection and mapping. *Remote Sensing Applications: Society and Environment*, 10, 198-208.

Ramoelo, A., Cho, M., Mathieu, R., and Skidmore, A.K., 2015: Potential of Sentinel-2 spectral configuration to assess rangeland quality, *Journal of Applied Remote Sensing*, 9.

Reyers, B., Tosh, C.A., 2003: National Grasslands Initiative: concept document. Johannesburg: Gauteng Department of Agriculture, Conservation and Land Affairs.

Reynolds, C. and Symes, C.T., 2013: Grassland bird response to vegetation structural heterogeneity and clearing of invasive bramble. *African Zoology*, 48 , 228-239.

Richardson, D.M., and Van Wilgen, B.W., 2004: Invasive alien plants in South Africa: how well do we understand the ecological impacts?. *South African Journal of Science*, 100, 45-52.

Richter, R., Schlaepfer, D., and Mueller, A., 2011: Operational atmospheric correction for imaging spectrometers accounting the smile effect, *IEEE Transactions on Geoscience and Remote Sensing*, 1772-1780

Robinson, T.P., Wardell-Johnson, G.W., Pracilio, G., Brown, C., Croner, R., and Klinken, R.D., 2016: Testing the discrimination and detection limits of WorldView-2 imagery on a challenging invasive plant target. *International Journal of Applied Earth Observation and Geoinformation*, 44, 23-30.

Rocchini, D., Andreo, V., Förster, M., Garzon-Lopez, C.X., Gutierrez, A.P., Gillespie, T.W., Hauffe, H.C., He, K.S., Kleinschmit, B., Mairota, P. and Marcantonio, M., 2015: Potential of remote sensing to predict species invasions A modelling perspective. *Progress in Physical Geography*.

Sahu, D.K., and Parsai, M.P., 2012: Different image fusion techniques - A critical review, *International Journal of Modern Engineering Research*, 2, 4298-4301.

Sameen, M.I., Nahhas, F.H., Buraihi, F.H., Pradhan, B., and Shariff, A.R.B.M., 2016: A refined classification approach by integrating Landsat Operational Land Imager (OLI) and RADARSAT-2 imagery for land-use and land-cover mapping in a tropical area, *International Journal of Remote Sensing*, 2358-2375.

Sano, E.E, Ferreira, L.G., and Huete. A.R., 2005: Synthetic aperture radar (L band) and optical vegetation indices for discriminating the Brazilian savanna physiognomies: A comparative analysis. *Earth Interactions* 9: 1-15.

Santoro, M., Beer, C., Cartus, O., Schmullius, C., Shvidenko, A., McCallum, I., Wegmüller, U., and Wiesmann, A., 2014: Retrieval of growing stock volume in boreal forest using hyper-temporal series of Envisat ASAR ScanSAR backscatter measurements, *Remote Sensing of Environment*, 490-507.

Schirmel, J., Bundschuh, M., Entling, M.H., Kowarik, I., and Buchholz, S., 2016: Impacts of invasive plants on resident animals across ecosystems, taxa, and feeding types: A global assessment, *Global Change Biology* 22: 594–603.

Schmidt, J., Fassnacht, F.E., Förster, M., and Schmidlein, S., 2017: Synergetic use of Sentinel-1 and Sentinel-2 for assessments of heathland conservation status. *Remote Sensing in Ecology and Conservation*.



Schmullius, C.C., and Evans, D.L., 1997: Review article Synthetic aperture radar (SAR) frequency and polarization requirements for applications in ecology, geology, hydrology, and oceanography: A tabular status quo after SIR-C/X-SAR, *International Journal of Remote Sensing*, 2713-2722.

Sentinel-1 Team, 2013: *Sentinel-1 User Handbook*, European Space Agency.

Shah, M.A., and Reshi, Z.A., 2014: Characterization of alien aquatic flora of Kashmir Himalaya: implications for invasion management, *Tropical Ecology* 55: 143-157.

Shafri, H.Z.M., Salleh., M.A.M., and Ghiyamat, A., 2006: Hyperspectral remote sensing of vegetation using red edge position techniques. *American Journal of Applied Sciences*, 3, 1864-1871.

Shang, J., McNairn, H., Champagne, C., and Jiao, X., 2009: Application of multi-frequency synthetic aperture radar (SAR) in crop classification. *Advances in Geoscience and Remote Sensing*, 557-568.

Shao, Y., and Lunetta, R.S., 2012: Comparison of support vector machine, neural network, and CART algorithms for the land-cover classification using limited training data points. *ISPRS Journal of Photogrammetry and Remote Sensing*, 70, 78-87.

Shezi, I.Z., and Poona, N.K., 2010: An investigation into using different satellite remote sensors and techniques to identify, map, monitor and predict the spread and distribution of some of the major current and emerging invasive alien plant species in KwaZulu-Natal, Submitted to: *Invasive Alien Species Programme (DAEA)*.

Shi, J., Du, Y., Du, J., Jiang, L., Chai, L., Mao, K., Xu, P., Ni, W., Xiong, C., Liu, Q. and Liu, C., 2012: Progresses on microwave remote sensing of land surface parameters. *Science China Earth Sciences*, 55, 1052-1078.

Silva WF, Rudorff BET, Formaggio AR, Paradella WR and Mura JC 2009: *ISPRS Journal of Photogrammetry and Remote Sensing*, 64, 458-463.

Simberloff, D., 2010: Invasive species, In: *Conservation biology for all*, 131-152, Oxford University Press.

Simental, E., Guthrie, V. and Blundell, S.B., 2005: Polarimetry band ratios, decompositions, and statistics for terrain characterization. In Proceedings, Pecora 16 Conference, ASPRS, Sioux Falls, SD-USA.

Simone, G., Farina, A., Morabito, F.C., Serpico, S.B. and Bruzzone, L., 2002: Image fusion techniques for remote sensing applications. *Information fusion*, 3, 3-15.

Sims, D.A., and Gamon, J.A., 2002: Relationships between leaf pigment content and spectral reflectance across a wide range of species, leaf structures and developmental stages. *Remote Sensing of environment*, 81, 337-354.

Singh, K., Forbes, A., and Akombelwa, M., 2013: The evaluation of high resolution aerial imagery for monitoring of bracken fern, *South African Journal of Geomatics*, 2, 296-208.

Slaton, M.R., Hunt, E.R. and Smith, W.K., 2001: Estimating near-infrared leaf reflectance from leaf structural characteristics. *American Journal of Botany*, 88, 278-284.

SNAP - ESA Sentinel Application Platform v3.0, URL: <http://step.esa.in>

Solberg, A.H., 2006: Data fusion for remote sensing applications, 249-271, In: *Signal and image processing for remote sensing*, CRC Press, Florida.

Somodi, I., Carni, A., Ribeiro, D., and Podobnikar, T., 2012: Recognition of the invasive species *Robinia pseudacacia* from combined remote sensing and GIS sources. *Biological Conservation*, 150, 59–67.

Song, Q., Xu, F. and Jin, Y.Q., 2018: Radar Image Colorization: Converting Single-Polarization to Fully Polarimetric Using Deep Neural Networks. *IEEE Access*, 6, 1647-1661.

South African Department of Environmental Affairs and Tourism (DEAT), 2009: National Environmental Management: Biodiversity Act (10/2004): Draft Alien and Invasive Species Regulations, Pretoria: Government Gazette.

Srivastava, H.S., Patel, P., Sharma, Y., and Navalgund, R.R., 2009: Multi-frequency and multi-polarized SAR response to thin vegetation and scattered trees, *Current Science*, 97.

Steidl, R.J., Litt, A.R. and Matter, W.J., 2013: Effects of plant invasions on wildlife in desert grasslands, *Wildlife Society Bulletin*, 37, 527-536.

Stratoulas, D., Balzter, H., Sykioti, O., Zlinszky, A. and Tóth, V.R., 2015: Evaluating sentinel-2 for lakeshore habitat mapping based on airborne hyperspectral data. *Sensors*, 15, 22956-22969.

Sun, J., Ai, T., Zhao, C., Yan, H., 2007: Assessing vegetation degradation in loess plateau by using potential vegetation index. *IEEE*, 1794-1797.

Talab-Ou-Ali, H., Niculescu, S., Sellin, V., and Bougault, C., 2017: November. Contribution of the new satellites (Sentinel-1, Sentinel-2 and SPOT-6) to the coastal vegetation monitoring in the Pays de Brest (France). In: *Remote Sensing for Agriculture, Ecosystems, and Hydrology XIX*, International Society for Optics and Photonics, 10421, 1042129.

Tan, D.T., Thu, P.Q., and Dell, B., 2012: Invasive Plant Species in the National Parks of Vietnam, *Forests* 3: 997-1016.

Taylor, M.H., Rollins, K., Kobayashi, M., and Tausch, R.J., 2013: The economics of fuel management: Wildfire, invasive plants, and the dynamics of sagebrush rangelands in the western United States. *Journal of Environmental Management*, 126, 157-173.

Teeb, T., 2009: *The Economics of Ecosystems and Biodiversity for National and International Policy Makers - Summary: Responding to the Value of Nature*.

Te Beest, M., Cromsigt, J.P., Ngobese, J. and Olf, H., 2012: Managing invasions at the cost of native habitat? An experimental test of the impact of fire on the invasion of *Chromolaena odorata* in a South African savanna. *Biological Invasions*, 14, 607-618.

Terblanche, C., Nanni, I., Kaplan, H., Strathie, L.W., McConnachie, A.J., Goodall, J. and Van Wilgen, B.W., 2016: An approach to the development of a national strategy for controlling invasive alien plant species: The case of *Parthenium hysterophorus* in South Africa. *Bothalia-African Biodiversity and Conservation*, 46,1-11.

Tittensor, D.P., Walpole, M., Hill, S.L., Boyce, D.G., Britten, G.L., Burgess, N.D., Butchart, S.H., Leadley, P.W., Regan, E.C., Alkemade, R. and Baumung, R., 2014: A mid-term analysis of progress toward international biodiversity targets. *Science*, 346, 241-244.

Trombetti, M., Riaño, D., Rubio, M.A., Cheng, Y.B., and Ustin, S.L., 2008: Multi-temporal vegetation canopy water content retrieval and interpretation using artificial neural networks for continental USA. *Remote Sensing of Environment*, 112, 203-215.

Tsai, F., Lin, E.K., and Yoshino, K., 2007: Spectrally segmented principal component analysis of hyperspectral imagery for mapping invasive plant species. *International Journal of Remote Sensing*, 28, 1023-1039.

Turkar, V., Deo, R., Rao, Y.S., Mohan, S., and Das, A., 2012: Classification accuracy of multi-frequency and multi-polarization SAR images for various land covers. *IEEE Journal of Selected Topics in Applied Earth Observations and Remote Sensing* 5, 936-941.

Turner, W., Spector, S., Gardiner, N., Fladeland, M., and Sterliug E., 2003: Remote sensing of biodiversity 610 science and conservation, *Trends in Ecology and Evolution*, 18, 306-314.

Tyson, P.D., Preston-Whyte, R.A., and Schulze, R.E., 1976: The climate of the Drakensberg, Natal Town and regional planning report, 31.

Underwood, E., Ustin, S. and DiPietro, D., 2003: Mapping nonnative plants using hyperspectral imagery, *Remote Sensing of Environment*, 86, 150-161.

Ustin, S.L., DiPietro, D., Olmstead, K., Underwood, E., and Scheer, G.J., 2002: Hyperspectral remote sensing for invasive species detection and mapping. In *Geoscience and Remote Sensing Symposium, 2002. IGARSS'02. 2002 IEEE International*.

Vaglio, G.L., Chen, Q., Guerriero, L., and Valentini, R., 2013: Optical and SAR sensor synergies for forest and land cover mapping in a tropical site in West Africa, *International Journal of Applied Earth Observation and Geoinformation* 21, 7-16.

Van den Berg, E.C., Kotze, I., and Beukes, H., 2013: Detection, Quantification and Monitoring of *Prosopis* in the Northern Cape Province of South Africa using Remote Sensing and GIS, *South African Journal of Geomatics*, 2.

van Beijma, S., Comber, A., and Lamb, A., 2014: Random forest classification of salt marsh vegetation habitats using quad-polarimetric airborne SAR, elevation and optical RS data, *Remote Sensing of Environment*, 149, 118-129.

van Rossum, G., and Drake, F.L. 2012: *The Python Language Reference Release 3.2.3*, Python Software Foundation.

van Wilgen, B.W., Forsyth, G.G., Le Maitre, D.C., Wannenburg, A., Kotzé, J.D., van den Berg, E., and Henderson, L., 2012: An assessment of the effectiveness of a large, national-scale invasive alien plant control strategy in South Africa, *Biological Conservation* 148, 28-38.

Vapnik, V., 1979: Estimation of Dependencies Based on Empirical Data. Nauka, Moscow.

Verbesselt, J., Hyndman, R., Newnham, G., and Culvenor, D., 2009: Detecting trend and seasonal changes in satellite image time series. *Remote sensing of Environment*, 114, 106-115.

Viña, A., Gitelson, A.A., Nguy-Robertson, A.L., and Peng, Y., 2011: Comparison of different vegetation indices for the remote assessment of green leaf area index of crops. *Remote Sensing of Environment*, 115, 3468-3478.

Vyjayanthia, N., and Nizalapur, V., 2010: Synthetic Aperture radar data analysis for vegetation classification and biomass estimation of tropical forest area, Unpublished PhD thesis, Jawaharlal Nehru Technological University.

Walsh, S.J., 2018: Multi-scale Remote Sensing of Introduced and Invasive Species: An Overview of Approaches and Perspectives, In: *Understanding Invasive Species in the Galapagos Islands*, 143-154, Springer, Cham.

Wang, J.F., Stein, A., Gao, B.B. and Ge, Y., 2012: A review of spatial sampling. *Spatial Statistics*, 2, 1-14

Weisberg, P.J, Dilts, T.E., Baughman, O.W., Meyer, S.E., Leger, E.A., Van Gunst, K.J., and Cleaves L 2017: Development of remote sensing indicators for mapping episodic die-off of an invasive annual grass (*Bromus tectorum*) from the Landsat archive. *Ecological Indicators* 79, 173-181.

White, R.P., Murray, S.M., Rohweder, M., 2000: *Pilot Analysis of Global Ecosystems: Grassland Ecosystems*. World Resources Institute, Washington, DC.

Wilson, J.R., Ivey, P., Manyama, P. and Nänni, I., 2013: A new national unit for invasive species detection, assessment and eradication planning. *South African Journal of Science*, 109, 01-13.

World Resources Institute (WRI)., 2001: *People and Ecosystems: The Fraying Web of Life*. World Resources Institute, Washington, DC.

Xue, J., and Su, B., 2017: Significant remote sensing vegetation indices: A review of developments and applications, *Journal of Sensors*.

Yilmaz, M.T., Hunt, E.R. and Jackson, T.J., 2008: Remote sensing of vegetation water content from equivalent water thickness using satellite imagery. *Remote Sensing of Environment*, 112, 2514-2522.

Zeng, Y., Zhang, J., and Van Genderen, J.L., 2006: Comparison and analysis of remote sensing data fusion techniques at feature and decision levels, In ISPRS Commission VII Mid-term Symposium Remote Sensing: From Pixels to Processes.

Zhao, D., Huang, L., Li, J., and Qi, J., 2007: A comparative analysis of broadband and narrowband derived vegetation indices in predicting LAI and CCD of a cotton canopy. *ISPRS Journal of Photogrammetry and Remote Sensing* 62, 25-33.

Zhang, H., Wang, T., Liu, M., Jia, M., Lin, H., Chu, L.M. and Devlin, A.T., 2018: Potential of Combining Optical and Dual Polarimetric SAR Data for Improving Mangrove Species Discrimination Using Rotation Forest. *Remote Sensing*, 10, 467.

Zhang, J., 2010: Multi-source remote sensing data fusion: status and trends, *International Journal of Image and Data Fusion*, 1, 5-24.

Zhang, X., Sun, R., Zhang, B., and Tong, Q., 2008: Land cover classification of the North China Plain using MODIS EVI time series, *ISPRS Journal of Photogrammetry and Remote Sensing* 63, 476-484.

Zheng, B., Myint, S.W., Thenkabail, P.S. and Aggarwal, R.M., 2015: A support vector machine to identify irrigated crop types using time-series Landsat NDVI data. *International Journal of Applied Earth Observation and Geoinformation*, 34, 103-112.

Zhu, Z., Woodcock, C.E., Rogan, J., and Kellndorfer, J., 2012: Assessment of spectral, polarimetric, temporal, and spatial dimensions for urban and peri-urban land cover classification using Landsat and SAR data, *Remote Sensing of Environment*, 72-82.

Ziolkowski, D., Malek, I. and Budzynska, M., 2013: Dual Polarimetric signatures of vegetation: a case study Biebrza. *Geoinformation Issues*, 5, 5.